ALMA MATER STUDIORUM A.D. 1088
UNIVERSITÀ DI BOLOGNA

SCUOLA DI SCIENZE

Corso di Laurea Magistrale in Geologia e Territorio

Dipartimento di Scienze Biologiche, Geologiche ed Ambientali

Tesi di Laurea Magistrale

Mediterranean Outflow interaction with the seafloor of the Gulf of Cadìz, a numerical ocean modelling approach

Candidato:
Giovanni Fantini

Relatore:
Prof. Claudia Romagnoli

Correlatori:
Prof. Alfredo Izquierdo
Prof. Nadia Pinardi

Sessione Marzo 2019
Anno Accademico 2017-2018

Si chiudano gli occhi, si presti attento ascolto e, dal più leggero soffio fino al più selvaggio rumore, dal più elementare suono fino al più complesso accordo, dal più veemente e appassionato grido fino alle più miti parole della ragione, sarà sempre la natura a parlare, a rivelare la propria presenza, la propria forza, la propria vita e le proprie connessioni, cosicchè un cieco, a cui l'infinitamente visibile fosse negato, in ciò che è udito potrà cogliere un infinitamente vivente.

Johann Wolfgang von Goethe

Table of contents

Riassunto

Il fondale del Golfo di Cadice è uno dei settori marini più studiati al mondo in quanto registra, con la costruzione di un sistema deposizionale conturitico, gli effetti della corrente legata all'uscita d'acqua mediterranea dallo Stretto di Gibilterra. Le conturiti ("drift") sono depositi di mare profondo, che si formano principalmente grazie alla circolazione di acque dense, lungo le scarpate dei margini continentali (Rebesco et al., 2014). Attraverso l'utilizzo di batimetria multibeam ad alta risoluzione e un modello numerico oceanografico (*Med-currents*), in questa tesi è stato riprodotto il flusso d'acqua Mediterranea sul fondale del Golfo di Cadice e valutato il suo impatto sul fondale a scala giornaliera nell'arco temporale di un anno. L'analisi si è basata sulla riproduzione della velocità sul fondale della corrente Mediterranea e sul calcolo dello stress di taglio che si genera. La variabilità spazio-temporale dello stress di taglio agente sul fondale, confrontata con valori assunti di stress di taglio critico, ci ha permesso di individuare aree in prevalente erosione e i principali centri deposizionali e di compararle con le figure erosive e deposizionali precedentemente definite dalla abbondante letteratura sul sito. I risultati di questo lavoro mostrano come i principali elementi strutturali del fondale deviano e modificano il flusso d'acqua Mediterranea, evidenziando in oltre , il ruolo della discontinua attività della corrente nell'erodere, trasportare e depositare i sedimenti.

Abstract

The seafloor of the Gulf of Cadiz is one of the most studied marine environment of the world because it records, with construction of a Contourite depositonal system (CDS), the effects of the Mediterranean outflow (MOW) current from the Gibraltar Strait. Contourite drifts are giant accumulation of deep-sea sediment, they are largely found along the middle slope of the continental margin, typically associated to high bottom currents activity (Rebesco et al., 2014). Through the use of high-resolution multibeam bathymetry and a numerical ocean model (Med-currents), we simulate the Mediterranean outflow spreading pattern on the Gulf of Cadiz seafloor, estimating its impact at an daily time scale in a period of one year. The analysis is based on the simulations of the bottom current speed and on the calculations of the bottom shear stress generated by the current-seafloor interaction. The spatial and temporal variability of the bottom shear stress, compared with the assumed bed critical shear stress, allow to individuate areas where the erosion prevails and the main depositional centers. Our results show how the bathymetry steers and modifies the flow and highlight the role of intermittent bottom current activity in sediment erosion, transport and subsequent drift deposition.

Introduction

The transitional zone between the Mediterranean basin and the Atlantic ocean extends along the south Iberian margin and the northwest African margin including the Alboran sea and the Gulf of Cadiz. Its expression is highlighted by geological, climatological, biological and oceanographic evidence but mainly by the exchange of water through the Strait of Gibraltar. This gateway drives the exchange of water between these two basins and is characterized by the Atlantic inflow (AI) and the Mediterranean outflow (MOW). The Gulf of Cadiz seafloor records the footprint of the Mediterranean water exit since the opening of the Gibraltar strait with the construction of one of well know Contourite Depositional Systems (CDS) of the world. This CDS comprises several erosional features and giants sediment drifts distributed along the middle slope of the Gulf of Cadiz. The evident link between the Mediterranean bottom current activity and the formation of The CDS has already been demonstrated by several authors (Llave et al., 2001,2009; Mulder et al., 2003; Hernández-Molina et al., 2006, 2011,2014,2016; Rebesco et al., 2014; amongst others). Furthermore, these studies have revealed the importance of *along-slope* process in shaping the continental margin *sea-bottom* morphology and how they interact with *down-slope* process (see, for example: Hernández-Molina et al., 2006a,2011, García et al., 2009, Rebesco et al., 2014). However, due to the difficulty in reaching this deep environment, the direct observations of the drifts associated bottom currents are sporadic and don't allow to adequately represent the regional hydrodynamic setting and the principal contourite's formation mechanisms (Thran et al., 2018). For this reason, the use of ocean circulation models can help to investigating the spatial and temporal variability of the bottom currents responsible for drifts development. The model simulates these processes on the basis of physical restriction imposed by the fluid dynamics and its able to reproduce the MOW spreading pattern over the bathymetric data of the Gulf of Cadiz. The purpose of this work is to explain the Gulf of Cadiz contourites distribution from a computational point of view. Through a bottom shear stress analysis carried out using simulated bottom currents metrics and an high resolution bathymetry, we estimate where the bottom current activity is higher enough to erode, transport and subsequently where are the preferential areas for drifts accumulation. We firmly believe that the combination of ocean circulation models and observation from the geological record, represents a new method to investigate the interaction between the bottom current activity and the deep seafloor morphology.

Chapter 1 - Study area

The Gulf of Cadiz is located in the Eastern - Central Atlantic, bounded by the Southwest margin of the Iberian peninsula and the Northwest African margin (Fig.1.1). This area is characterized by one of the most important sea-ocean gateway of the world, the Strait of Gibraltar.

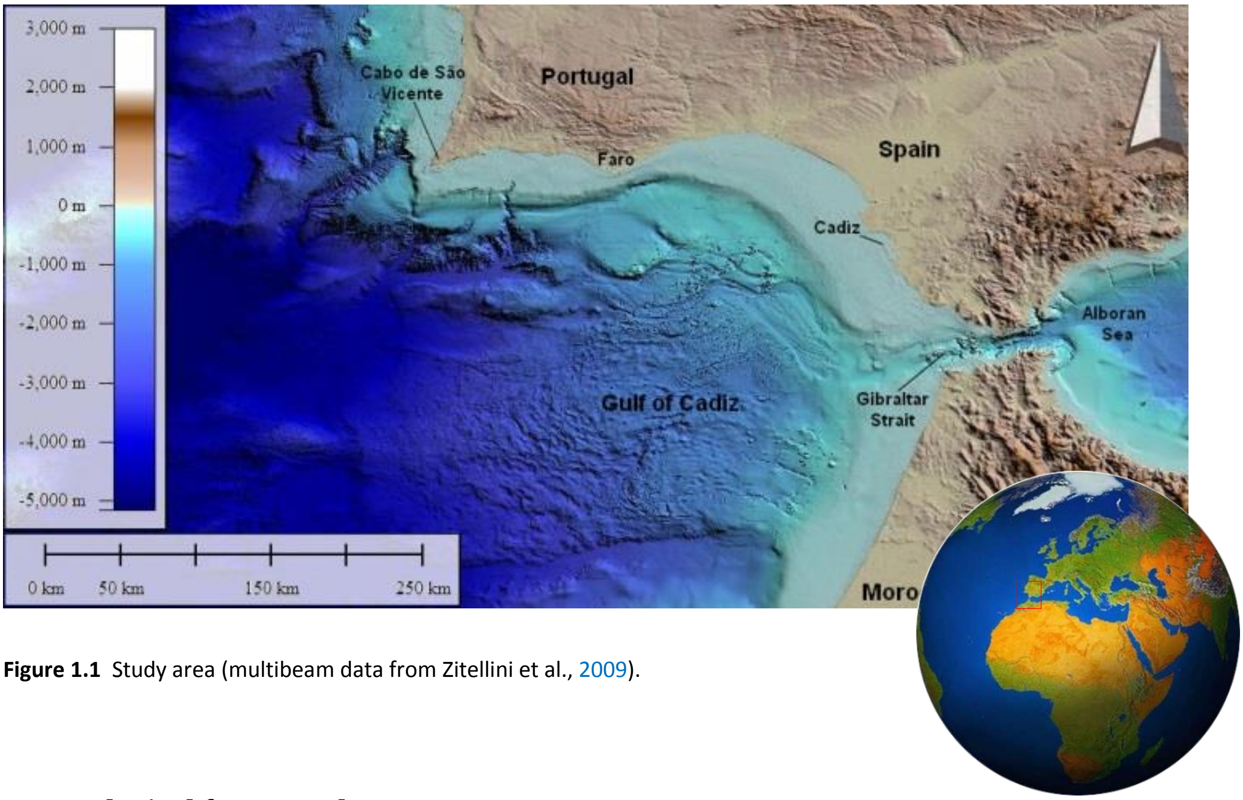

Figure 1.1 Study area (multibeam data from Zitellini et al., 2009).

1.1 Geological framework

The Northwest Africa– Southwest Eurasia plates boundary (Fig. 1.2b) extend along a west to east direction, from the Azores islands through the Gulf of Cadiz into the western Mediterranean across the Gibraltar Strait. At present, the pole of rotation of Africa with respect to Eurasia is located in the Atlantic near the Equator at a longitude ~20°W (Zitellini et al., 2009). For this reason, the central part of the Azores–Gibraltar plate boundary is a transform fault, the Gloria Fault (Fig. 1.2b). West of the Gloria Fault, the Terceira Ridge is an oceanic trans-extensional plate boundary where oceanic-crust accretion occurs at present. East of the Gloria fault, and already in the Gulf of Cadiz, the plate boundary is not well established because deformation is distributed over a broad elongated area in correspondence of an accretionary wedge (Fig. 1.2). Further East, to the east of the Straits of Gibraltar, the Nubia–Iberia plate boundary is defined by a right-lateral transpressive shear zone (Fig. 1.2b), the

Rif–Tell fault zone (Zitellini et al., 2009). The diffuse nature of the plate boundary segment of the Gulf of Cadiz has been a matter of debate since the early plate tectonic reconstructions of McKenzie (1970) and Dewey et al. (1973). The aim was connect the ocean plate boundary, from the Gloria transform fault to the right transpresional Rif–Tell fault of the western alpine orogenic termination.

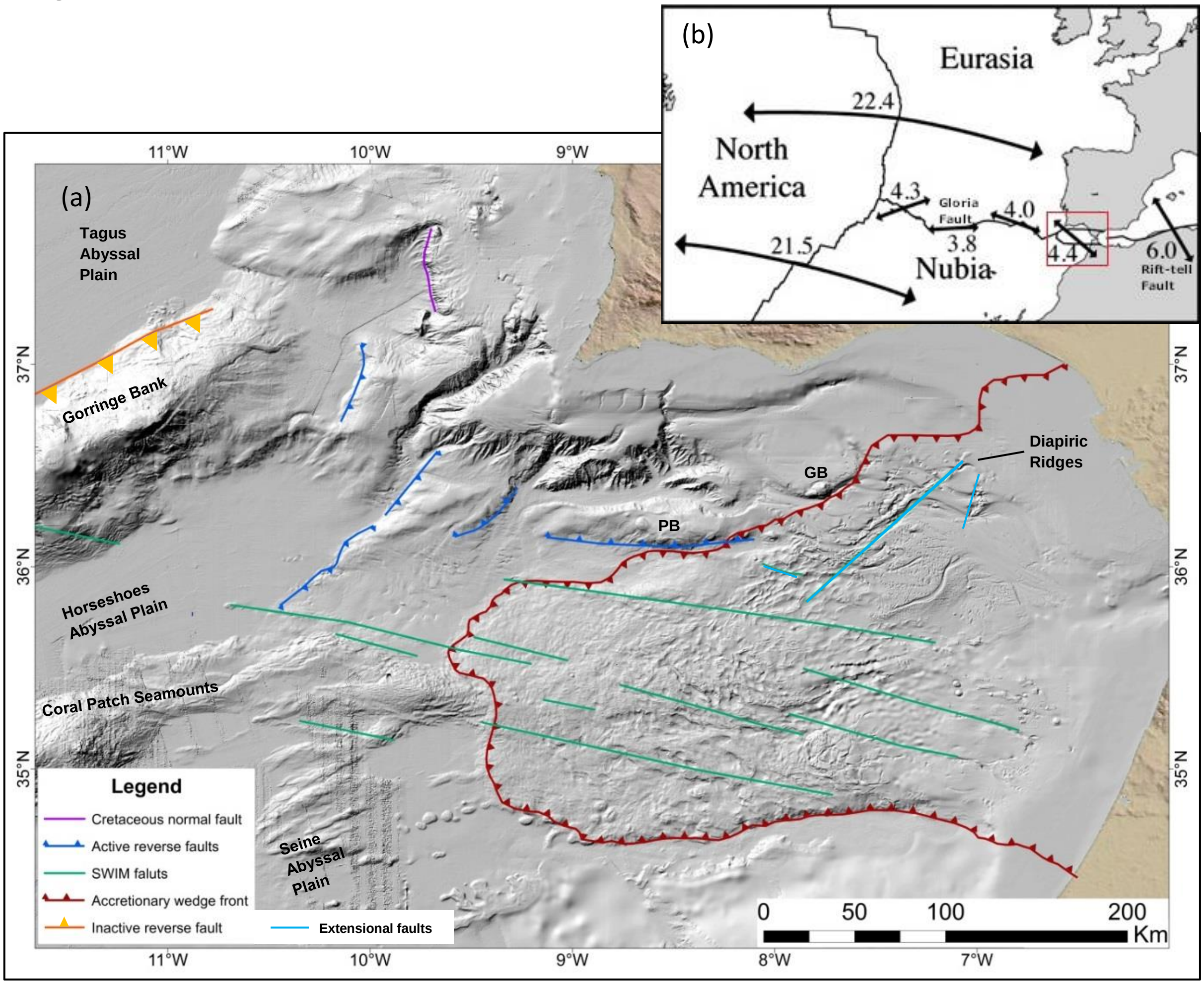

Figure 1.2 Structural map of the Gulf of Cadiz, modified from Zitellini et al., (2009); right top frame: actual North Atlantic plate movements (mm/yr) modified from Terrinha et al., (2009); GB = Gualdalquivir Bank, PB = Portimao Bank.

Zitellini et al. (2009) have successfully completed this goal, defining a series of sub-parallel WNW-ESE trending lineaments, which their refer to as the SWIM lineaments (Fig. 1.2). The SWIM Fault zone cross-cut the Horseshoes Abyssal Plain and the Gulf of Cadiz accretionary wedge. The SWIM lineaments are dextral strike-slip faults that often correspond to a series of narrow ridges and valleys defined on the seafloor morphology and are punctuated by several active mud volcanoes (Fig. 1.2).

Since the Jurassic continental break-up between north America, Africa and Eurasia, the Gulf of Cadiz has been marked by various change in the tectonic regimes. The opening of the Central Atlantic Ocean in the Mesozoic age and the relative rifting stage lead the formation of the SW Iberia and NW Morocco passive continental margin. Palinspastic reconstructions of the Atlantic (e.g. Srivastava et al., 1990) have shown that the continental margins of South Iberia and Northwest Africa were formed during the Jurassic opening between North America and Africa, while the western continental margin of Iberia resulted from separation of Iberia with respect to North America in Cretaceous times. During the late Cretaceous-Early Paleogene the Iberia sub-plate moved independently from Eurasia and Africa (Gradstein & Ogg, 2004) but subsequently Iberia became welded to Africa and their boundary became passive (Zitellini et al., 2009). At about 35 Ma the plate boundary between Africa and Iberia returned active with the occurrence of compressional regime, conditioned by N–S Africa–Eurasia convergence (Fig. 1.3). This compressional condition led to the formation of the Betic–Rif orogeny that was coeval with the opening of the Western Alboran Sea (Fig. 1.1), during Oligocene through Miocene times (Zitellini et al., 2009; Gutscher et al., 2002). The westwards directed thrusting of the Gibraltar orogenic produced a complex imbricated and thrusted allocthonous masses arc in the Gulf of Cadiz, called ‘‘olistostrome unit’’ (Hernández-Molina et al., 2016), detached from a decollement surface located at the top of the Cretaceous sedimentary units.

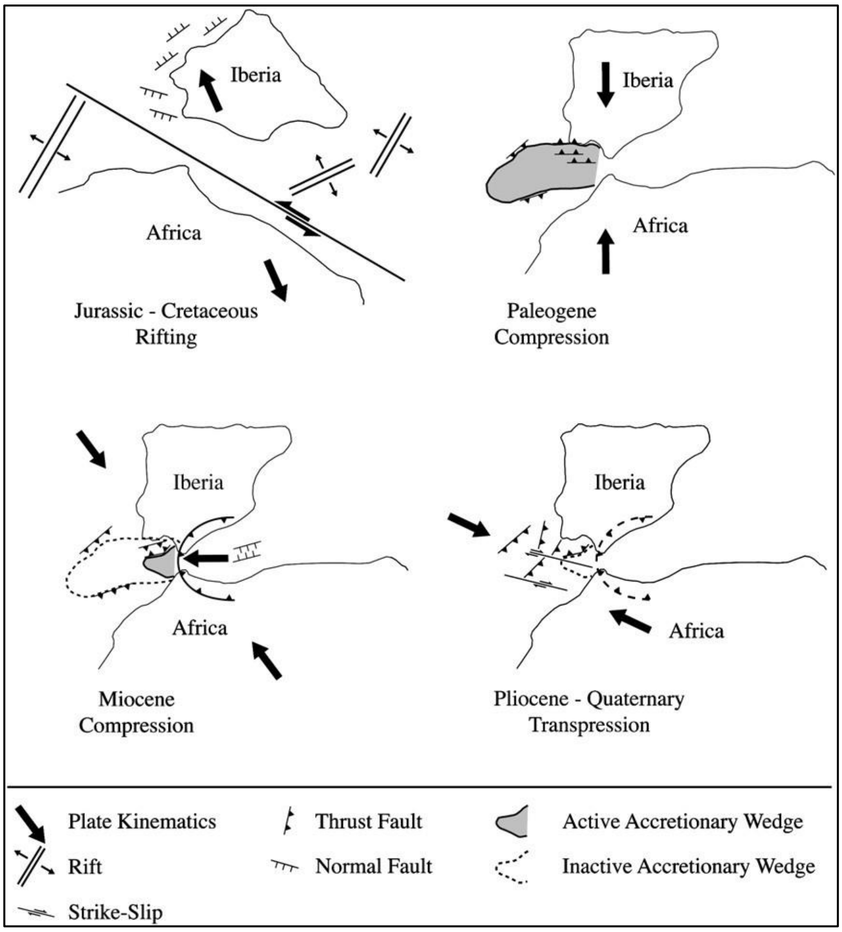

Figure 1.3 Plate kinematics reconstruction from Terrinha et al. (2009).

This resembles a subduction accretionary complex (Gutscher et al., 2002), clearly defined by the seafloor morphology (see Fig. 1.2). From Late Oligocene to present time, the convergence between Africa and Eurasia plates gradually changed the direction, from N-S thought NW-SE to the present-day transpressional WNW-ESE (Fig.1.3). The submarine mountains that border the abyssal plains, such as Gorringe Bank, Coral Patch Seamounts and Ridge, and the series of elongated hills in the northern Seine Abyssal Plain (Fig. 1.2), were formed by the NW–SE trending compression due to the Iberia– Nubia convergence (Fig. 1.3). Even, the Guadalquivir and Portimao bank are two pop-up structures formed during this NW-SE trending compression (Fig. 1.2). Although at the present-day, the southern flanks of this structures, are undergoing extensional deformation (Terrinha et al., 2009). On the Est of the Guadalquivir bank (Fig. 1.2), the Donãna, Guadalquivir and Cadiz ridge are Triassic salts, gypsum and shallow-marine carbonate deposits emplaced as diapiric extrusion, that arises along the thrust migrating structure of the stretched accretionary prism, during the Tortonian collapse of the Betic-Rift orogenic front (Hernandez-Molina et al., 2016). From the late Pliocene age (~2.4 Ma), the margin evolve toward more stable conditions (Hernández-Molina et al., 2016). Since this time, the present-day regional circulation setting of the Gulf of Cadiz and the water exchange through the Gibraltar gateway were established.

1.2 Morphological setting

The complex geodynamic evolution of the Gulf of Cadiz continental margin lead the division of the area in three main morphostructural zones, clearly recognizable on the seafloor morphology (Fig. 1.4). Firstly, it may be observed the area located offshore the SouthWest Portuguese margin (1); it was formed by tectonic inversion of a pre-rifted continental margin (Terrinha et al., 2009) and it is crossed by deeply incised submarine canyons, oriented NE-SW, with steep margins and erosive floor. The second morpho-structural zone (2) is located offshore of the Guadalquivir basin and shows a broad continental middle slope that strongly interact with the Mediterranean outflow. In this area, the Guadalquivir Basement High and the Donãna, Guadalquivir and Cadiz diapiric ridges (Fig. 1.4) are the main structural highs. Attached to these features, there are several contourite channels, clearly visible on the bathymetry (Fig. 1.4). The third zone (3) is bounded by the offshore configuration of the Betic-Rift orogenic accretionary wedge, characterized by numerous pockmarks and diffuse instability features (Mulder et al., 2003) also it presents a well-defined low gradient smooth platform on middle slope (profile in Fig. 1.5) and a relevant structural high, in front of the exit of the strait, the First basement high.

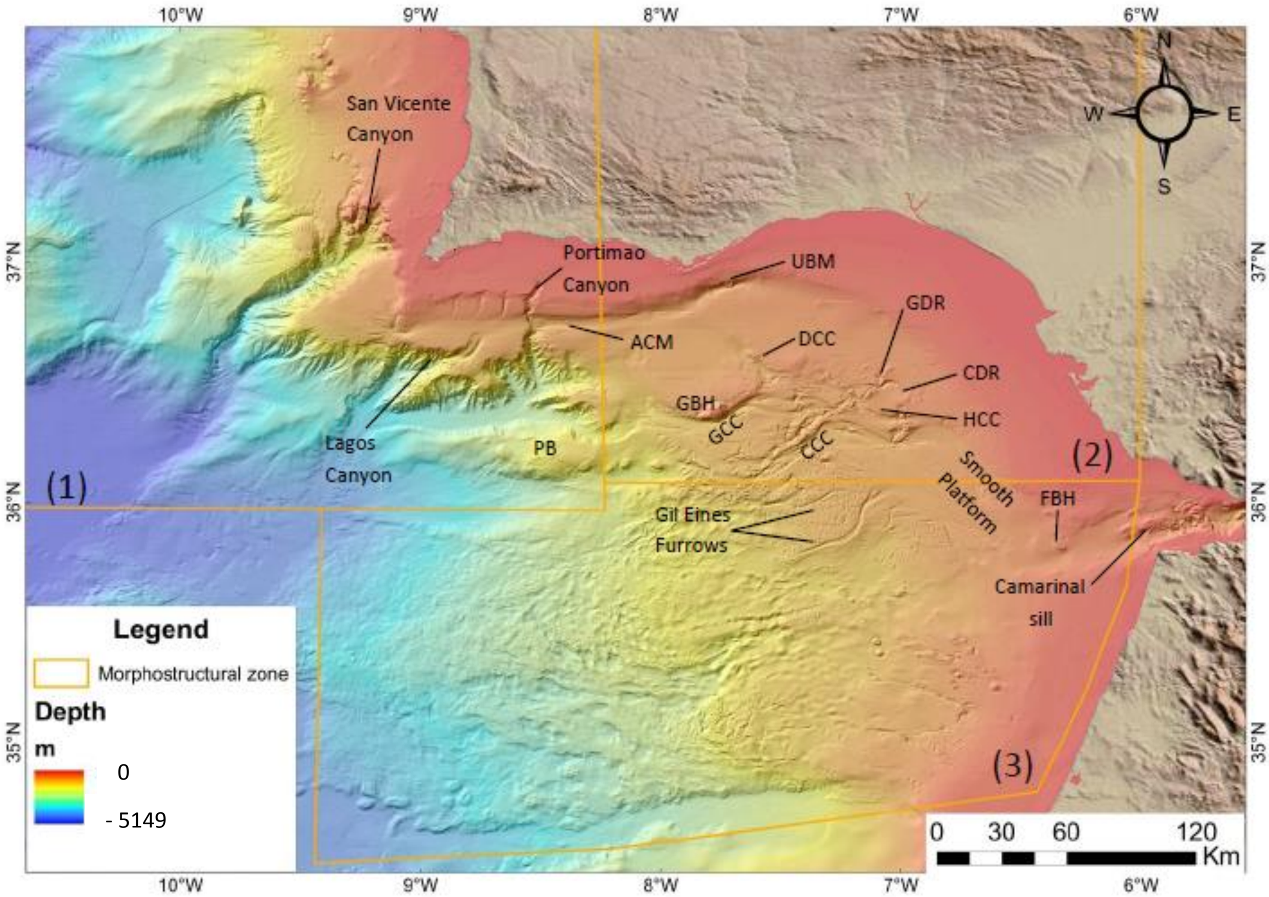

Figure 1.4 Geomorphological map of the Gulf of Cadiz (multibeam data from Zitellini et al., 2009). Subdivision in 3 morphostructural zone: orange polygons. *Legend of the main morphological features that interact with the MOW, in alphabetic order:* ACM: Alvarez Cobral Moat, CCC: Cadiz contourite channel, CDR: Cadiz diapiric ridge, Cs= Camarinal sill, DCC: Diego Cao Contourite Channel, FBH: First Basement High, GDR: Guadalquivir diapiric ridge, GCC: Guadalquivir contourite channel, GHB: Guadalquivir Basement High, HCC: Huelva contouite channel, PB: Portimao Bank, UBM: Upper slope Basal Moat.

The Gulf of Cadiz continental margin shows a well-defined continental shelf, slope and abyssal plain. The continental shelf exhibits a variable width, wider in the central area of the Spanish zone (~ 30 km), narrower towards Portugal (~ 17 km), generally the shelf-break is located at a water depths between 120 and 140 m (profile in Fig. 1.5,1.6). As well, the continental slope exhibits pronounced difference between the Algarve and the Spanish zones (profile in Fig. 1.5 and 1.6). Along the Algarve margin the slope is very steep and narrow with an extension of about 100 Km from the shelf edge to the abyssal plain. On the other side, submarine canyons are not present in the Spanish zone.

Here, the continental slope is very extensive (~ 300 Km) because of the offshore configuration of the Gibraltar orogenic arc external front represented by the accretionary wedge, emplaced since Oligocene, in the eastern and central part of the margin (Hernandez-Molina et al., 2016).

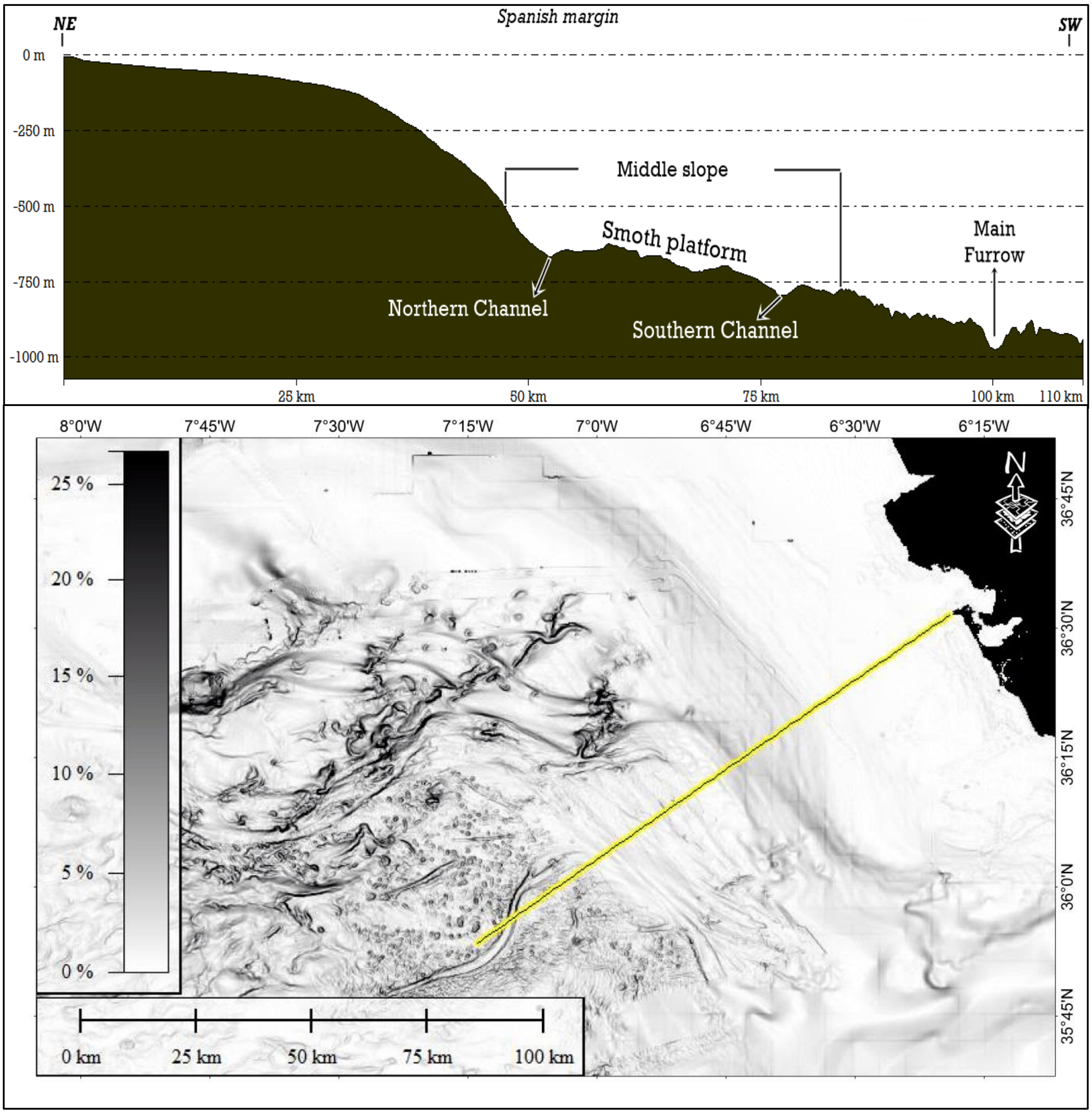

Figure 1.5 a) Spanish margin slope profile; b) Slope steepness in percent grade and path profile (multibeam data from Zitellini et al., 2009). Colorbar = Slope Acclivity (%).

In general, the continental slope in the Gulf of Cadiz, has a very irregular relief and can be divided in upper, middle and lower slope (Fig. 1.7).

The upper slope occurs from 120-140 to 400 m water depth and is 10 km wide on average (locally ~ 20 km), and has a gradient between 1° and 3°. The middle slope occurs at depth of about 400-1200 m and is characterized by an extensive slope terrace with a low average gradient between 0.5° and 1°.

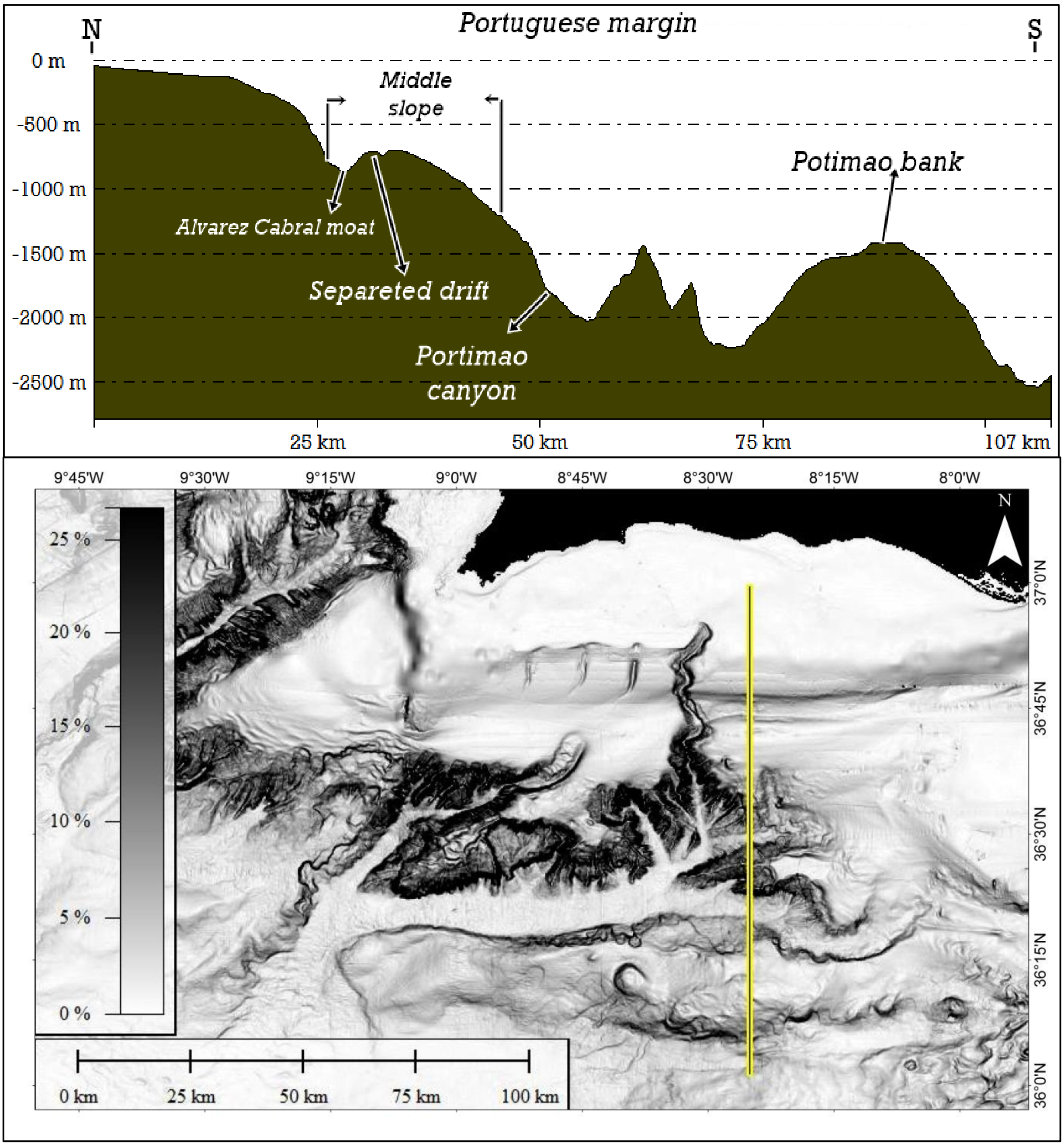

Figure 1.6 **a)** Portuguese margin slope profile; **b)** Slope steepness in percent grade and path profile (multibeam data from Zitellini et al., 2009). Colorbar = Slope Acclivity (%).

The lower slope starts at about 1200 m water depth, with a slope gradient between 2° and 4° and it connects with the abyssal plain at about 4000 m water depth (see profiles in Fig. 1.5 and 1.6).

The existence of a low gradient terrace along the middle slope (Fig. 1.7) has been one key factor for the development of the Gulf of Cadiz contourite depositional systems (Hernández-Molina et al., 2006).

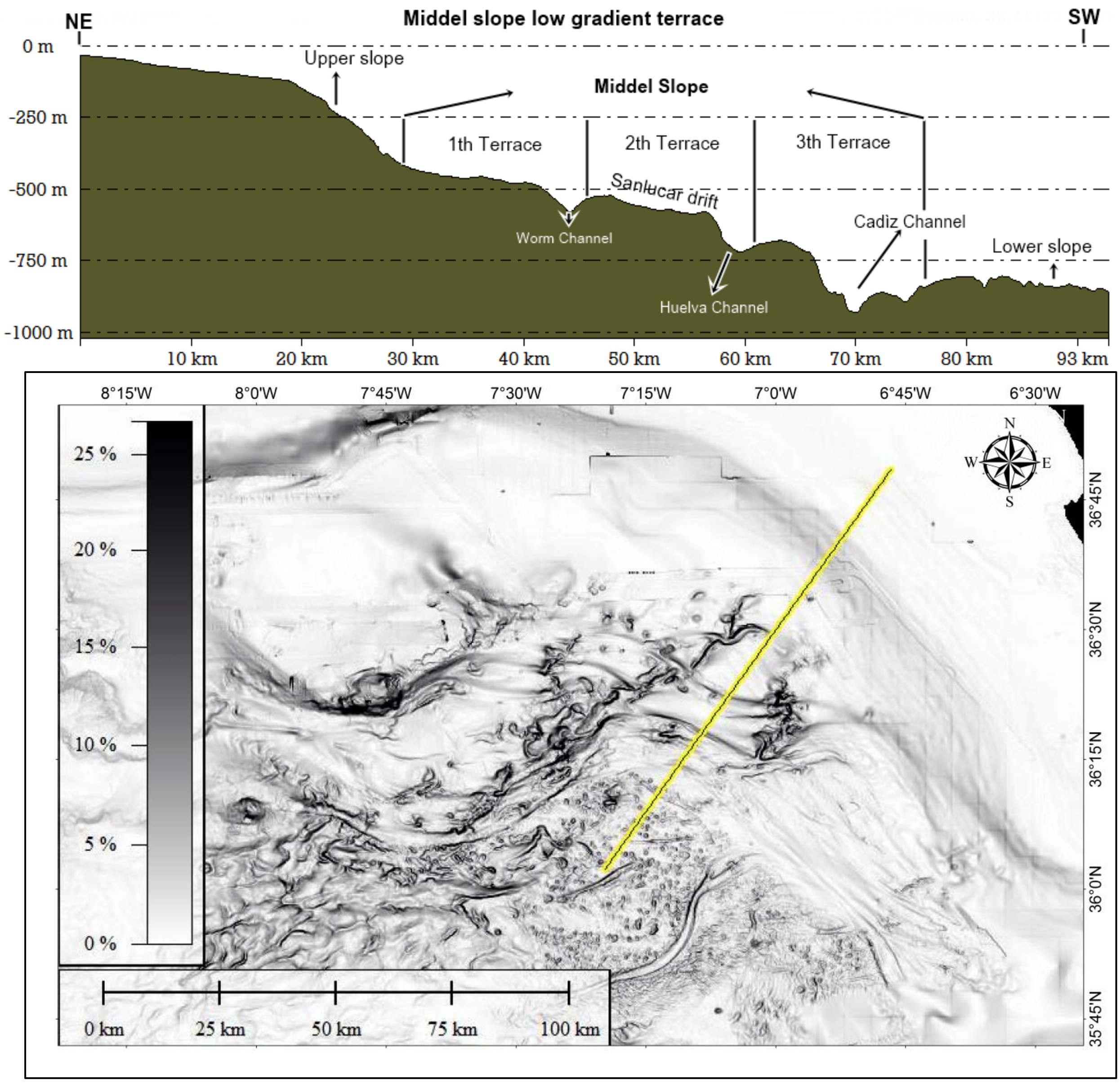

Figure 1.7 a) Middle slope low gradient terrace; **b)** path profile over the multibeam bathymetry (multibeam data from Zitellini et al., 2009). Colorbar = Slope Acclivity (%).

.

1.3 Oceanographic setting

The Strait of Gibraltar physically control the exchange of water between the Mediterranean Sea and the Atlantic Ocean. This exchange determines the circulation pattern of the Gulf of Cadiz and along the western Portuguese margin (Fig. 1.9). The Mediterranean outflowing waters spreads into the interior of the Atlantic Ocean forming a prominent basin-scale termohaline anomaly at mid-depths (Izquierdo et al., 2016).

The MOW (or Mediterranean undercurrent) is a mixture of waters sourced from the Mediterranean Basin, composed mainly of Levantine Intermediate Water (LIW) and a small component of Western Mediterranean Deep Water (WMDW; Ambar et al., 2002). This strong, warm and high saline current, averaging 13°C and 36.5 PSU, accelerates through the Strait of Gibraltar reaching velocities of up to 300 cm/s (Mulder et al., 2003) and flows towards NW along the continental slope of the Gulf of Cadiz, between 400-1400 m water depth, beneath the Atlantic inflow water (AIW) and above the Nord Atlantic Deep Water (NADW). The AIW is a combination of the Nord Atlantic central Water (NACW) and the Eastern North Atlantic Central Water (ENASW).

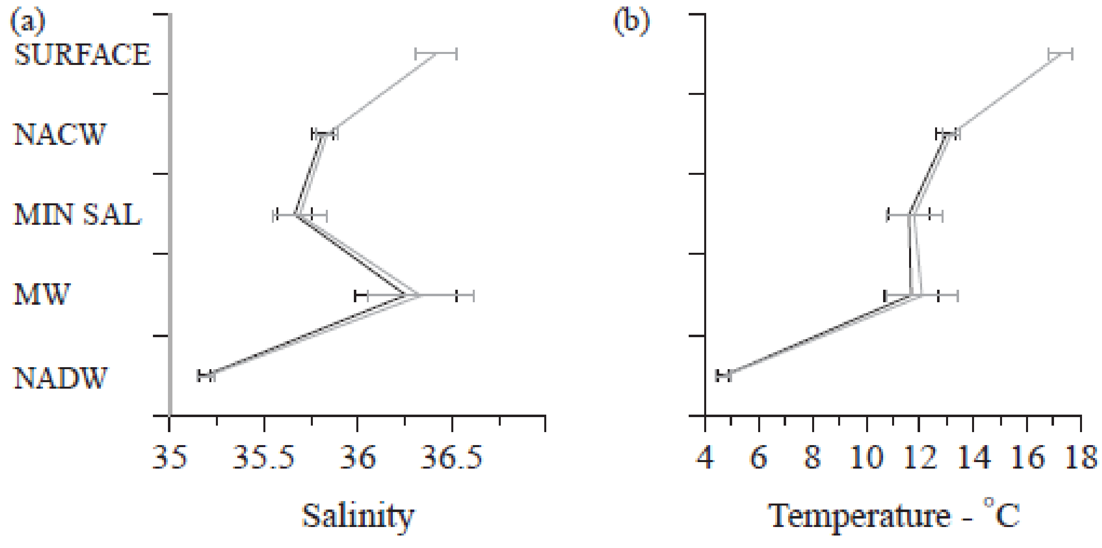

Figure 1.8 Plot of the main water mass of the Gulf of Cadìz (year averaged in the 1997); in a) salinity (PSU) and b) potential temperature (°C). From Ambar et al. (2002)

The AIW flows at a depth between 100-700 m water depth and averages 12-16°C and 34.7-36.25 PSU (Fig.1.8). The underlying NADW is a cold (3-8°C) and less saline (34.95-35.2 PSU) water mass (Fig. 1.8) flowing at a depth >1500 m from the Greenland-Norwegian sea region towards the south (Baringer & Price, 1999; Ambar et al., 2002). Furthermore, the modified Antarctic Intermediate Water (AAIW) was recently identified in the Gulf of Cadiz and it represents, in the eastern part of the Gulf of Cadiz, the coldest water mass above the MOW with a bottom boundary identified down to 600–625 m (Louarn & Morin, 2011).

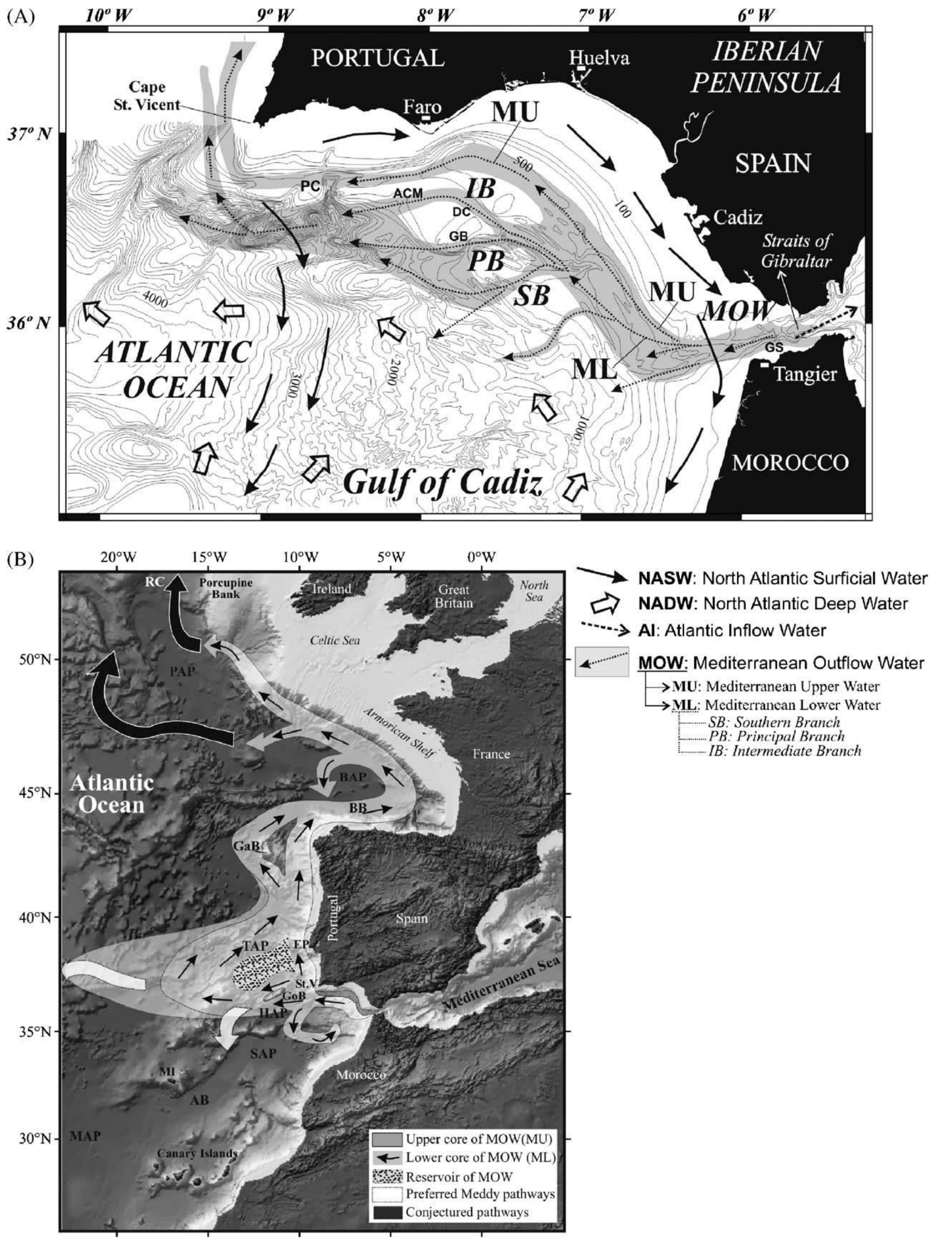

Figure 1.9 **a)** General circulation pattern of the gulf of Cadìz; **b)** general circulation pattern of the MOW in the North Atlantic. *Legend of the physiographic reference points in A and B, in alphabetical order:* AB= Agadir Basin; ACM= Alvarez Cabral Moat; BAP= Biscay Abyssal Plain; BB= Bay of Biscay; EP= Extremadura Promontory; DC= Diego Cao Channel; GB= Guadalquivir Bank; GaB= Galicia Bank; GoB= Gorringe Bank; GS= Gibraltar Seamounts; HAP= Horseshoe Abyssal Plain; MAP= Madeira Abyssal Plain; MI= Madeira Island; PAP= Porcupine Abyssal Plain; PC= Portimao Submarine Canyon; RC= Rockall Channel; SAP= Seine Abyssal Plain; StV= Cape Sant Vicent; TAP= Tagus Abyssal Plain. From Hernàndez-Molina et al. (2006).

Exiting with a South-west direction from the Gibraltar gateway, the MOW deflects in a north-west direction (Fig. 1.9) steered by the Coriols force effect (Zenk & Armi, 1990). Flowing toward NW, the MOW systematically decelerates from a 100-150 cm/s out of the Strait, through a range of 50 – 90 cm/s in the central part of the Gulf of Cadiz, to 20-50 cm/s around the Cape St. Vicente (Hernández-Molina et al., 2011). At about 6.2 °W, the Mediterranean water splits in two main core: the Mediterranean Upper core (MU) and the Mediterranean Lower core (ML, Hernández-Molina et al., 2014). The MU flows slope parallel (Fig.1.8), between 400-800 m water depth and is warmer and less saline (13-14°C and 35.7-37 PSU) in respect to the ML. The ML flows in a range between 800-1400 m depth and it's colder but more saline (10.5-11.5°C and 36.5-37.5 PSU) than the MU (Ambar et al., 2002; Fig. 1.8). At ~ 7.2°W, the ML divides into three distinct branches (Hernández-Molina et al., 2006). Following the thermohaline characteristics and the morphological restrictions the Southern Branch (SB), the Principal Branch (PB) and the Intermediate Branch (IB) are formed (Fig. 1.9a). On the other side, the MU is kept unite until it reaches the Portimao Canyon, where parts of its water mass is captured (Serra et al., 2010). After exiting the Gulf of Cadiz and passing Cabo St. Vicente, the Mediterranean Outflow splits in other three principal branches (Fig. 1.9b). The first branch moves to the south reaching the Canary island, the second goes to the West and the main branch flows Northwards along the western Iberian margin until it reach the Nordic seas, where notably impact the water temperature (Hernández-Molina et al., 2011). Its saline signal is tracked as far north as 50°20'N (Iorga & Lozier, 1999) and is now widely recognized its importance in the maintenance of the Atlantic Meridional Overturning Circulation (Rogerson et al.,2012).

1.4 The Contourite Depositional System

Since the opening of the Strait of Gibraltar at the end of the Messinian salinity crisis (about 5.3 Ma) a Contourite Depositional Systems (CDS) has been develops by the Mediterranean outflow water (MOW) and its strong impact on the bottom morphology of the Gulf of Cadiz. Contourite drifts are giant accumulation of deep-sea sediment, they are largely found along the middle slope of the continental margin, typically associated to high bottom currents activity. They can preserve high resolution sedimentary record, useful in order to investigate paleoclimatic and paleoceanographic evolution (Rebesco et al., 2014). Flowing in proximity of the seafloor, in fact the MOW produced different types of erosive features: contourite channels, moat and furrows; and several types of sediment drifts: sheeted, mounded, plastered and separated drifts (García et al., 2009; Hernández-Molina et al., 2003, 2006, 2016). The drifts consist primarily of muddy, silt and sandy sediments of mixed terrigenous and biogenic composition, while coarse sand and sporadic gravel are found mainly inside contourite channels (Fig. 1.10a, Hernández-Molina et al., 2016).

Llave et al., (2001) and Hernández-Molina et al., (2003) defined five morphosedimentary sector (Fig. 1.10), primarily related with the systematic decreasing of the MOW bottom velocity toward NW; these are, from east to the west: (1) proximal scour and sand ribbonst; (2) overflow sedimentary lobe sectort; (3) channels and ridges ; (4) contourite depositional sector and (5) submarine canyons sectors. This decreasing in the flow velocities, as it descends the continental slope is due to different factors: a decreasing density anomaly, induced mainly by mixing with the overlying Atlantic waters, which reduces the pressure force of the outflow; the effect of the Coriolis force in deflecting the current to the right (looking in a downstream direction); the bottom frictional effect produced by the roughness of the seafloor and especially of the channels floor (Hernández-Molina et al., 2006). The proximal sector (1) is dominated by abrasive surface and erosive scour lineaments oriented SE-NW and with a "V" shape profile. This zone is characterized by a smooth platform oriented along-slope (NW-SE) between 500 and 800m water depth that presents in the initial part (looking downstream) an evident rock outcrop (Fig. 1.10). While, on the final part of this platform, one of the exceptionally thick (~815 m) sandy sheeted drift has developed within the Cadiz depositional Basin (CB, Fig. 1.11). Connected with this slope platform, there are three furrows, produced by the erosional action of detached filaments of the ML (Fig. 1.10).

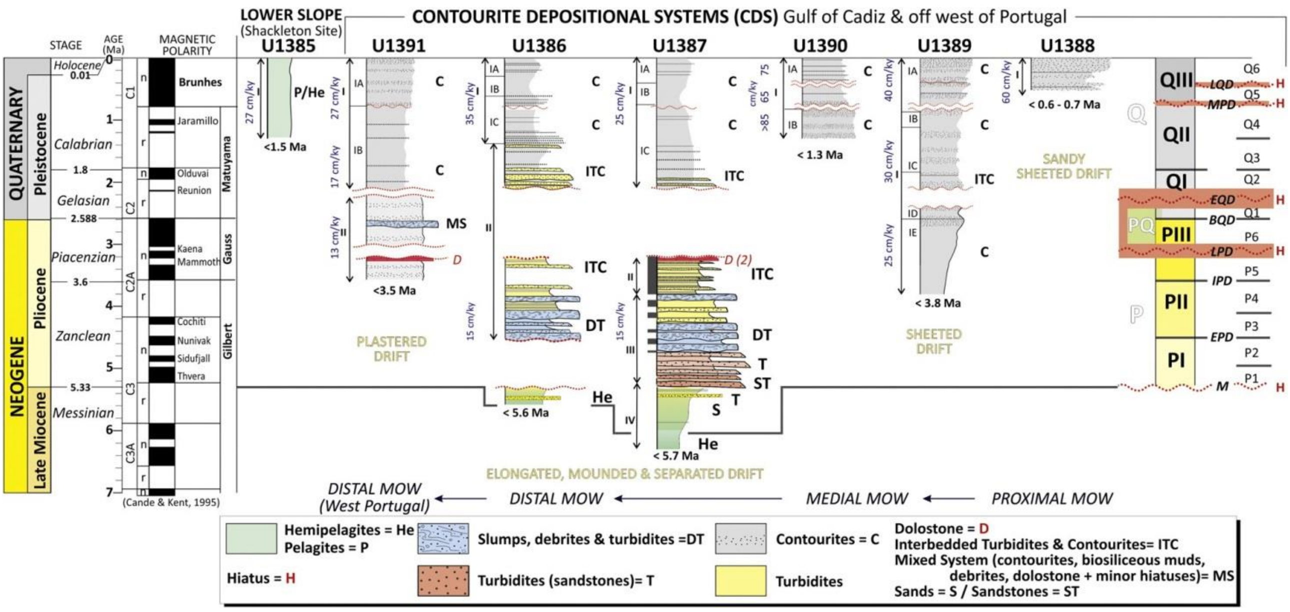

Fig. Following below

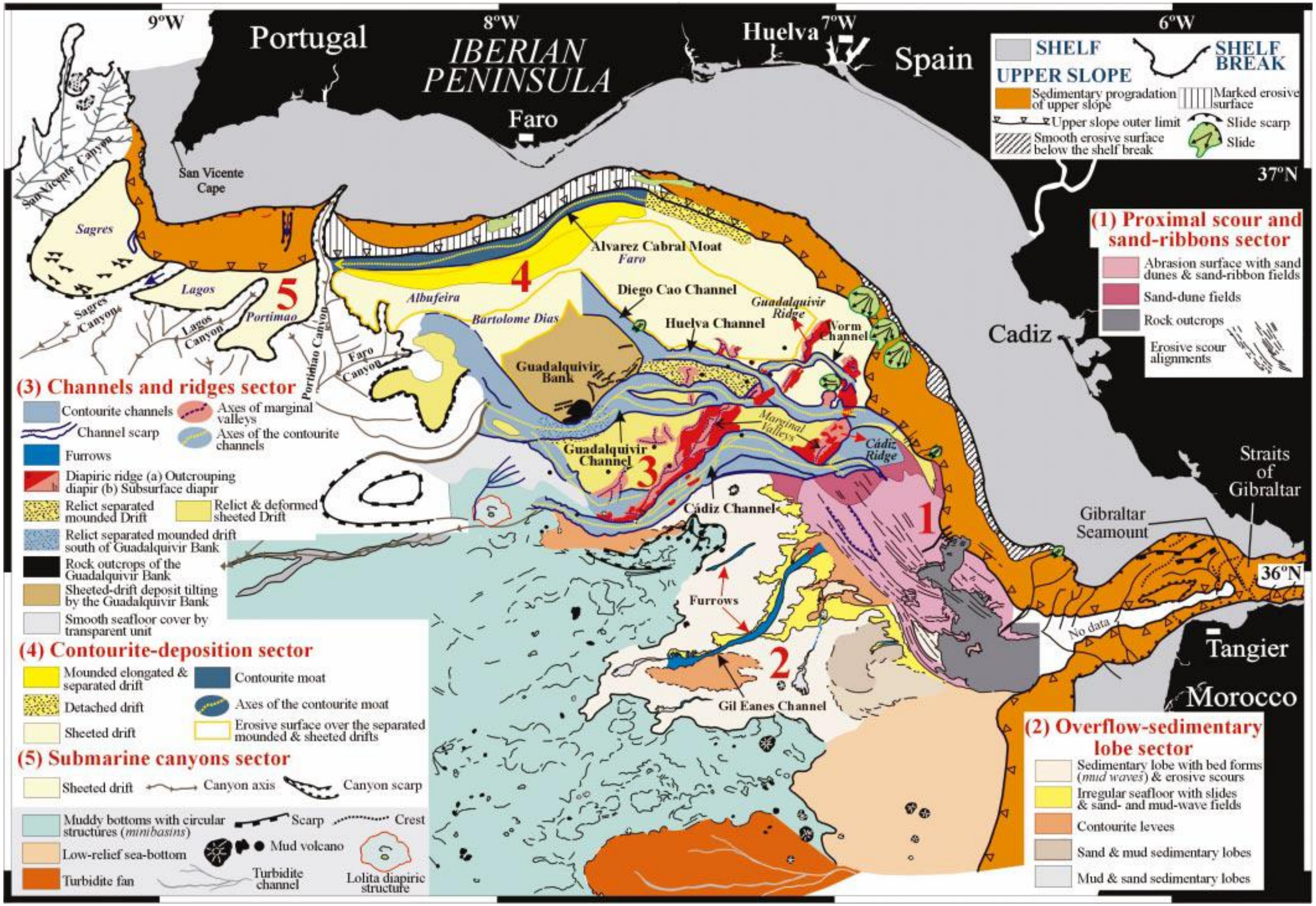

Figure 1.10 **a)** Lithologic summary for sites drilled during IODP Exp. 339. A general interpretation for the proximal area close to the Strait of Gibraltar to the distal area off west Portugal, from Hernàndez-Molina et al. (2016). **b)** Contourite Depositional System from Hernàndez-Molina et al. (2003).

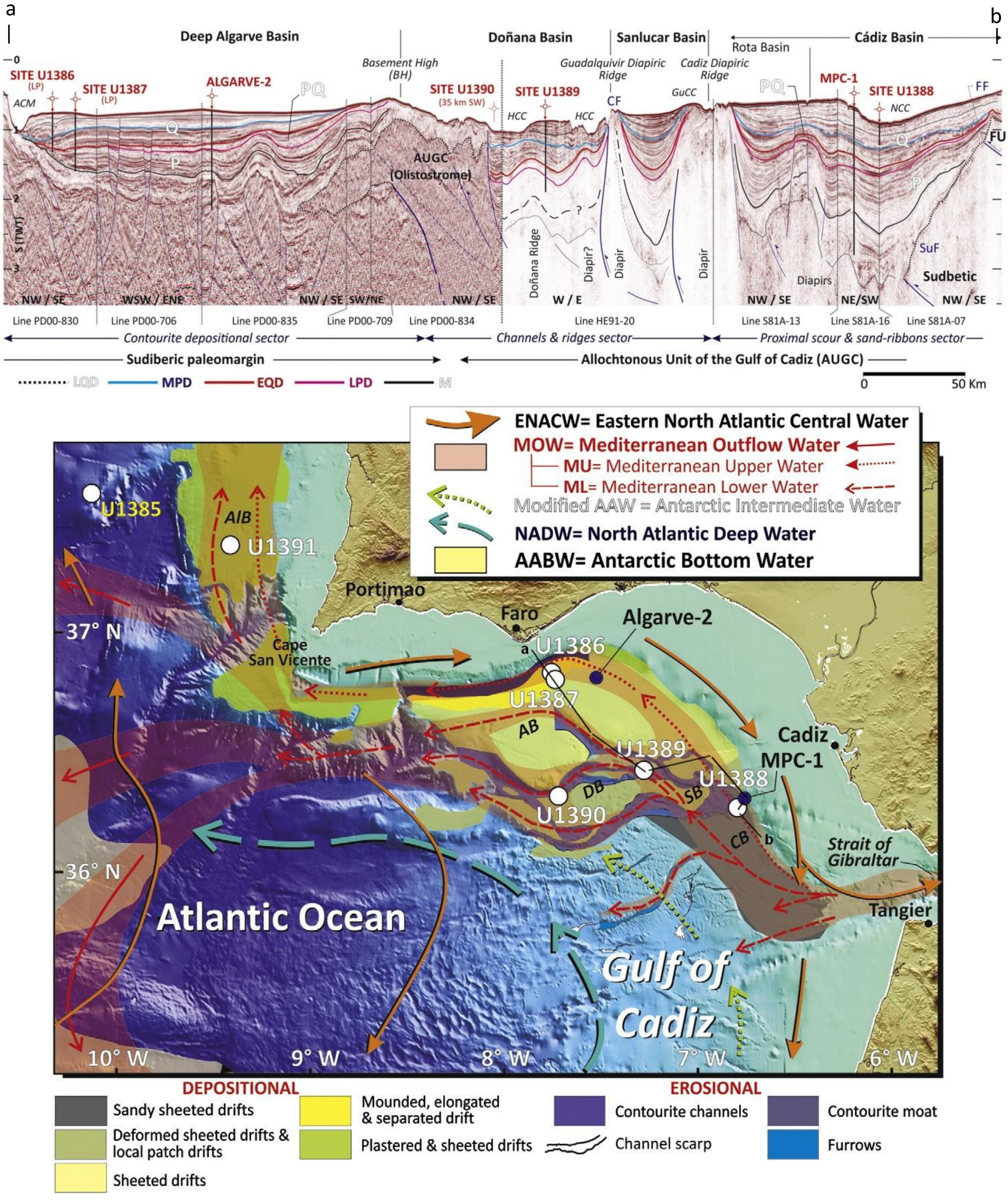

Figure 1.11 above) Composite seismic profile (~500 km long) along themiddle slope of the Gulf of Cadiz, from the proximal area near the Strait of Gibraltar (right) to the distal area along the Southern Algarve basin (left). Neogene sedimentary basins and the main morphosedimentary sectors of the contourite depositional system are shown within the regional tectonic framework. The Cadiz, Rota, Sanlucar and Doñana basins overly the Allochthonous Unit of the Gulf of Cadiz (AUGC). The Deep Algarve basin is located on the Sudiberic paleomargin. The major discontinuities occur at the Miocene–Pliocene boundary (M), late Pliocene (LPD), early Quaternary (EQD), mid Pleistocene (MPD) and late Quaternary (LQD). **below)** Gulf of Cadiz, showing the pathway of Mediterranean OutflowWater (MOW), as well as the regional depositional and erosional features it generates along the mid-slope. IODP Exp. 339 sites shown as solid white circles and the two wells drilled by petroleum exploration companies are shown as blue circles. Bottom water masses and ocean currents are also shown. Legend for the sedimentary basins along the southern Iberian margin: AB=Algarve basin; AlB=Alentejo basin; CB=Cadiz basin; DB=Doñana basin; RB = Rota basin; SB= Sanlucar basin. Both Modified From Hernàndez-Molina et al. (2016). Location profilein the Fig. below.

This narrow channels are inside the over-flow sedimentary lobes sector (2) and present, on the seaward side, a well-defined sedimentary lobes (Hernández-Molina et al., 2006). In the channels and ridge sector (3), five main contourite channels have been recognized by García et al., (2009): Cadiz Contourite Channels (CCC), Guadalquivir Contourite Channel (GCC), Huelva Contourite Channel (HCC), Worm Contourite Channel (GCC) and Diego Cao Contourite Channel (DCC).

This sector is characterized, in the middle of the Guadalquivir diapiric ridge (GDR) and Cadiz diapiric ridge (CDR) by the Sanlucar and between the GDR and the Guadalquivir B. H. by the Doñana basins (Fig. 1.11b). The sedimentation of this two basins is characterized by deformed sheeted drifts (profile in Fig. 1.11a)and are both stratigraphically correlated with the adjacent Rota and Cadiz basin (Hernández-Molina et al., 2016). Furthermore, the deep Algarve basin is located over the Guadalquivir Bank (GB; Fig. 1.11b) and is composed by a very extensive mounded sheeted drift that has formed inside the contourite depositional sector (4, Fig. 1.10). This main depositional sector is characterized by the Faro–Albufeira system (Llave et al., 2001) and comprises one main erosional features represented by the Alvarez Cabral Moat that is placed in the transition zone between the upper and middle slope (Fig. 1.12). attached to the ACM there is a separated drift that shows a characteristic upslope migrating depositional sequence (profile in Fig. 1.11a, Hernández-Molina et al., 2003).

Further NW, the occurrence of deep incised submarine canyons, the Portimao, Lagos, Sagres and San Vicente submarine canyons (Fig. 1.4), that are orientated approximately NE–SW, define the submarine canyon sector (5). Within this sector, there are the Portimao, Lagos, and Sagres drifts (Fig. 1.4) that are located on the narrow terrace of the middle slope that characterize this area.

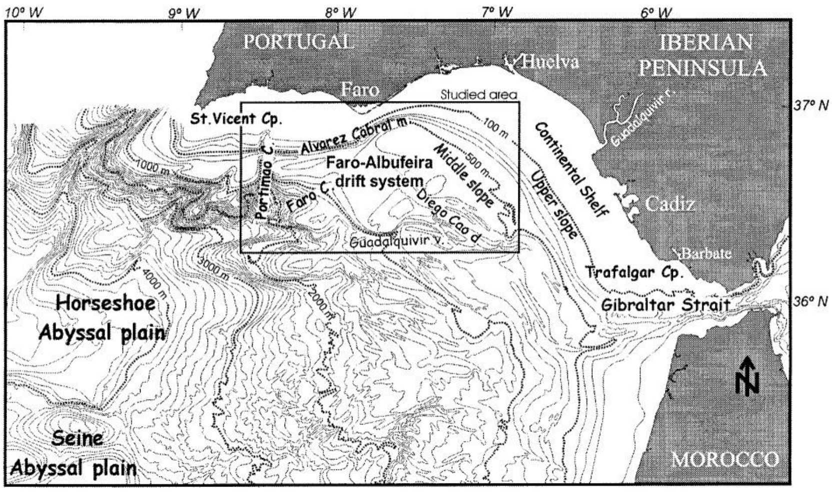

Figure 1.12 Location of the Faro-Albufeira contourite system in the Gulf of Cadiz; from Llave et al. (2001).

Turning around Cabo St. Vicente and passing the San Vicente canyon, on western Algarve margin, the Mediterranean bottom current produces a silty buried mounded drift that constitutes the Alentejo Basin (AIB; Fig. 1.11).

Chapter 2 - Materials and Methods

In this work we use a numerical modelling approach in order to relate some seabed morphologies widely present on the Gulf of Cadiz slope (Contouritic Depositional System, CDS) with the Mediterranean bottom current pattern. The study is based on high-resolution bathymetric data (section 2.1), used for the bottom morphology analysis, and on the Med-currents ocean model (section 2.2) provided by INGV (Istituto Nazionale di Geofisica e Vulcanologia). The Med-currents ocean model permits to simulate the present-day currents circulation of the Gulf of Cadiz and the Mediterranean Outflow Water hydrodynamics. Simulated bottom current speeds (e.g., time-mean and maximum bottom current speed, speed standard deviation) were estimated and overlapped on the high-resolution bathymetry. Then, bottom currents metrics were examined in relation to the distribution of depositional drift and erosional channels that characterize CDS of the Gulf of Cadiz.

Finally, a bottom shear stress (see section 2.3) and critical bed shear stress analysis (section 2.4) was carried out to estimate the force per unit area of the Mediterranean outflow current impacting the seafloor, and for a comparison with the long-term patterns of erosion and deposition in the study area. In this analysis we take in account only the shear stress produced by the MOW over the seafloor (bed load), excluding other types of alongslope and downslope processes due to different bottom water movements that characterize the deep ocean environment (for examples: tidal internal waves). The identification of the sediment sources of the CDS and quantification of the MOW suspended sediment load is beyond the scope of this work. These analysis would require, in fact, an integrated and advanced study, including an estimate of fluvial sediment input and Mediterranean sea sediment supply, the localization of the paths of principal turbidity currents in the area, etc. etc..

2.1 Bathymetry

After several years of marine geology investigations, the bathymetry of the Gulf of Cadiz has been acquired by means of high-resolution multibeam data. Zitellini et al. (2009) published a bathymetric compilation map (Fig. 2.1) merging data from different surveys performed in the last ten years by several oceanographic institutions from all over the world (see Diez et al., 2005, Zitellini et al., 2009). The results is a bathymetric map with 250 m x 250 m grid spacing that improve the knowledge of the whole area. For surrounding areas, the General Bathymetric Chart of the Oceans (GEBCO) data (0.5° resolution) are available, and were used to integrated the map. For the purposes of this Thesis, the bathymetric data were processed and analyzed using Global Mapper, ArcGIS and Spider (Python language) software.

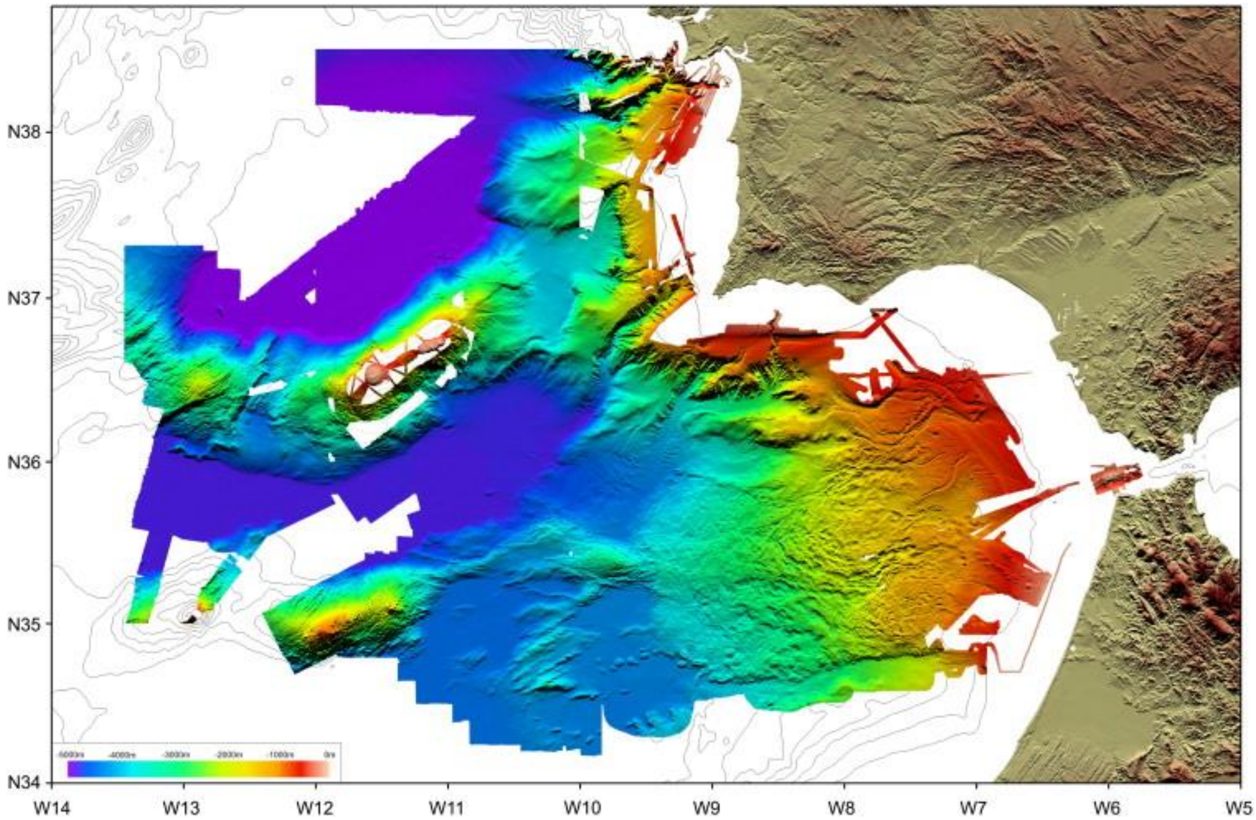

Figure 2.1 "Bathymetry of the Gulf of Cadiz, North-East Atlantic: the SWIM multibeam compilation" (Zitellini et al., 2009).

2.2 Ocean Circulation Model

A numerical ocean model is a set of equation describing physical processes in order to simulate the oceanic system. Different oceanic variables, such as temperature, salinity, meridional and zonal velocity, obtained by assimilation of observed data and several processing stages, constitute the initial condition of the models. Forcing this initial conditions with a set of boundary conditions and letting the model's equations shape its dynamical state for an adequate time, allow to reproduce the evolution in space and time of the ocean circulation. To simulate the MOW bottom current activity, we use a regional ocean model (Med-currents) that covers the whole Mediterranean Sea and also extends into the Atlantic (Fig. 2.2), in order to better resolve the water exchanges with the Atlantic Ocean through the Strait of Gibraltar. The data assimilation system is the 3DVAR scheme developed by Dobricic and Pinardi (2008) and modified by Storto et al. (2015), while the physical base of this model is the Mediterranean Forecasting System, MFS (Pinardi et al., 2003, Pinardi and Coppini, 2010, Tonani et al., 2014).

The oceanic equations of motion of Med-currents model are solved by an Ocean General Circulation Model (OGCM) based on NEMO (Nucleus for European Modelling of the Ocean) version 3.6 (Madec et al., 2016).

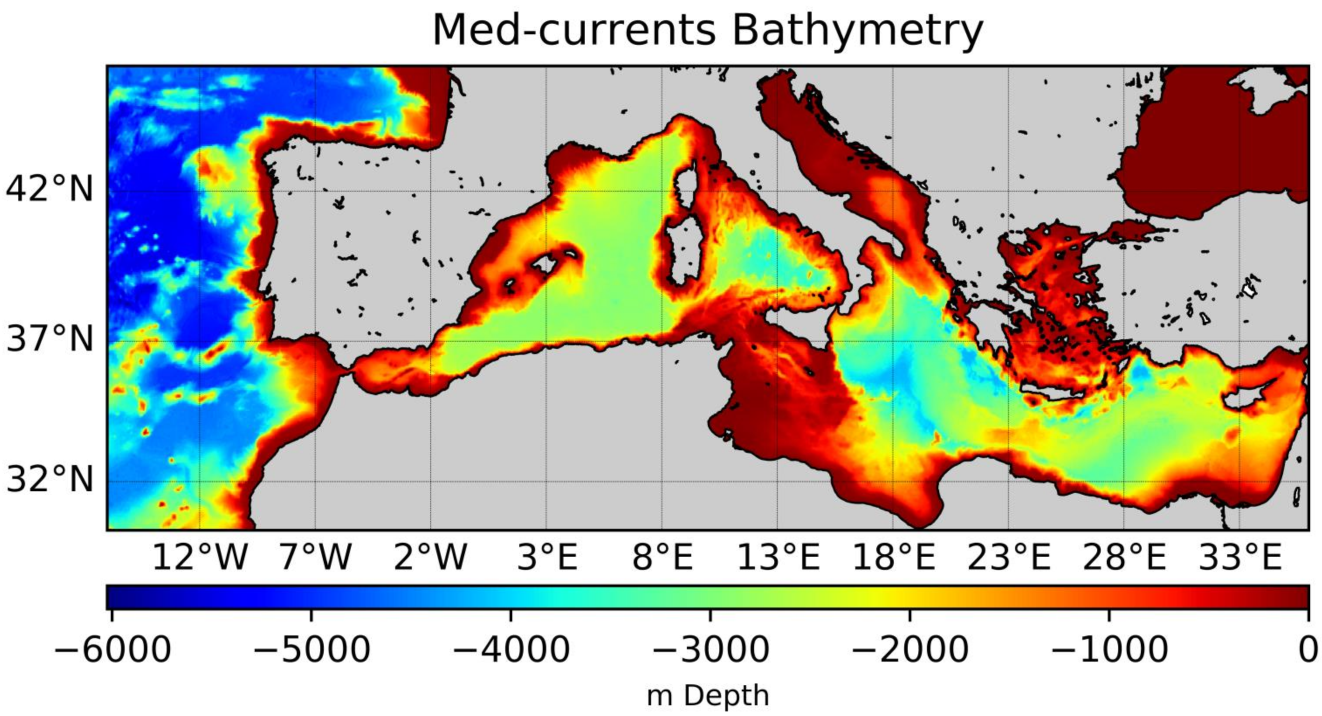

Figure 2.2 Med-currents domain and bathymetry.

NEMO has been implemented in the Mediterranean at 1/24° x 1/24° horizontal resolution (≈ 4 km) and 141 unevenly spaced vertical levels (Clementi et al., 2017a) with time step of 300 seconds. The structure of the horizontal and verical indexing of the latitude/longitude grid of Med-current ocean model are show in figure 2.3. The horizontal viscosity and diffusion operators are assumed to be bi-laplacian with coefficients of 5×109 ms-1 and 3×109 ms-1 for viscosity and diffusion, respectively (Madec and NEMO team, 2008).

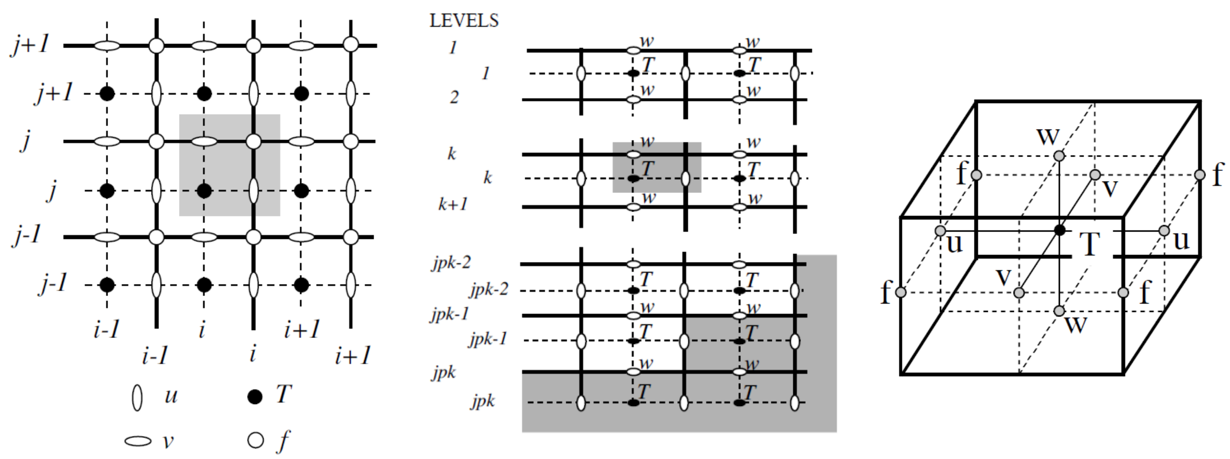

Figure 2.3 Structure and indexing of the grid used by Med-currents ocean model (same of NEMO); on the left, horizontal grid, in the center, vertical grid and on the right, arrangement of variables in one cell. Where the dashed area indicates the cell in which variables contained in arrays have the same i (longitude) and j (latitude) indices. u: zonal velocity component; T: tracer; v: meridional velocity component. Modified from Madec and NEMO team, 2008.

The model's atmospheric forcing is the 3-hours forecast NWP (*Numerical Weather Predictions*) from the European Centre for Medium-Range Weather Forecasts (ECMWF) and includes precipitations. Rivers runoff are parametrized on the basis of the Global Runoff Data Centre dataset (Fekete et al., 1999) for Po, Ebro, Nile, Rhone and for the Adriatic rivers (Vjosë, Seman) from the dataset of Raicich et al. (1996). The Med-currents model has a very good capability to reproduce the termohaline propriety of the main water masses of the study area (Fig. 2.4).

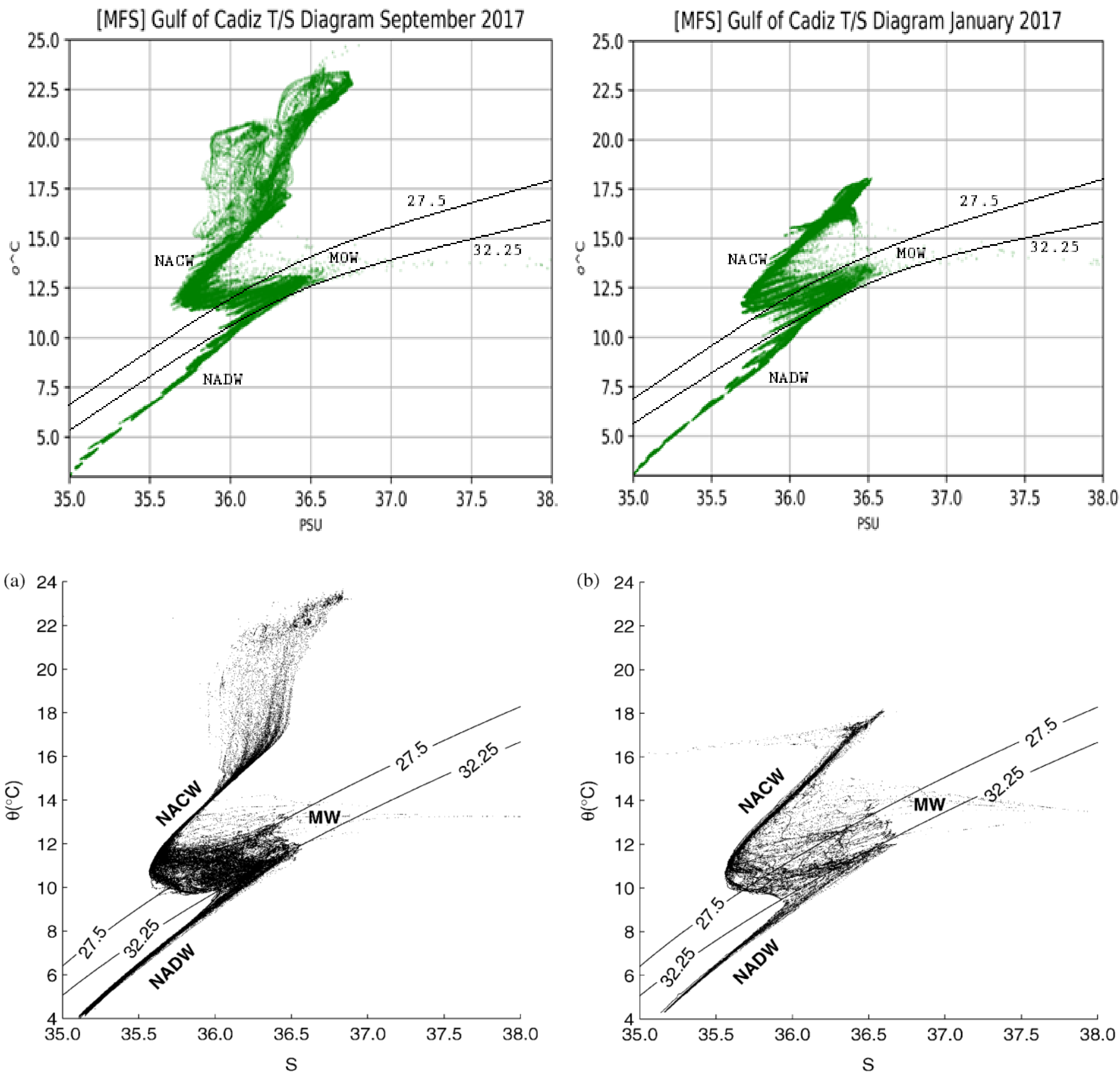

Figure 2.4 Temperature/Salinity multiplots of Gulf of Cadiz in September and January 2017 from the Mediterranean Forecasting system (MFS) compared with those of the CTD data collected (a) in September 1997, aboard N/O Thalassa and (b) in January 1998, aboard B/O Cornide de Saavedra. Lines of constant potential density anomaly γ_θ= 27,50 and γ_l= 32,25 kgm^{-3} (γ_l---potential density anomaly referred to the 1000-dbar level) are shown within the density range of the MW (from Ambar et al., 2002). The field of the main water masses (NACW, MW and NADW, see chapter 1) is indicated.

T/S diagrams (Temperature/Salinity) for the whole Gulf of Cadiz water for summer (September) and winter (January) conditions (Fig. 2.4) are in agreement with the observed data (Ambar et al., 2002).

The model's bathymetry (Fig. 2.2) is derived from the GEBCO 30arc-second grid, filtered (using a Shapiro filter) and manually modified in critical areas such as: islands along the Eastern Adriatic coasts, Gibraltar and Messina straits, Atlantic box edge, etc. to solve the hydrodynamics of the model's bottom layer. Figure 2.5 shows the Med-currents/MFS bathymetry (a) compared with the high-resolution multibeam SWIM compilation (b). In order to estimate the distribution of the bathymetry model's error (Fig. 2.5c), the SWIM multibeam bathymetric data (spatial resolution: 250 x 250 m) have been interpolated on the model's grid (spatial resolution: ≈ 4 x 4 km) and subtracted from the model's bathymetry. Fig. 2.5c shows the obtained difference (error map).

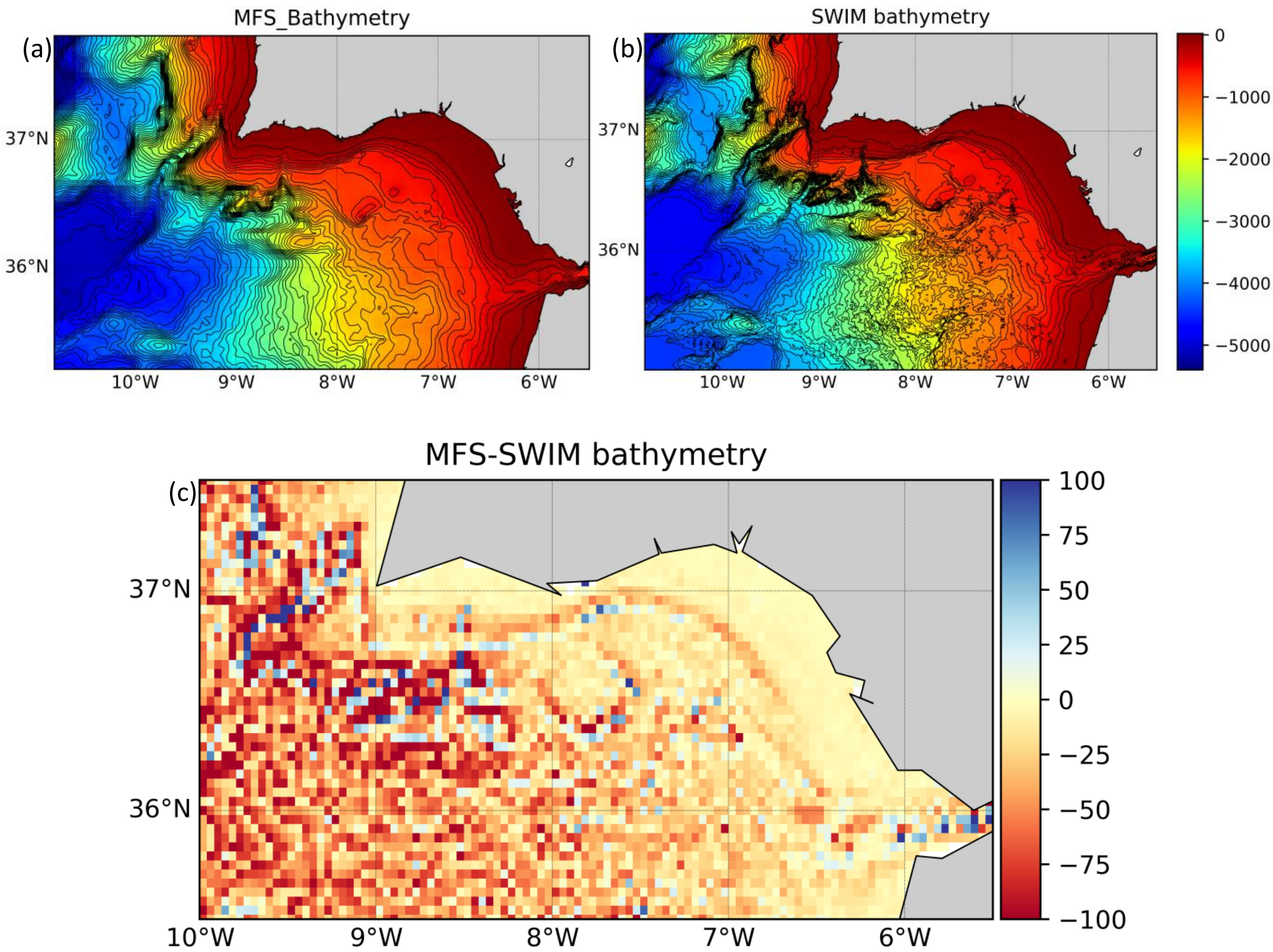

Figure 2.5 a) Med-currents bathymetry; **b)** the SWIM multibeam compilation from Zitellini et al. (2009). [Isobaths spacing: 100 m] **c)** Med-currents bathymetry error map (in meters).

It can be noted that the areas with higher error values are the deepest part of the seafloor, and those where the morphology is steep and uneven (i.e. submarine canyons). The difference between the Med-currents/MFS and SWIM bathymetry just occasionally reaches or exceeds 100 m error. In the areas interested by the CDS, the higher errors rarely exceed 20 m and are located in the deepest part of the contourite channels. The effects of the multi-dimensional linear filter on the GEBCO bathymetry (30arc-seconds grid) is heavy, but in our opinion it doesn't hardly impact the MOW bottom current simulations carried out in this study.

2.3 Bottom shear stress

As the scientific community recognizes, the bottom current velocity at the closest particle of the seafloor is 0 (Fig. 2.6). At the base of this statement there is the concept of viscosity that is strictly related to the shear stresses existing between the molecules of the fluid. In fact, the contact between a moving fluid and a surface ("wall"), generates changes in the flow movements inside the layer close to the wall, depending on the viscosity that stick the fluid itself to the wall. In fluid dynamics *"the law of the wall"*, firstly published by Theodore von Kármán (1930), states that the average velocity of a turbulent flow at a certain point is proportional to the logarithm of the distance from that point to the "wall", or the boundary of the fluid region. This law it's only theoretically applicable to part of the flow that is close to the wall (< 20% of the flow thickness, Fig. 2.6) called Bottom Boundary Layer (BBL), and provides a good method to estimate the shear stress generated between natural streams and planetary boundary, such as air ocean interface and sea bottom interface. The BBL (Fig. 2.6) extracts energy and momentum from the ocean currents and provides a mechanism for sediment resuspension and transport, generating also bedforms such as seabed ripples and dunes (Trowbridge and Lentz, 2018).

The shear stress (τ) produced by the motions of the fluid over the sea bottom interface is responsible for the erosion, transport and deposition of the previously deposited sediment grains (Guarnieri et al., 2014). Erosion occurs when the shear exceeds a certain critical stress value that characterize the sediments ($\tau_b > \tau_c$). On the other hand, deposition occurs when the shear is lower than the critical value for deposition ($\tau_b < \tau_c$).

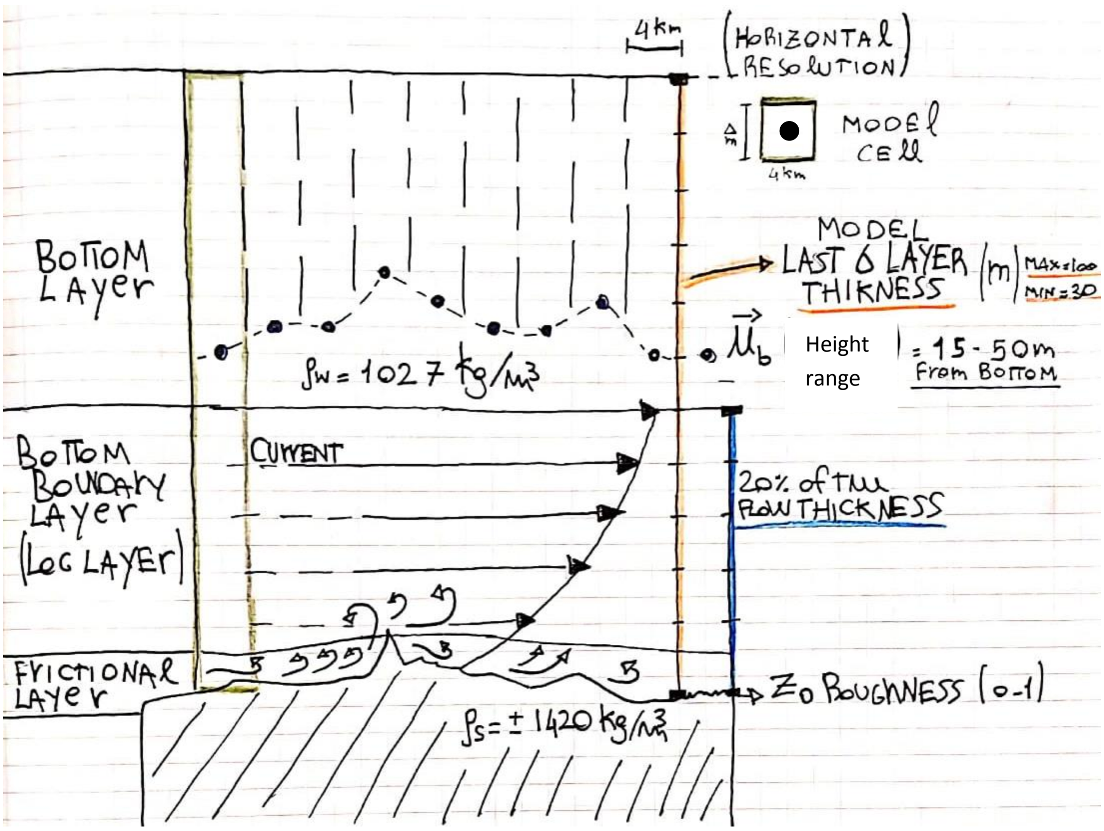

Figure 2.6 Bottom Boundary Layer scheme, with indications of seabed and water density ($\boldsymbol{\rho_s}, \boldsymbol{\rho_w}$). The "last $\boldsymbol{\sigma}$ layer" of the model (ranging in thickness from 30 to 100 m) is represented by the orange bar; black dots represent the location of the fields inside the bottom model cells (represented by the half of "last $\boldsymbol{\sigma}$ layer" and ranging from 15 to 50 m of height from bottom), U_b = bottom current speed module (computed using the zonal and meridional velocity values from the Med-currents ocean model), Z_0 = roughness.

The bottom shear stress (τ_b[N/m^2]) acting over the Gulf of Cadiz seafloor was calculated following the "*law of the wall*" set of equations:

$$\tau_{x=}\rho_w C_D\,|U_b|\,u_b \qquad \tau_{y=}\rho_w C_D|U_b|\,v_b \tag{1}$$

$$\tau_{b=}\sqrt{\tau_x{}^2\,\tau_y{}^2}$$

where the water density (ρ_w) is 1027 Kgm^{-3} (for the Mediterranean water), U_b is the bottom current speed module, u_b and v_b are the zonal and meridional component of the bottom velocity (ms^{-1}) respectively. The special power of the bottom shear stress equation (1) is that it links the bottom current speed with the seafloor characteristics that directly involve the Bottom Boundary Layer (BBL) dynamics (Fig. 2.6). The Drag coefficient (C_D), in fact, describes the BBL dynamics and physically links the current speed height from the bathymetry with the seabed asperity; it is estimated as follows:

$$C_D = \left[K/\ln\left(\frac{z}{z_0}\right)\right] \qquad (2)$$

Where K is the Von Karman constant, empirically determined to be 0,4 (dimensionless), z is the elevation of the speed value from bottom, represented by half height of the last σ layer of the model (last σ layer/2; Fig. 2.6). In the study area this parameter has been estimated as having a range varying from 15 to 50 m (Fig. 2.7).

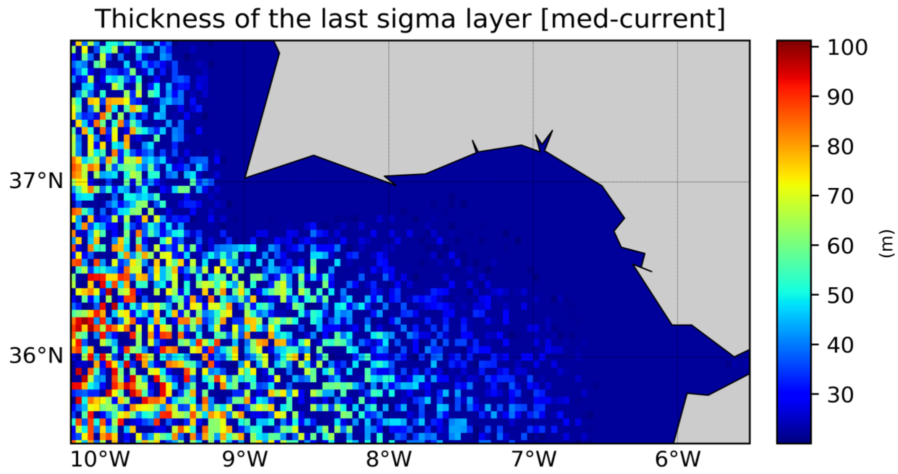

Figure 2.7 Thickness of the last ***σ*** layer of the Med-currents model.

Z_0 represents the roughness; it is a local elevation index that quantify the terrain asperity. It's also called "relative Topographic Position Index" (TPI; Jenness, 2002). Bathymetric position of each pixel is identified with respect to its local neighborhood, thus its "relative" position. The determination of Z_0 is difficult because it depends on the nature of the boundary as, for example, if the seabed is characterized by erodible sediments, basement highs and bedrock outcrops modelled by strong flows. Therefore, an established general relationship between the physical characteristic of the boundary and the hydrodynamic roughness parameter Z_0 does not exist for geophysical flows (Trowbridge and Lentz, 2018). Thus, this parameter can occupy a wide range of scales involving the scale of particles through bedforms such as ripples and dune, to seamount scale. Considering the thickness and the extension of the Mediterranean Outflow current, values of roughness in the study area have been calculated on a "wide scale".

As previously indicated, the bathymetric data have a spatial resolution of 250 m x 250 m (Fig. 2.1 and 2.8a). For this reason, we estimate a value for the roughness for each 18 x 18 cell grid by taking the MEAN, MAX and MIN DEM (Fig. 2.8 b, c, d) of the SWIM bathymetry, in order to have the same spatial resolution of the model (≈ 4 km x 4 km) and to better interpolate the field on the regular longitude-latitude grid (Fig. 2.9). Then, Z_0 has been calculated normalizing the MEAN, MAX and MIN DEM:

$$\left(\frac{DEM_{mean}-DEM_{min}}{DEM_{max}-DEM_{min}}\right) = Z_0(Roughness) \qquad (3)$$

obtaining a positive value between 0-1 (Fig. 2.9). This parameter thus represents the "relative bathymetry position" and describes the seabed unevenness.

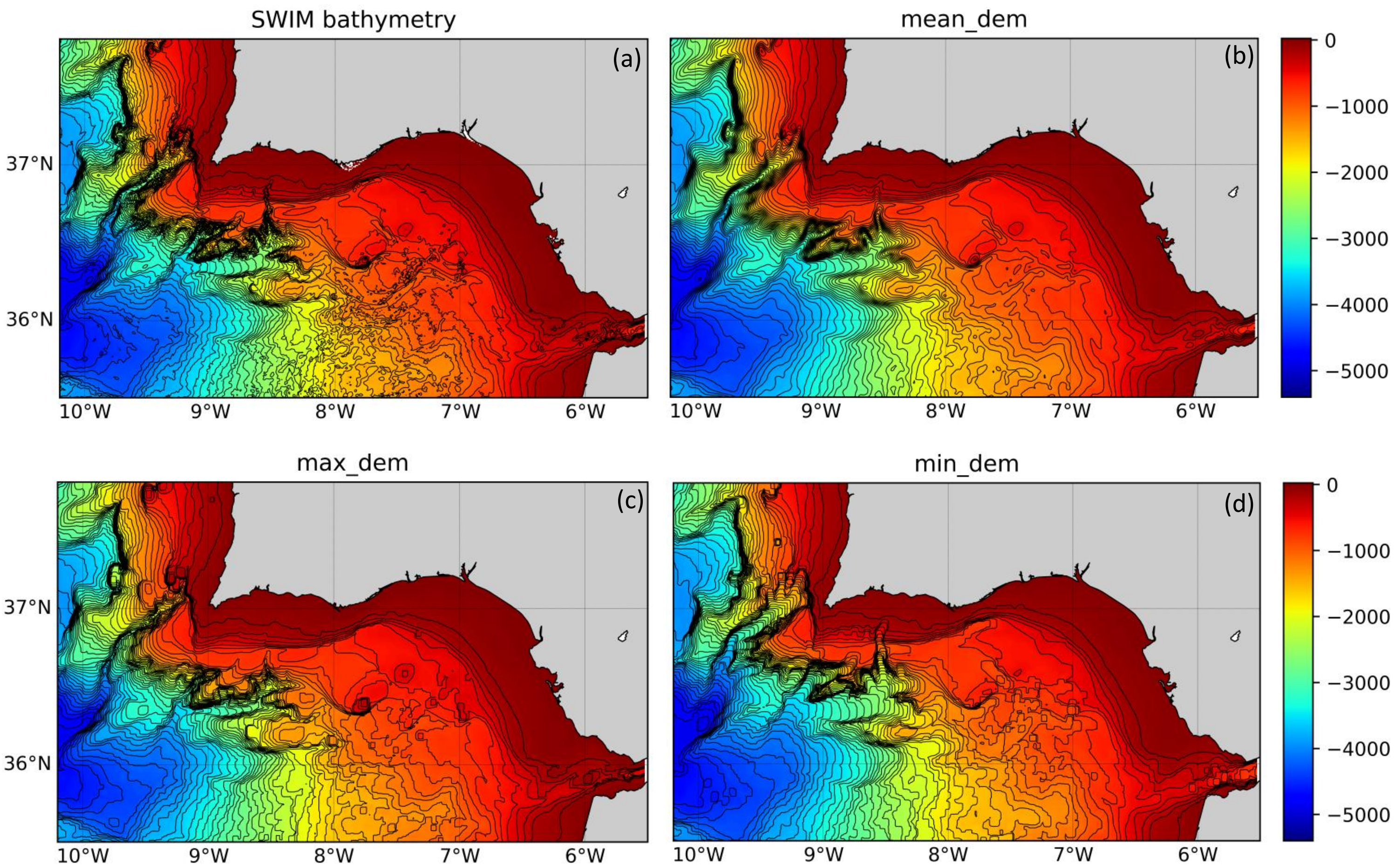

Figure 2.8 **a)** original DEM from the SWIM multibeam compilation (Zitellini et al., 2009); **b)** averaged smoothed DEM; **c)** maximum DEM; **d)** minimum DEM.

The choice of this method to compute the roughness differs from that adopted by various authors (i.e. Grant and Madsen, 1979,1986; Lou and Schwab, 2000) which also consider the median grain size and the dominant ripple wavelength and height for this estimate.

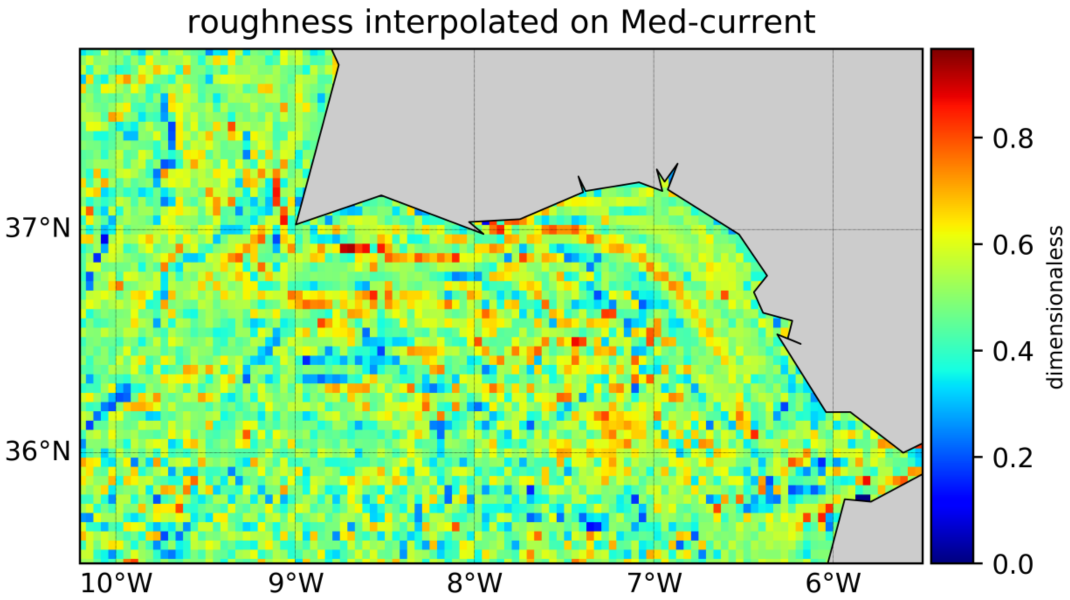

Figure 2.9 Roughness values calculated as "relative bathymetric position" and interpolated on the Med-currents ocean model grid (horizontal spacing = 4 x 4 km).

In figure 2.10 the relations between the variables that compose the bottom stress equations (1) and (2) can be appreciated. Obviously, the Drag coefficient (C_d) increases when the roughness (Z_0) is high, while it decreases by growing of the last σ layer thickness, both with a logarithmic trend as described by the equations (2). Also, the bottom shear stress increases with a logarithmic trend by increasing the bottom current speed. Conversely, between bottom stress and C_d there isn't any linear trend, but it can be noted that the highest stresses have a drag coefficient ranging from 0.008 to 0.018.

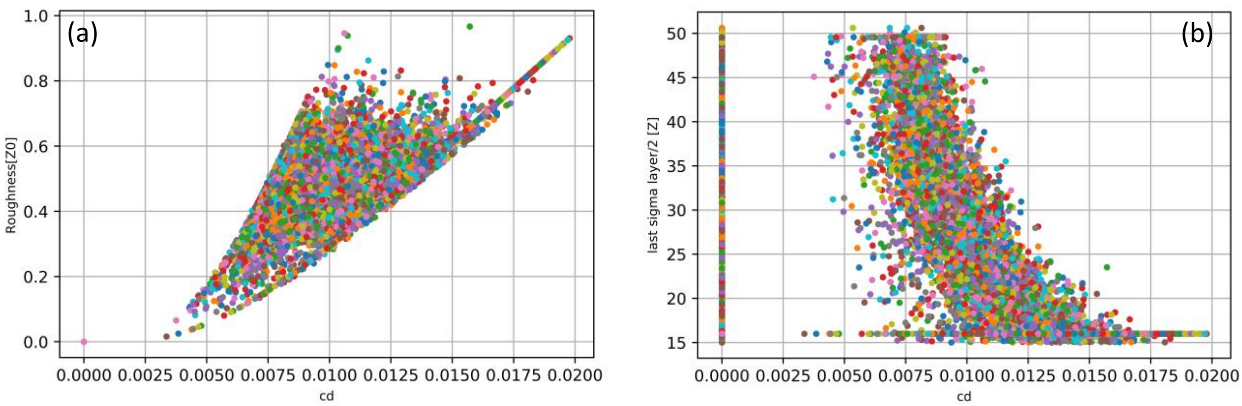

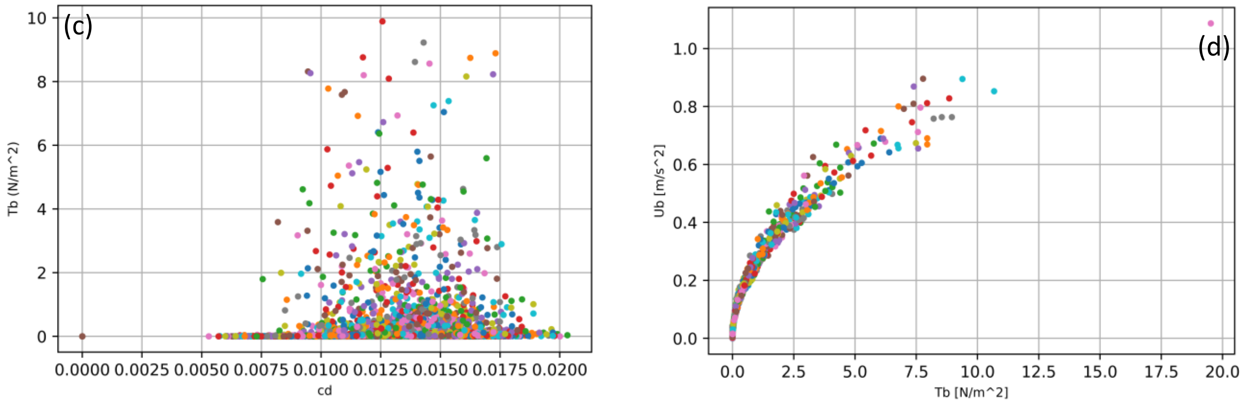

Figure 2.10 Multiplot of the "law of the wall equations" variables : **a)** y= Roughness, x= Drag coefficient; **b**) y= last sigma layer thickness, x= Drag coefficient; **c)** y= Drag coefficient, x= Bottom shear stress; **d)** y=Bottom current speed, x=bottom shear stress.

2.4 Critical bed shear stress

The calculation of the erosion and deposition threshold for the contouritic deposits in the study areas requires the determination of a mean bottom critical shear stress for the Gulf of Cadiz seafloor. As the roughness, also the critical shear stress (τ_c[N/m^2]) is highly variable on the seafloor and principally depends on the sediment grain size and on the degree of cohesion and consolidation of the deposits.

Considering a median grain size of non-cohesive sediments, the critical shear stress (τ_c[N/m^2]) can be estimated as (U.S. Geological Survey, see Berenbrock and Tranmer, 2008):

$$\tau_c = \theta^*(S-1)\rho_w g d_{50} \qquad (4)$$

in which, θ^* is the Shield parameter for a given particle size (dimensionless), used to calculate the initiation of motion of sediment in a fluid flow and derived by the Shield's curve (Shield, 1936). S is the specific gravity of the particles and is calculated as the dimensionless ratio of specific weight of sediments (γ_s) to the specific weight of water (γ_w). ρ_w is the density of the water in Kg/m^3, g is the gravitational acceleration constant in m/s^2 and d_{50} is the median grains size in m.

In our scenario, the contouritic deposits of the CDS can be considered as a mixture of fine-very fine sand (from 0,063 to 0,25 mm of diameter) with a variable percentage of mud (< 0,063 mm of diameter), the latter increasing in the distal area far from the Gibraltar Strait (see chapter 1.4; Hernandez Molina et al., 2016). The percentage of mud in turn determines the degree of cohesion of the sediments, while the settling time defines the deposit consolidation.

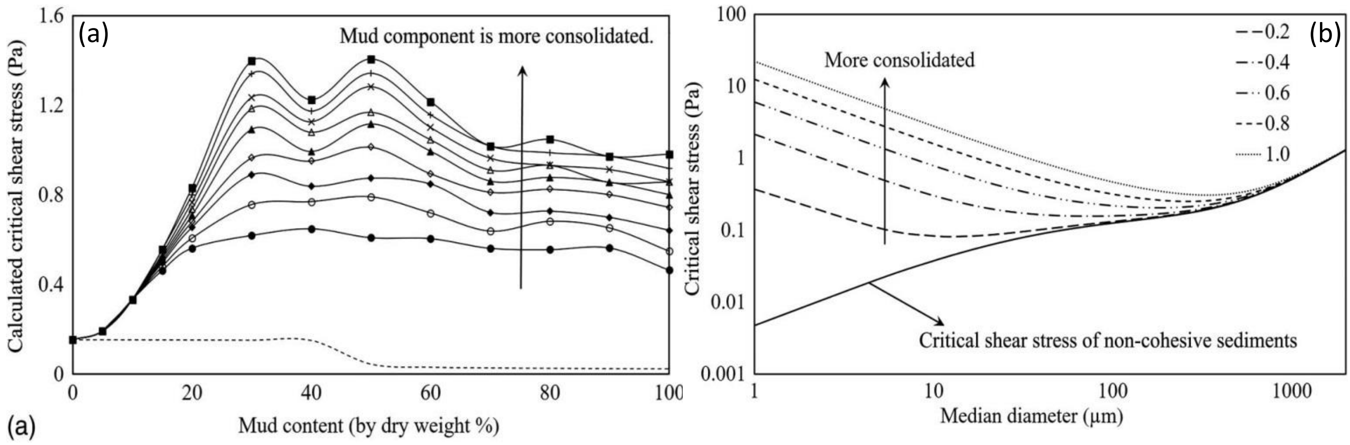

Figure 2.11 a) Critical shear stresses curves calculated with the % of mud and **b)** with respect to a median grain diameter. The figure indicates the consolidation/cohesion increment also controlling erosion and deposition. Modified from Dake Chen et al. (2018).

In recent laboratory studies, Dake Chen et al. (2018) found how critical stress increments, in agreement with an increase in the percentage of mud and the degree of consolidation. The plots in Figure 2.11 show several key concepts about the relationships between the critical shear stress and the % of mud, median grain size and the degree of consolidation of the deposits. Overall, the required stresses for inducing erosion grows with increasing the particle size diameter. However, for cohesive sediment, mostly clay but also silt, the erosion stress threshold increases with decreasing grain size, as the cohesive forces are relatively more and more important when the particles get smaller, as it is shown aslo by the Hjulström curve (Hjulström , 1932; Fig. 2.12). On the other hand, deposition occurs when the bottom stress is lower than the critical stress, determining the end of sediment transport, and when the suspended sediment load of the current reaches his characteristic settling velocity, For example, following this diagram (Fig. 2.12), the settling velocity for mud with a diameter of 0,03 mm is about 0,4 cm/s while for fine sand with 0,2 mm of diameter it is about 1,5 cm/s.

Deposition and erosion are thus primarily the consequence of spatial and temporal changes in bottom shear stress. On the base of these considerations, we decided to take into account, for the contouritic deposits of the CDS, a range of erosion shear stresses for a sand-mud mixture, ranging from 0.4 to 1.2 pascal (N/m^2). In order to evaluate the long-term patterns of erosion and deposition in the study area, the maps of the simulated bottom shear stress averaged in the 2017 (Fig. 3.10 in the next section) and of the time % in the year 2017 that the current induces a bottom shear stress greater than the assumed critical bed shear stresses values (τ_{c1} = 0.4 pa, τ_{c2} = 0.8 pa, τ_{c3} = 1.2 pa, Fig. 3.12) were produced.

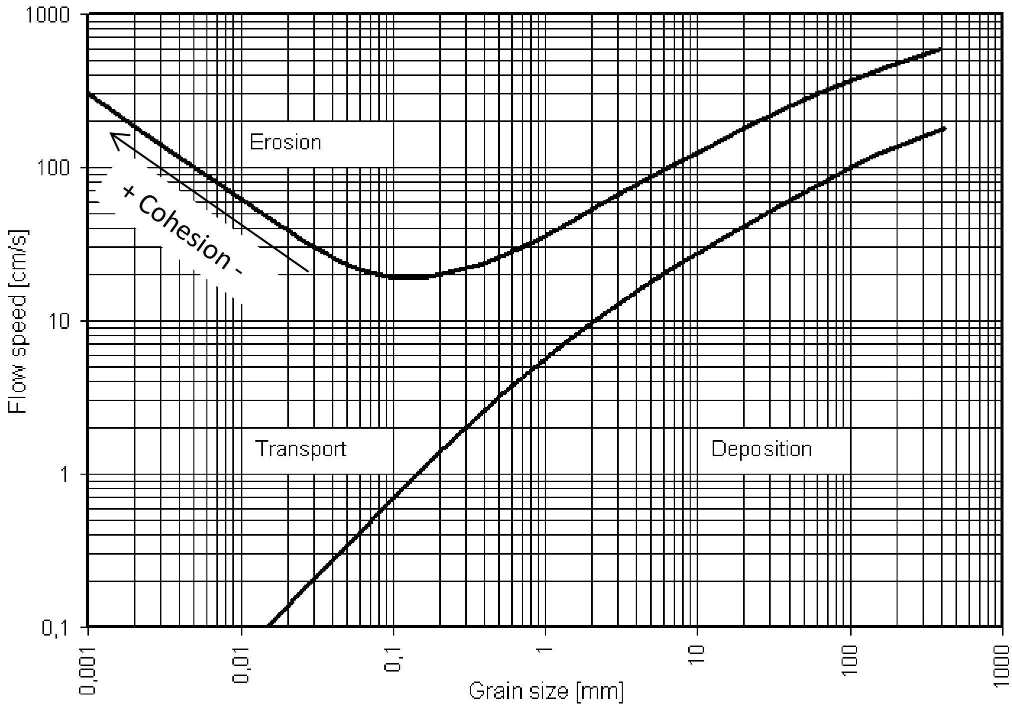

Figure 2.12 Hjulström curve (1932); upper curve = erosion threshold; lower curve = deposition threshold; in the middle = field of sediment transport.

Chapter 3 – Results

In this chapter, the results of simulations (made with the Med-currents model) of the bottom current pattern in the Gulf of Cadiz are described, and compared with the distributions of seabed morphologies and deposits in the CDS. The results of our attempts to estimate the bottom shear stress and critical bed shear stress will be also discussed.

3.1 Simulated Bottom Speed and Contourite distribution

The simulated annual bottom current speed (2017), plotted over the high-resolution SWIM bathymetry (Fig. 3.1) reveals the topographically-controlled spreading pattern of the MOW and suggests which seabed erosional features may be associated to the most energetic branches of the current.

The Mediterranean Outflow undercurrent pathway, exiting from the strait, enters in the Gulf of Cadiz with a West-South-West flow direction at depths of 250–300 m, then it is forced by the Coriolis effect towards North-West and flows parallel to contours all along the Gulf margin to Cabo San Vicente (Fig. 3.1). Its path and activity are reflected by computed bottom current metrics (i.e., mean and maximum annual bottom current speed and bottom current speed standard deviation). Between these simulated metrics there is an evident overlap: areas with the highest mean annual bottom current speed (Fig. 3.1a) also show the highest maximum annual speed (Fig. 3.1b) and standard deviation values (Fig. 3.1c). Areas with particularly intense bottom currents exhibit, in fact, a wider range of mean annual current speeds. The MOW bottom current velocity has a range from > 90 cm/s near the strait, to > 50 cm/s several kilometers downstream and drop off to < 20 cm/s in the North-Western part of the gulf and turning around Cabo San Vicente (Fig. 3.1). The highest standard deviation values of the bottom current speed were found in the “Channels and Ridges” sector (compare with Fig. 1.10), reaching a maximum value of about 40 cm/s (Fig. 3.1).

One key observation is that areas with the stronger simulated bottom current activity closely correspond to the main contourite channels and moat of the Gulf of Cadiz (see chapter 1), while over the drift accumulations areas the mean annual bottom currents speeds are generally less than 20 cm/s (Fig. 3.1).

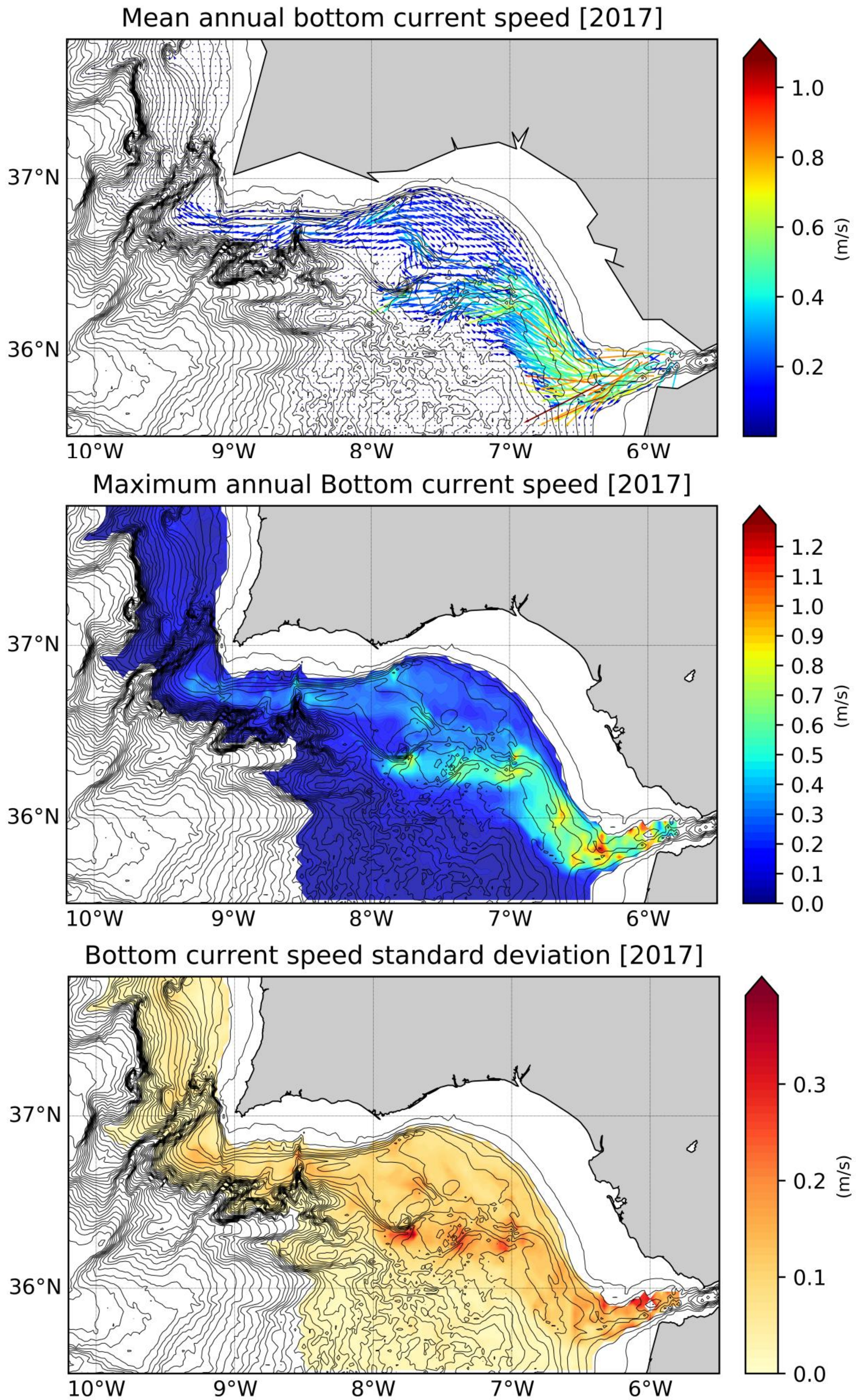

Figure 3.1 Simulated mean annual (a) and maximum annual (b) bottom current speed, and related standard deviation (c) on the bathymetry from "the SWIM multibeam compilation"(isobaths spacing = 100 m; Zitellini et al., 2009). Data refers to the year 2017.

A comparison has been made between specific sectors of the simulated current pattern and the bathymetric map in some key areas (Fig. 3.2).

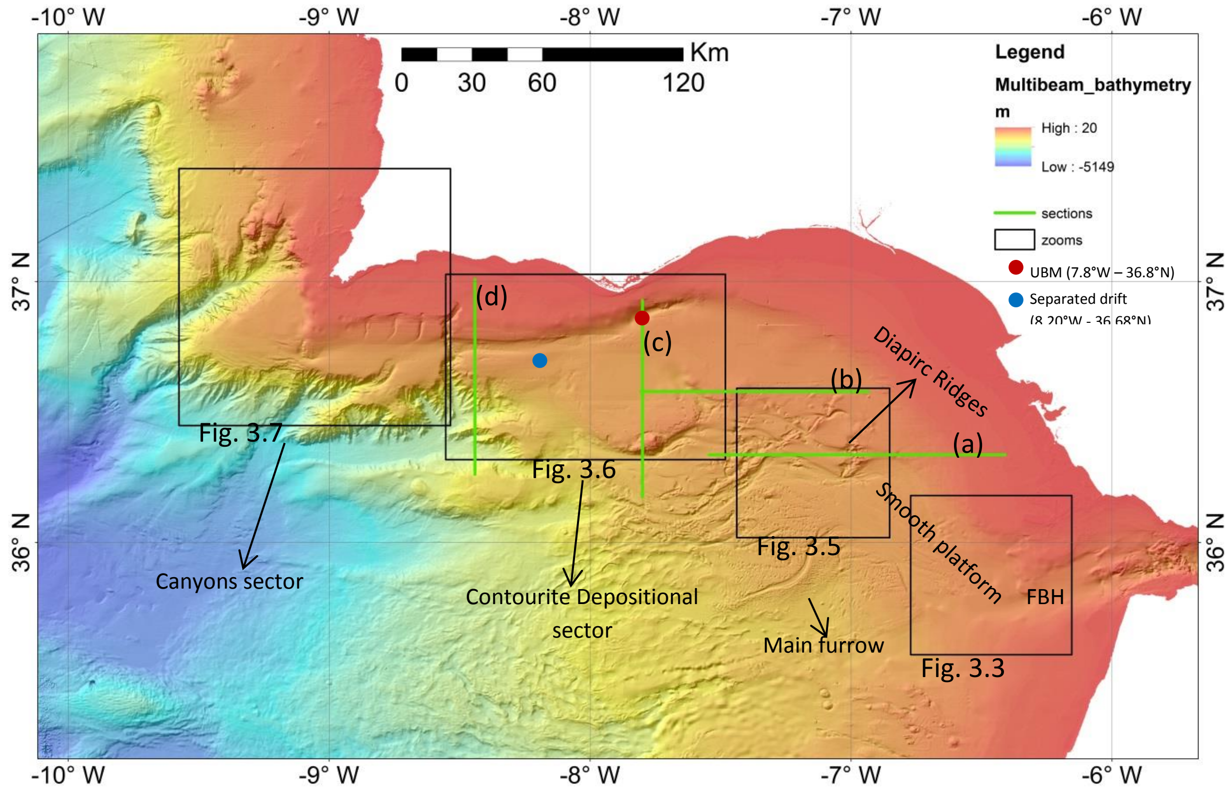

Figure 3.2 Location of areas of Figs. 3.3 to 3.7 and of sections of reconstructed currents speed (Fig. 3.4; green lines) on the bathymetric map from Zitellini et al. (2009). Reconstructed sections are located: (a) along latitude 36.3N (Fig. 3.4a), (b) along latitude 36.6N (Fig. 3.4b), (c) along longitude 7.8W (Fig. 3.4c), (d) along longitude 8.4W (Fig. 3.4d). FBH= First Basement High, UBM = Upper slope Basal Moat (red dot), Blue dot = Separated drift.

As already indicated, the MOW enters in the Gulf of Cadiz with a West-South-West flow direction at depths of 250–300 m (Fig. 3.3). Due to the vicinity of the strait, the most energetic simulated bottom current are located in correspondence of the "Proximal scour and sand ribbons" sector (Hernandez Molina et al., 2006; Fig. 1.10). In particular, the highest mean and maximum simulated bottom speed of the study area were found on the downstream flank of the First Basement High (FBH), at about 6.2°W/35.8°N, reaching an intensity up to 1.2 m/s (Fig. 3.3).

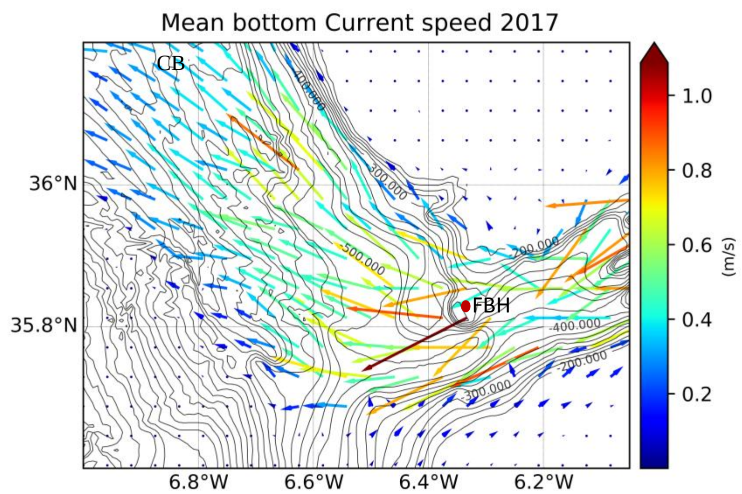

Figure 3.3 MOW reconstructed mean current speed and interaction with the First Basement High (FBH); CB = Cadiz basin.

In this location, the FBH splits the current into an upper and a lower core (Hernández-Molina et al., 2014). As it shown by the simulated bottom speed vectors over the FBH, the Mediterranean upper core (MU) takes a NW direction, while the Mediterranean lower core (ML) takes a WNW direction (chapter 1 and Fig. 3.3). These two cores have different densities, thus they flow at different depths (sections in Fig. 3.4) along the middle slope terraces (sections in Fig. 1.4, 1.6, and Fig. 3.4).

Passing the FBH, the MOW flows over a rock outcrop connected, further downstream, with a smooth platform characterized by erosional scour lineaments, NW-SE oriented, and sand dunes (Fig. 3.2 and 1.4). Here, it flows with general NW direction and with a range of mean current speed varying from 30-40 cm/s in the distal part, over the Cadiz basin (CB, Fig. 1.11 and 3.3), to 80-90 cm/s over the rock outcrop (see Fig. 1.10). Attached to this platform, the main NE-SW oriented furrow (Fig. 1.10 and 3.2) doesn't show particularly high values of simulated bottom current activity (Fig. 3.1), as expected.

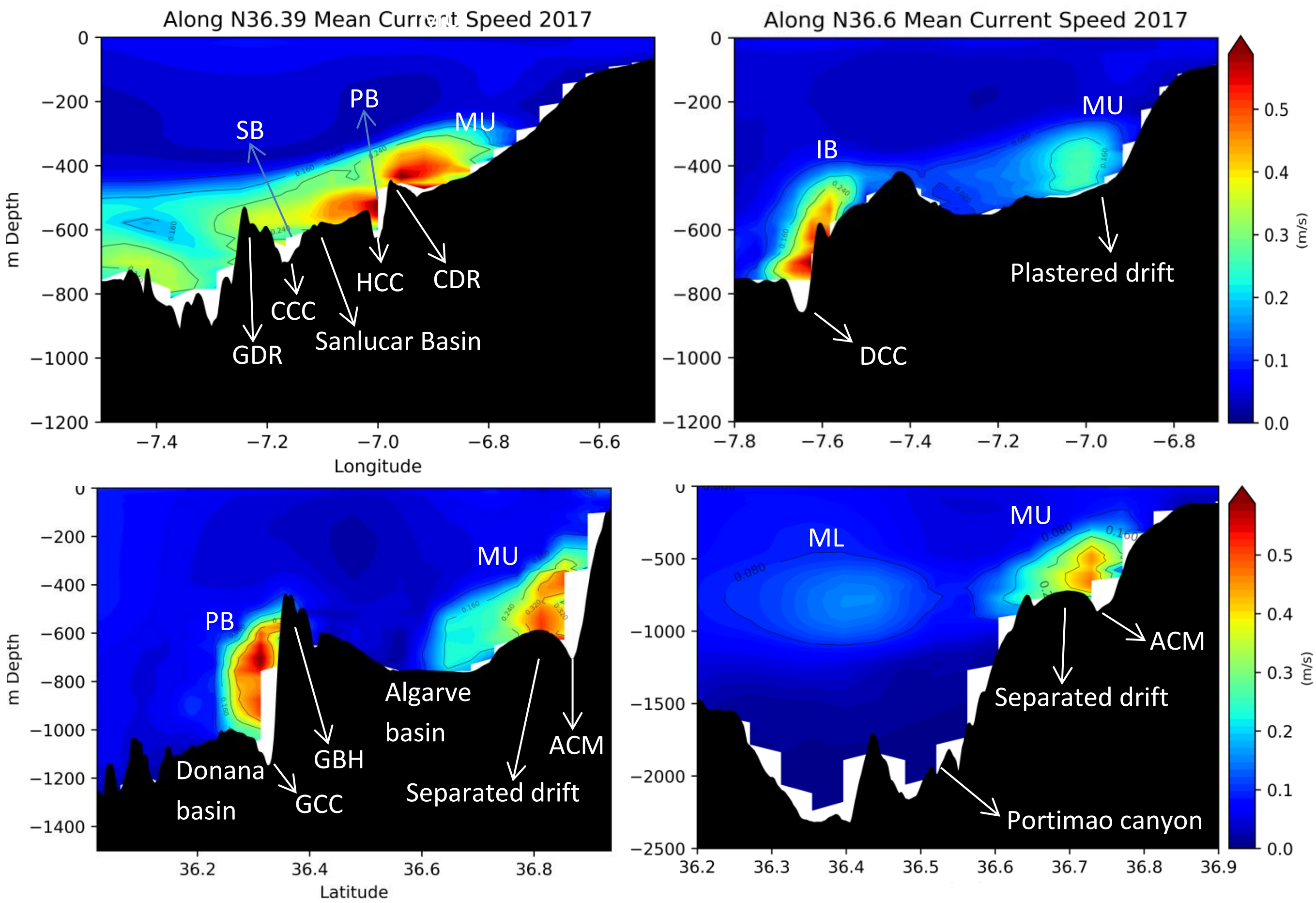

Figure 3.4 Reconstructed sections of current speed over bathymetry, from (a) to (d) in a downstream order. Mediterranean core and Branches: MU = Mediterranean upper core, ML = Mediterranean lower core, PB = Principal branch, IB = Intermediate branch, SB= southern branch; Channels and physiography features : ACM = Alvarez Cobral Moat, GCC = Guadalquivir contourite channel, DCC = Diego Cao contourite channel, HCC = Huelva contourite channel, CCC = Cadiz contourite channel, GBH = Guadalquivir basement high, CDR= Cadiz diapirc ridge, GDR = Gualquivir diapirc ridge.

At about 7°W, reaching the "Channels and ridges" sector (Fig. 1.10), the current impacts the Cadiz Diapiric Ridge and subsequently the Guadalquivir Diapiric Ridge (Fig. 3.5), that are perpendicular (NE-SW aligned) to the flow direction. In this sector, the higher computed bottom current speed (40 cm/s < U mean < 60 cm/s) are located at the entrance of the Cadiz, Worm and especially the Huelva contourite channels that cross cut the diapiric ridges, flowing at a depth ranging from 600 m to 900 m (Fig. 3.5). In this location, the ML splits in three branches (Hernandez-Molina et al., 2006; IB, PB and SB in Fig. 1.9) while the MU keep flowing intact, at the base of the upper slope. The simulated speed vectors clearly show the different directions of the three branches (Fig. 3.5). The Intermediate Branch (IB) and the Principal Branch (PB) take the direction of the Worms and Huelva contourite channels axes respectively, while the Cadiz contourite channel steers the Southern Branch (SB, Fig. 3.5 and profile in Fig. 3.4a) in a WSW direction. Located in the central "Channels and ridge" sector, the Sanlucar and Doñana basins (SB, DB, Fig. 1.11, 3.5 and 3.6) correspond to abnormally high values of simulated mean bottom current speed for deposition. Current speed, in fact, especially in the middle of the diapiric ridges, reaches an intensity of 30 cm/s with a maximum of about 50 cm/s (Fig. 3.5). Further West, the Guadalquivir channel (GCC) captures the Principal Branch (PB) that represents the major part of the ML water-mass (Fig. 3.6 and profile in Fig. 3.4c).

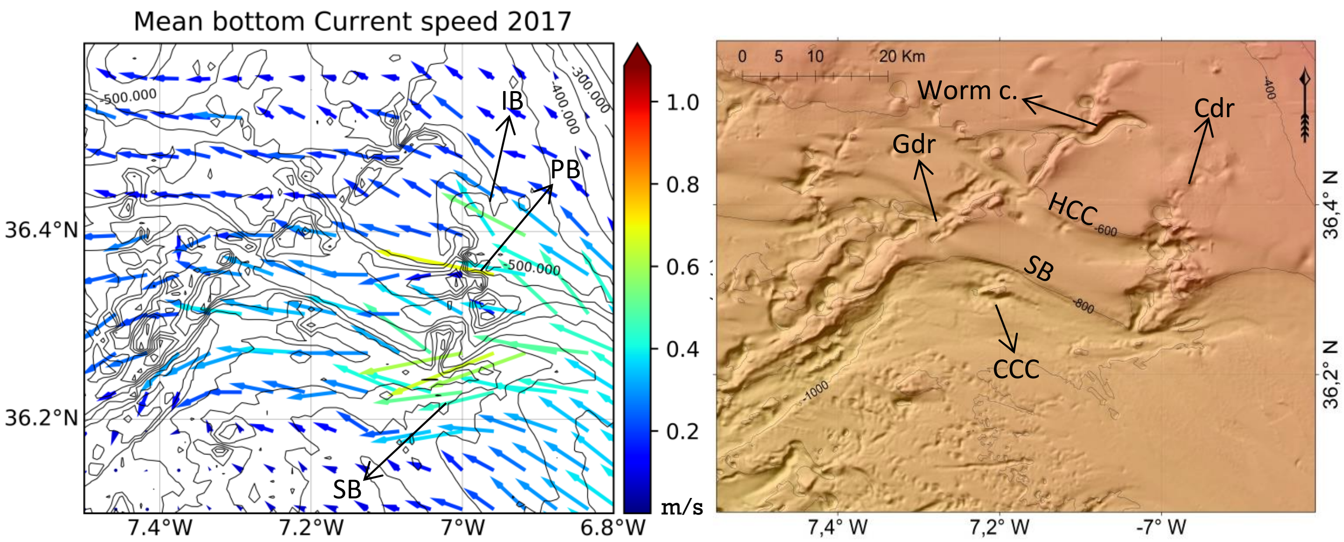

Figure 3.5 Cadiz and Gualquivir diapiric ridges (Cdr, Gdr) and interaction with 3 branches of the MOW lower core. Channels and Basins: HCC = Hulva contourite channel, CCC = Cadiz contourite channel, SB = Sanlucar basin and Worm contourite channel; MOW LOWER CORE branches: IB = Intermediate Branch, PB = Principal branch, SB = Southern Branch.

In this channel and especially at the southern base of the Guadalquivir Bank (at about 7.8W/36.3N), the highest bottom current speed standard deviation of the study area is observed, also highlighted by the strong difference between the maximum and mean speed intensity (Umean= 50 cm/s, Umax= 90 cm/s; Fig. 3.1 and profile in Fig. 3.4c). Entering in the “Contourite depositional” sector (Fig. 3.2 and 3.6, see also Fig. 1.10) vigorous bottom current activity is found at the exit of the Diego Cao contourite channel (DCC), where the IB reaches velocities up to 40 cm/s, almost flowing upslope (Fig. 3.6 and profile in Fig. 3.4b) and in correspondence of the erosional feature located at the base of the upper slope (Upper slope Basal Moat, UBM), in the SouthEast area offshore Faro lagoon (Fig. 3.6).

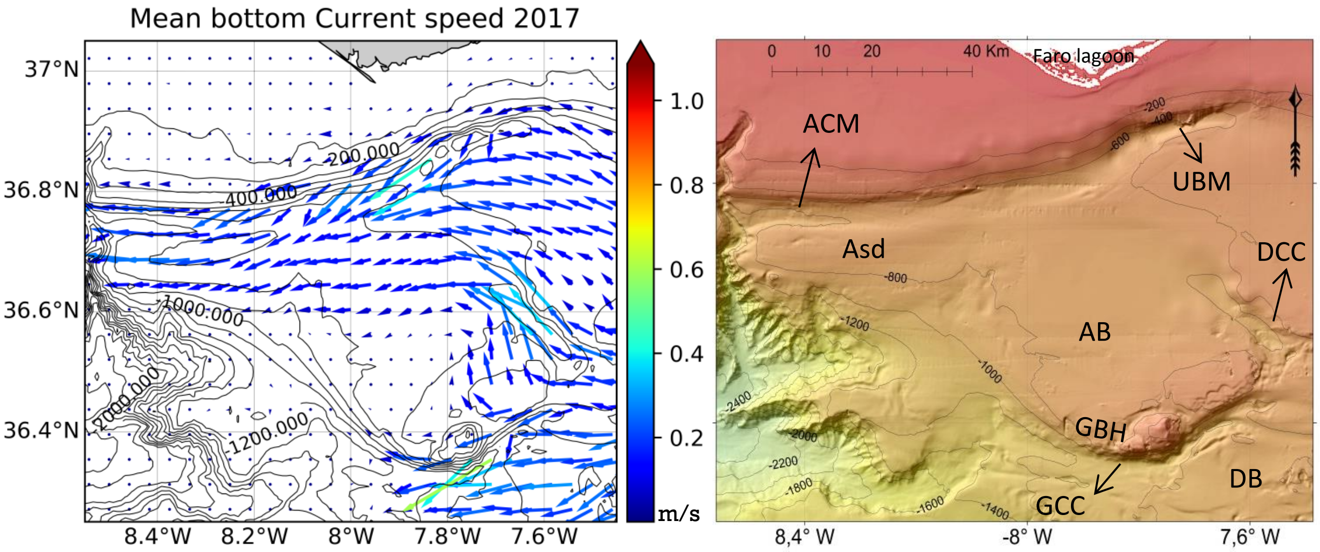

Figure 3.6 Bottom current speed in the Main contourite depositional sector, simulation averaged on 2017. Depositional basin: AB = Algarve basin, DB= Doñana basin; Moat and channels: ACM = Alvarez cabral moat, UBM = Upper slope basal moat, DCC = Diego Cao contourite channel, GCC = Gualquivir contourite channel; GBH = Gualquivir basement high, Asd = Alvarez Cabral separated drift.

Moving from the Diego Cao channel, the IB of the Mediterranean lower core is steered by the front of the slope towards the West (Fig. 3.6) and starts flowing over the central part of the Algarve basin with about 10 cm/s of speed beside the MU that, coming from the UBM, starts flowing in the Alvarez Cabral moat (ACM), accelerating as it gets closer to the Portimao canyon (Fig. 3.6).

In the “Submarine canyon” sector (Fig. 3.7), the Bottom current activity decreases notably (Fig. 3.2). This area does not show any incised erosional features created by the MOW and the mean simulated bottom current speed rarely exceed 20 cm/s over the Portimao, Lagos and Sagres drift (Fig. 3.7). Finally, the part of the current with the thermohaline and speed characteristics needed to jump the San Vicente canyon reaches the western Algarve margin and starts flowing on the Alentejo basin (AIB, Fig. 3.7), where the simulated mean annual bottom current speed hardly reaches 10 cm/s with a maximum of about 15 cm/s (Fig. 3.1).

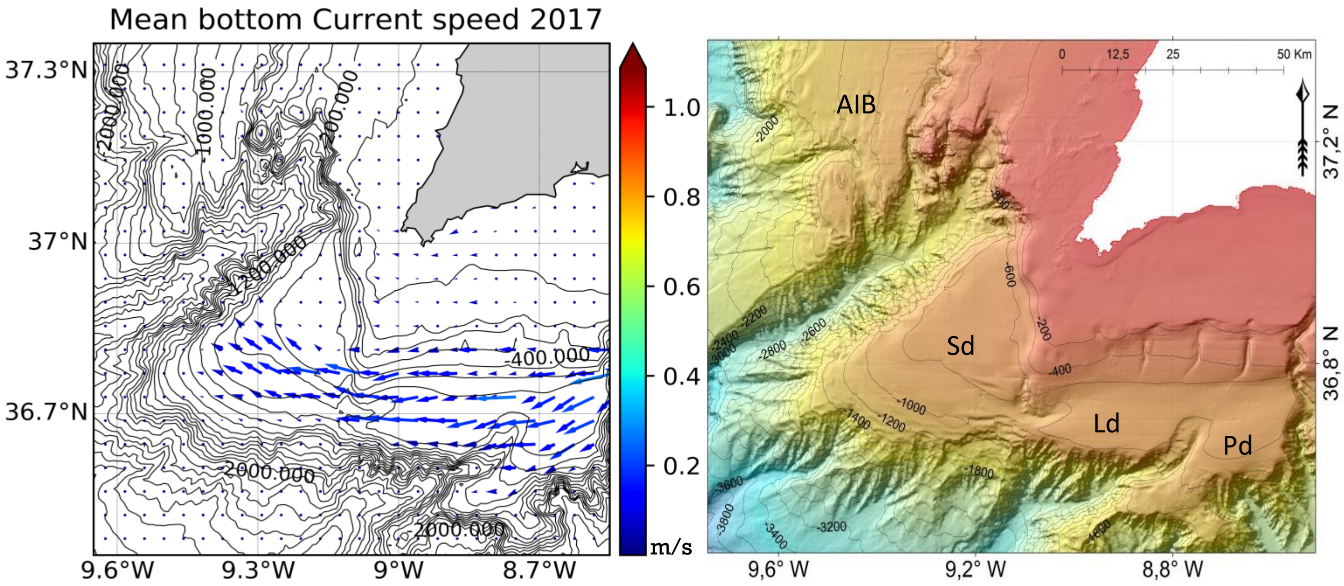

Figure 3.7 Bottom current speed in the Submarine canyon sector, simulation averaged on 2017. Basin and drifts : Pd = Portimao drift, Ld = Lagos drift, Sd= Sagres drift, AIB = Alentejo basin.

3.3 Simulated bottom shear stress and critical bed shear stress

One of the most important physical quantity for contourite drift formation is the bottom shear stress, which drives the mechanism of resuspension/deposition of the sediment grains. Naturally, there is a clear correspondence between the bottom current speed and the bottom shear stress, clear hint that the driving forcing for resuspension is the bottom current action, in accordance with all the literature in this area (Llave et al., 2002; Mulder et al., 2003; Stow et al., 2009; F. J. Hernández-Molina et al., 2006, 2011,2016; among others).

Through the approach described in section 2.3, where we indicate the equations adopted for calculating the bottom shear stress (1 and 2), we needed to estimate the Roughness in the study area. Taking in account that the Mediterranean current is a geostrophic flow, governed mainly by gravity (pressure gradient) and Coriolis force, when it reach bathymetric lows, its flowing is facilitated, while reaching bathymetric highs the bottom friction effect on the flow increments (Fig. 3.8).

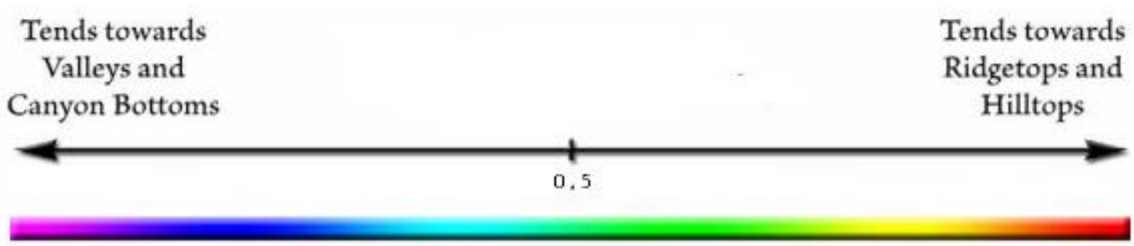

Figure 3.8 Roughness values and related morphological context; modified from Jenness, (2002).

Therefore, the roughness (Z0) of the Gulf of Cadiz seafloor, it's been calculated as " relative bathymetric position" (Jenness, 2002; Fig. 3.9). This parameter (Z0) in the equation (2) works as a "calibrator of the speed height (Z)": for example, for high roughness values, the ratio between Z and Z_0 decrease and vice versa, influencing the final shear stress produced.

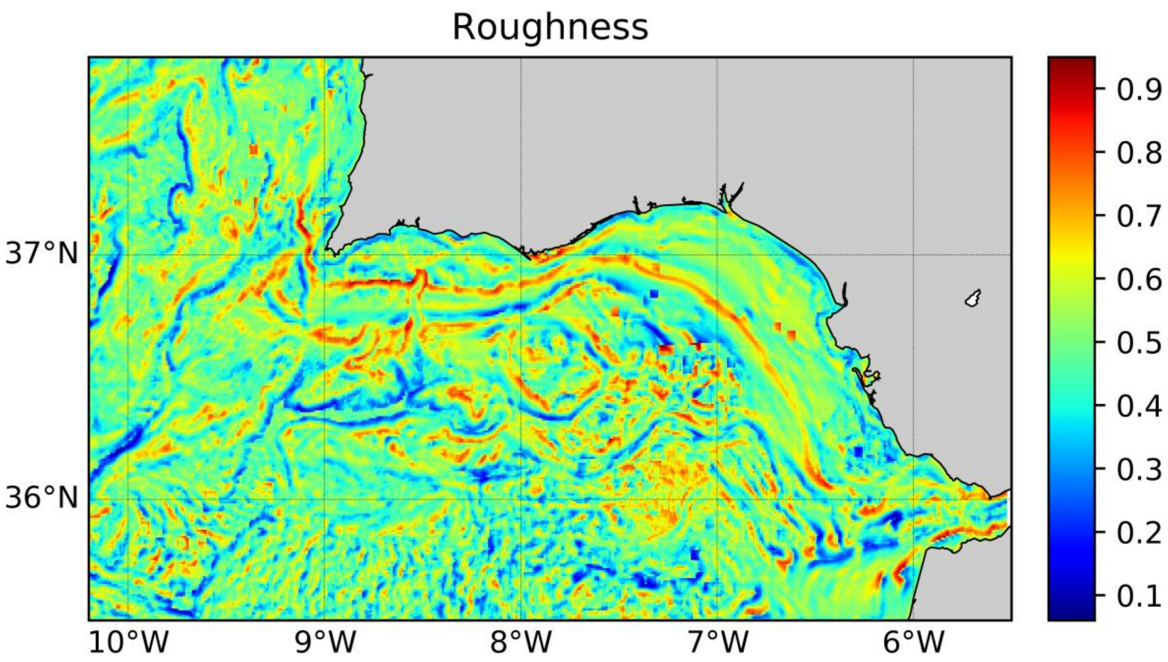

Figure 3.9 Seafloor roughness of the Gulf of Cadiz computed as " relative bathymetric position".

The average bottom shear stress simulated for year 2017 (Fig. 3.10) significantly matches with the erosional and depositional features of the study area. Overall, it shows the higher stresses (> 5 N/m^2) localized inside the erosional channels and moats and over the "Proximal scour and sand ribbons" sector, reflecting the mean annual bottom current speed spatial distributions (Fig. 3.2). On the other hand, over the depositional drifts just sporadically the bottom shear stress value exceeds 1 N/m^2.

The highest shear stress value of the study area is found on the FBH southern flank reaching about 18 N/m^2, and is confined just over this feature. Another very high shear stress spot is located at the intersection between the rock outcrop and the sand dune - ribbons fields, exceeding 10 N/m^2. For a better representation of the bottom shear stress pattern in a 0-9 N/m^2 scale, these two spots have been cut off from the plot, thus appear as no data value (white spots in Fig. 3.10). In the "proximal scour and sand ribbons" sector, the simulated bottom shear stress is particularly high over the rock outcrop, then it decreases over the Cadiz basin and then increase again when the current collide into the diapiric ridges.

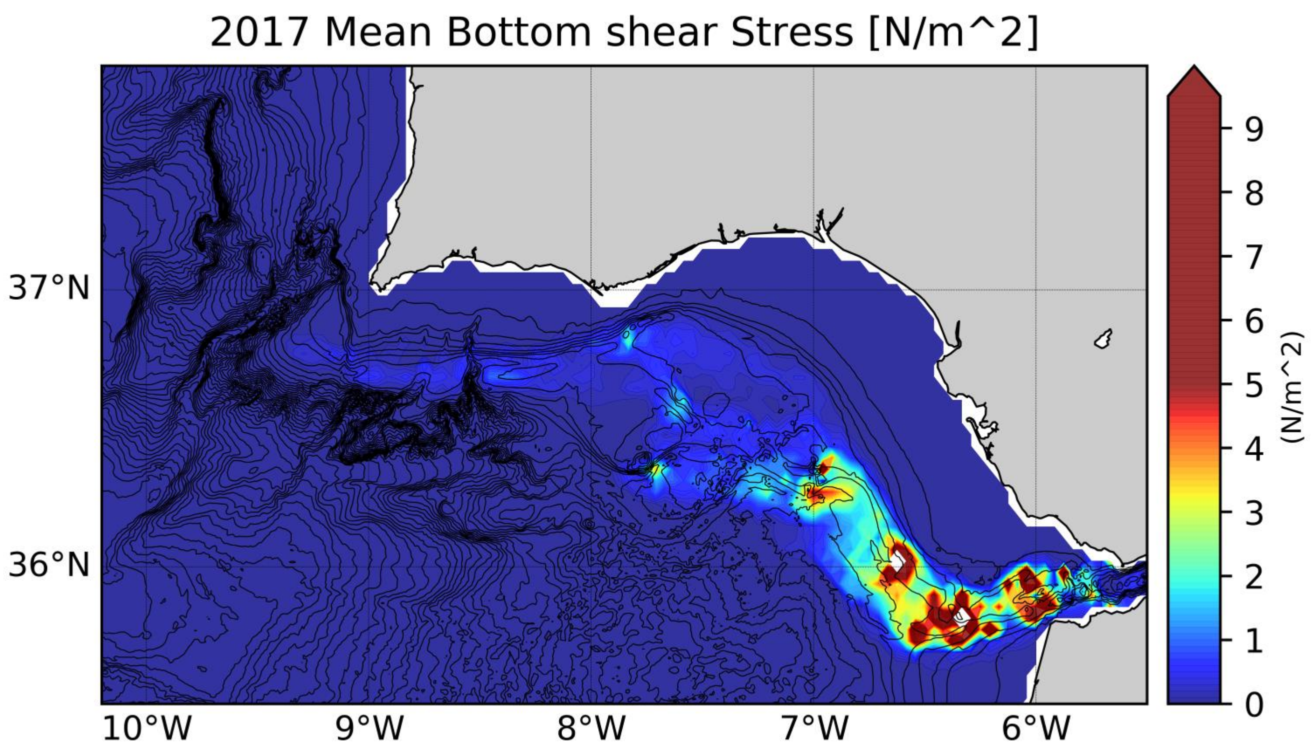

Figure 3.10 Simulated mean bottom shear stress, calculated in the year 2017.

In the "channel and ridge" sector, the Cadiz and Huelva channels show a shear stress of about 3 N/m^2, while on the surrounding Sanlucar basin it is around 1,5 N/m^2. Nevertheless, these shear stress values are high for sediment drift deposition and only in some areas of the Donana basin exhibit a similar range (exceeding 1 N/m^2). In the main contourite channels and moats of the "Contourite depositional" sector (Guadalquivir, Diego Cao contourite channels, Upper slope basal and Alvarez Cabral moats, GCC, DCC, UBM, ACM respectively; Fig. 3.6 and Fig. 1.10) the shear stress generally exceeds 2 N/m^2, with a maximum of about 4 N/m^2 at the southern base of the Guadalquivir Basament High. The only exception is the ACM where the simulated shear stress value remains less than 1 N/m^2. The sediment drifts of this sector, founded in the Deep Algarve basin, generally corresponds to low shear stress values (< 0.6 N/m^2), only in the western side of the separated drift attached to the Alvarez Cobral moat (Fig. 3.6) the shear is around 1 N/m^2. In the "Submarine canyon" sector, over the Portimao, Lagos and Sagres sediment drifts (Fig. 3.7) the mean simulated bottom shear stress is generally about 0.4 N/m^2, until Cabo San Vicente and over the Alentejo basin where the average shear is very low.

The estimated critical bed shear stresses concerning to the mixed sand and mud contouritic deposits have been compared with the daily annual (2017) bottom shear stresses (Fig. 3.11 and 3.12) in order to assess the long-term patterns of erosion and deposition in the Gulf of Cadiz.

Firstly, looking at the daily annual bottom shear stresses reported for two different locations in the Gulf (Figs. 3.2 and 3.11), it was possible to correlate their trends between erosional features and the associated depositional drifts. Figure 3.11a shows the correlation between peaks in the bottom shear stress estimated for the Upper slope Basal Moat (UBM) and the Separated drift further downstream from this feature (grid points location in Fig. 3.2). Their main peaks have a good correspondence, demonstrating their interaction. Furthermore, plotting the histograms of the bottom shear stresses acting over these features in the year 2017,

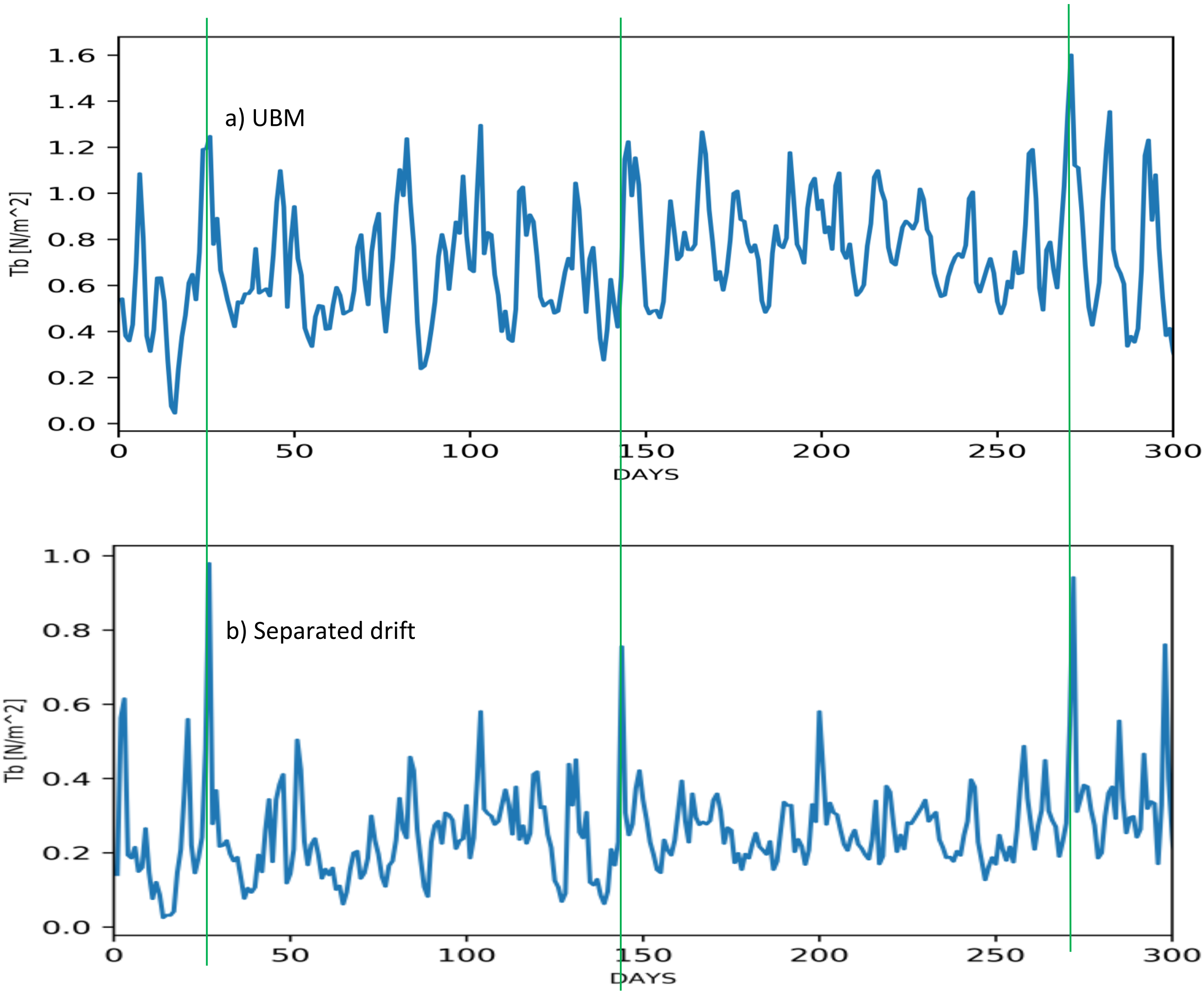

Fig. following below

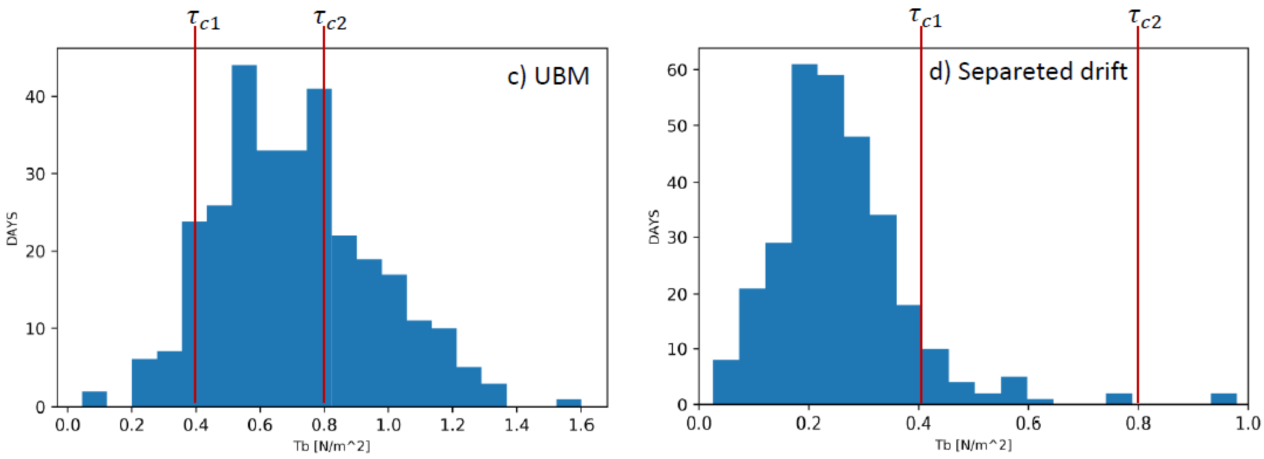

Figure 3.11 a) and b) 2017 daily time series of the Bottom shear stress; **c) and d)** Histogram of the N° of the days in the year 2017 for 20 categories of bottom shear stresses, **b) and d)** located over the separated drift (8.20°W - 36,68°N); **a) and c)** inside the Upper slope basal moat, UBM (7.8°W – 36.8°N); locations in Fig. 3.2.

it can be noted for how many days the bottom stress exceed a chosen critical shear stress for erosion, in the channels and in the related deposits. It appears that the bottom shear stress in the year 2017 exceeds the minimum selected critical shear stress (τ_{c1}= 0.4 pa) for a smaller percentage of time in the Separated drift (8.20°W - 36,68°N) than inside the UBM, where the shear exceeds this threshold for more than 50 % of the time (Fig. 3.11b).

As it is explained in section 2.4, the critical shear stress is extremely variable on the seafloor along the MOW pathway. For this reason, a further analysis was conducted considering three different critical shear stress for erosion (τ_{c1} = 0.4 pa, τ_{c2} = 0.8 pa, τ_{c3} = 1.2 pa; see Fig 3.12) and representing the percentage of time in a year in which the bottom shear stress exceeds the erosional threshold in the whole Gulf of Cadiz seafloor. Three percentage maps for each $T_{c,}$ were computed (Fig. 3.12) that express the spatial and temporal variability of the Mediterranean Overflow current effect on the seafloor. Areas where the daily bottom shear stress exceeds the threshold of critical stress for more of the 50% of time in the year 2017 are considered in prevalent erosion, while areas that don't exceed the erosion shear threshold for more than 50% of the time are considered dominated by deposition. The first plot (τ_{c1} = 0.4 pa; Fig. 3.12a) computed with the minimum adopted threshold, shows areas with dominant erosion also over the depositional basins as defined by Hernandez Molina et al. (2016; Fig. 1.11) and very diffused erosion areas all-around the main channels. The second plot (Fig. 3.12b), assuming τ_{c2} = 0.8 pa, is in agreement with the distribution of the depositional basins and the localization of erosion inside the contourite channels and moat of the study area, already defined by several author (Llave et al., 2001; Hernández-Molina et al., 2003; García et al., 2009; among others).

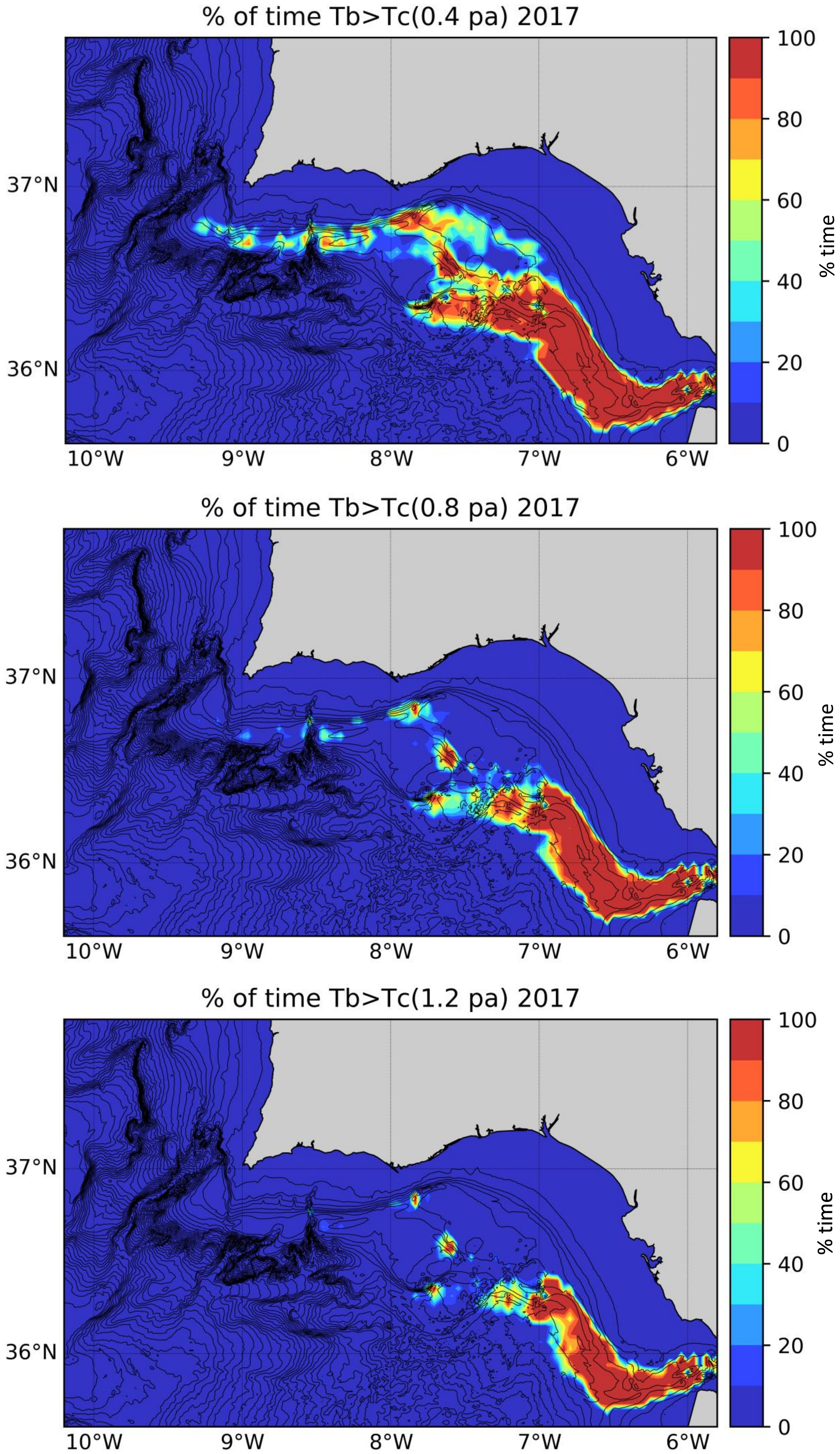

Figure 3.12 Percentage of Time in the year 2017 in which the bottom shear stress exceed the critical shear stress for erosion. **First plot**: Tc = 0.4 pa, **second plot** : Tc = 0.8 pa, **third plot** : Tc = 1.2 pa.

Finally, the third plot (τ_{c3}= 1.2 pa; Fig. 3.12c) generally underestimates erosion inside the main erosive features and over the sediment drifts that characterize the “Contourite depositional” sector and the “Submarine canyon” sector. Above the Sanlucar Basin and in some areas of the Doñana basin, the shear stress exceeds the critical threshold (0.8 pa) for more than 60% of the year and for more than 40%, using the threshold of 1.2 pa. Furthermore, the sandy sheeted drift characterizing the Cadiz basin appears to be permanently over the assumed highest erosion threshold (1.2 pa). The reason for of the widespread high bottom shear stress values observed over the basins will be discussed in the following chapter 4, together with the possible sources of uncertainty of the analysis.

Chapter 4 – Discussion

4.1 Evolution of the Gulf of Cadiz seafloor

The seafloor of the Gulf of Cadiz is the results of the interaction between several processes acting at different time scales, from millions-thousands years scale, where tectonic activity and sea level changes are the principal factors, to the scale of hundred years-decades, where more frequent phenomena shape the seabed through downslope processes (such as submarine slides, turbidity currents and other gravity instability phenomena; Teixeira et al., 2019) and alongslope processes, forming contourite deposits (drifts). Indeed, the Gulf of Cadiz is characterized by a mixed contourite-turbidite depositional system, formed by the interaction between these processes (Hernandez Molina et al., 2006).

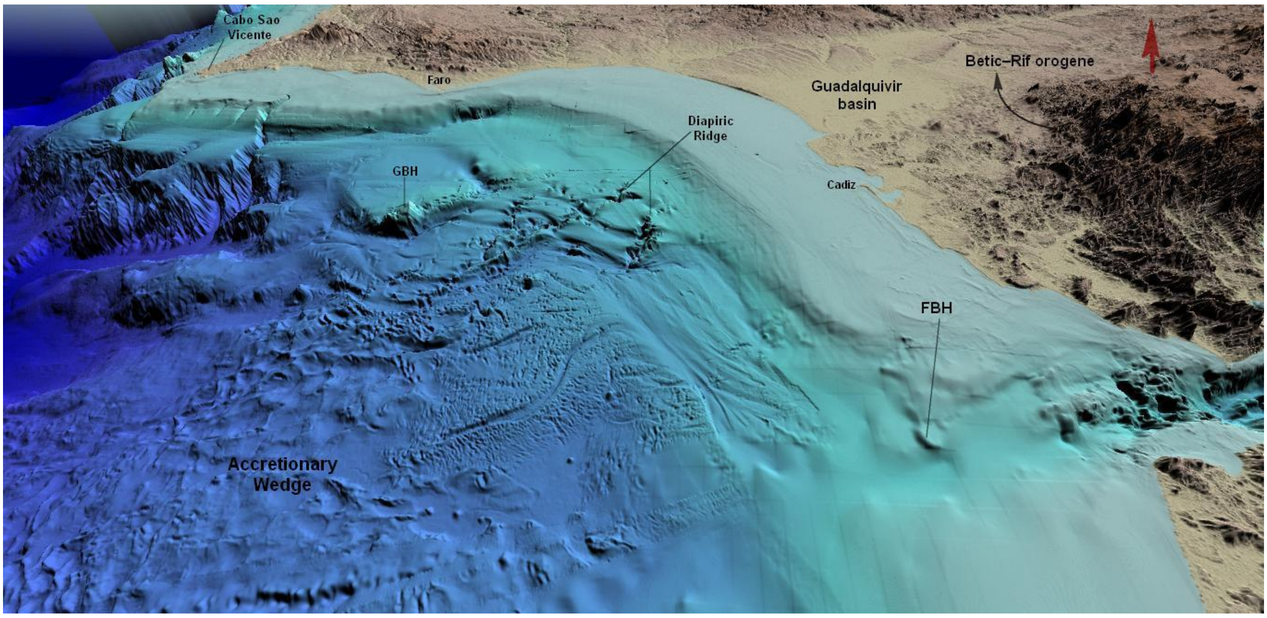

Figure 4.1 Gulf of Cadiz seafloor. FBH = First basement high, GBH = Guadalquivir basement high.

Plate tectonics set up the basal physiographic structure of the Gulf of Cadiz (Fig. 4.1). The formation of the accretionary wedge during the Betic–Rif orogenesis (Oligocene through Miocene times; Zitellini et al., 2009) and related deformations of the Spanish continental margin lead the development of the wide middle-slope area that deeply interacts with the MOW spreading pattern. Also, the FBH is the westernmost peak of the Betic–Rif orogene, that pop out from the ocean floor (Fig. 4.1). On the other side, the Portuguese margin has been less tectonically active in the last 30 Ma and is characterized by the occurrence of incised canyon that makes its slope steep and narrow. The Nubia-Iberia plates convergence (NW-SE) has created the Guadalquivir and Portimao structural highs, while the diapiric ridges of Triassic salts, gypsum and shallow-marine carbonate deposits arise along the thrust-migrating structure of the stretched accretionary prism, during the Tortonian collapse of the Betic-Rift orogenic front (Hernandez-Molina et al., 2016). Extensional and diapiric processes give also place to areas with a high subsidence rate that are perfect spots for sediment drifts deposition. These morphostructural conditions set out the main constraints, driving the spatial distribution of the channels and moats excavation and the location of the main drift accumulation areas. All drifts are, in fact, related to a combination of regional oceanographic conditions and the physiographic domains in which they develop (Hernandez Molina et al., 2006). The opening of the Gibraltar gateway in the late Miocene connects the Mediterranean Sea with the Atlantic Ocean (Roveri et al., 2014), establishing the water exchange between these two basins. From the late Pliocene age (~2.4 Ma), the margin evolves toward more stable conditions (Hernández-Molina et al., 2016). Since this time, the present-day regional circulation setting of the Gulf of Cadiz and the water exchange through the Gibraltar gateway were established. The circulation of the Mediterranean water mass has a strong impact on the middle slope morphology, leading to the formation of contourite erosional and depositional features that constitute the Contourite Depositional system of the Gulf of Cadiz.

4.2 Mediterranean current interaction with the bottom morphology

The spatial correspondence found between the MOW simulated bottom current speed and the simulated bottom shear stress is a clear hint that the bottom current action drives the construction of the Contourite Depositional Systems, in accordance with all the literature of this area (Llave et al., 2002; Mulder et al., 2003; Stow et al., 2009; F. J. Hernández-Molina et al., 2006, 2011,2016; among others). Nevertheless, due to the difficulty to survey the deep ocean bottom, the unavailability of observations does not allow to adequately represent the regional hydrodynamic setting and erosive-depositional processes leading the contourite formations. Therefore, is not clear how the Mediterranean outflow velocity affects the seafloor sediments. The “the law of the wall”, firstly mentioned by Theodore von Kármán (1930) and applied in this Thesis, provides a good method to estimate the shear stresses over a boundary, which are, in our case of study, primarily responsible for the movements of the seabed sediments.

Our simulations of the bottom shear stress link the bottom current behavior with the seafloor characteristics. The spatial and temporal variability of this parameter permits to discern areas where erosion prevails and areas dominated by deposition (Fig. 3.12). By combining these results with the previously defined contourite channels and drifts distribution, such comparison allows a further understanding on the dynamics of contourite depositional systems. The MOW pathway, firstly deflected towards NW by the Coriolis force, is largely steered by the bathymetry, splitting it in different cores and small branches and forcing the Mediterranean water mass to flow along the main contourite channels and moats of the study area. As the simulated bottom current speed and stress shows (Fig. 3.1, 3.10 and 3.12), areas with stronger erosional activity are linked to the main morphological constrictions (i.e. First Basement High, Diapiric ridges, Guadalquivir basement high and upper-middle slope intersection, Fig. 3.1, 3.10 and 3.12). Although the frictional effect of the bottom produces a deceleration of the current speed, the complex slope morphology may locally enhance the flows velocity (Fig. 3.1a), mainly inside the channels, through the known "channeling effects" (García et al., 2009). Furthermore, the flow–bottom interaction increments the variability of the bottom current speeds, as it is shown by the simulated annual bottom current speed standard deviation (Fig. 3.1c).

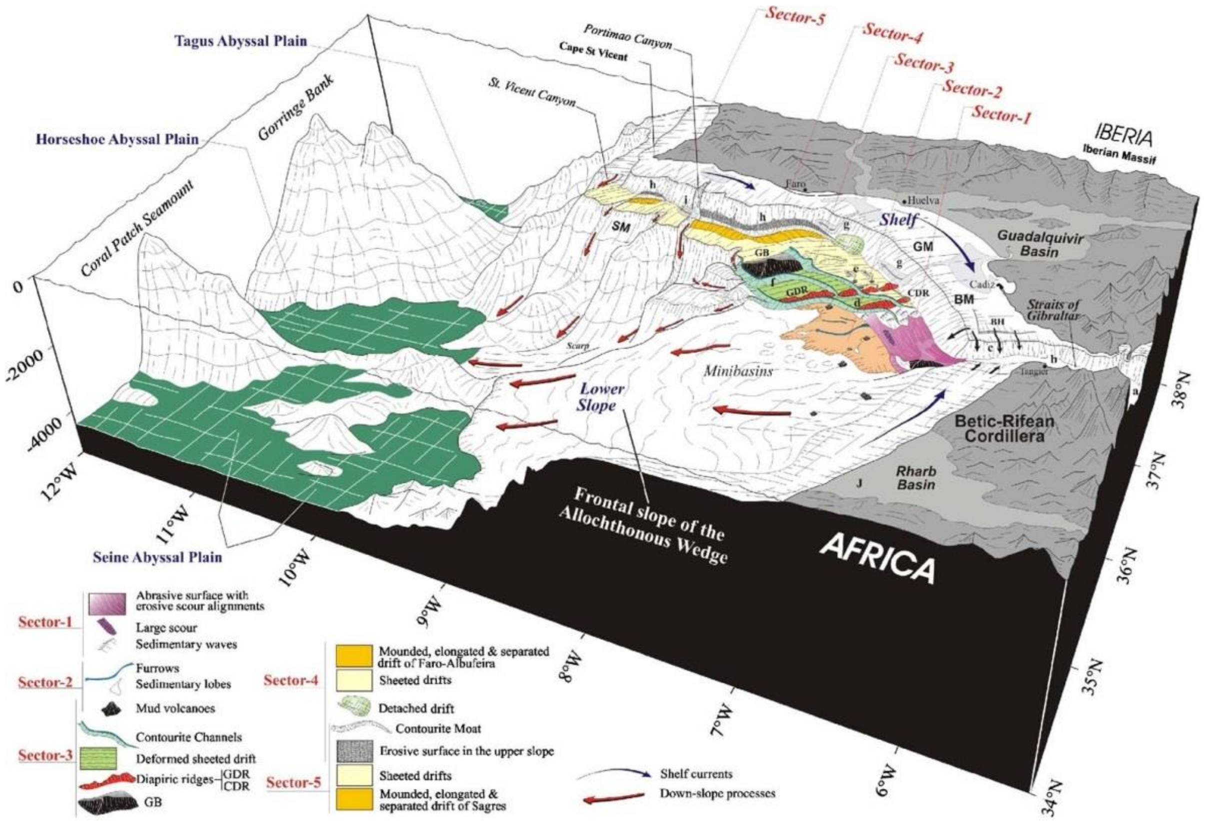

Figure 4.2 3D reconstruction from Hernandez Molina et al., (2006).

The five morphosedimentary sectors (Fig. 4.2) defined by Hernandez Molina et al. (2003) are thus related to the systematic decrease of the bottom current activity, also associated to mixing with the surrounding water masses (i.e. Nord Atlantic deep water, NADW and Nord Atlantic central water, NACW), enhanced by turbulence induced by the topography; this also causes the loss of part of the water mass and kinetic energy of the Mediterranean Outflow current. In detail, passing the Gibraltar Strait and flowing toward NW over the smooth platform, characterized by the rock outcrop and the drift founded in the Cadiz basin, the bottom shear stress largely exceed the critical stresses, defining that the whole area is dominated by erosion. The presence of the sandy sheeted drift is due to the facts that the faster parts of the current, flow in correspondence of the main erosional lineations, Fig. 4.3), allowing deposition between one and the other and forming a series of ribbons and dunes orientated along the flow directions (Fig. 4.3).

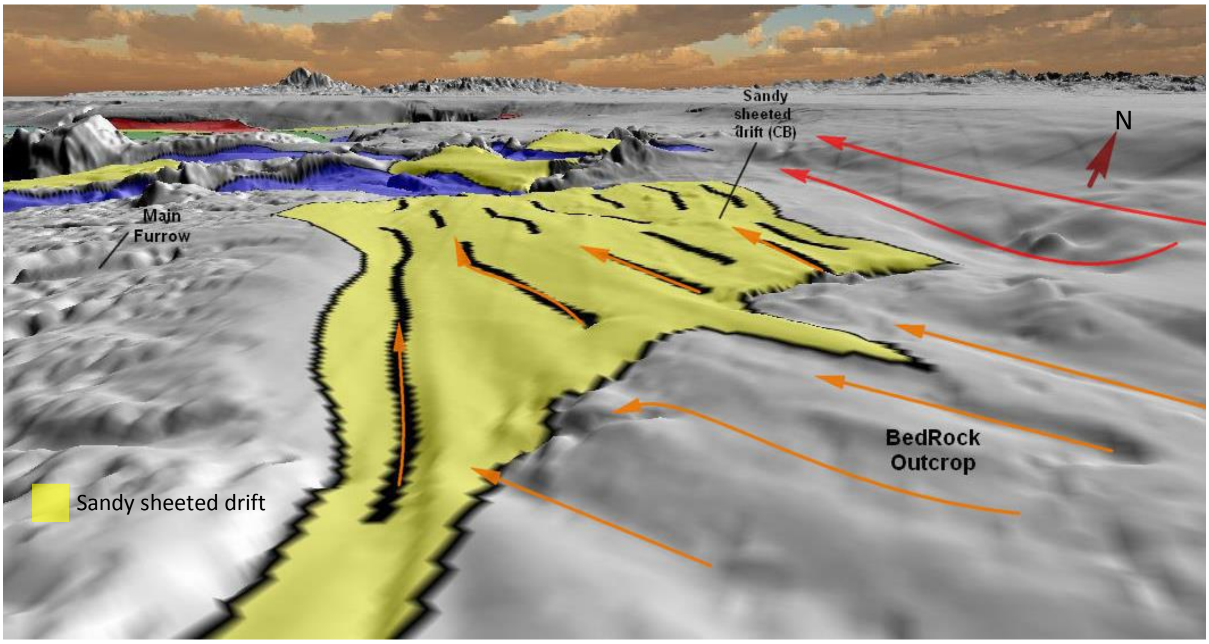

Figure 4.3 Smooth Platform with Bedrock outcrop and erosive lineaments (black lines), Red arrow = Mediterranean Outflow upper core (MU), Orange arrow = Mediterranean Outflow lower core (ML), CB = Cadiz basin.

Reaching the diapiric ridges, the current is strongly steered; the flow-ridge interactions allows deposition in the downstream flank of the Cadiz diapiric ridge, over the deformed sheeted drift founded in the Sanlucar basin (Fig. 4.4). The principal contourite channels of this area (Worm channel, HCC and CCC) host the main three current branches (IB, PB, SB) and show high stresses on their bottom, contributing to deposit on the adjacent drift (Fig. 4.4), likely thought some process of flow stripping (Hernandez Molina et al., 2006).

Entering in the Guadalquivir contourite channel (GCC), the PB erodes at the southern base of the Guadalquivir basement high (GBH) and feeds the Donana basin (DB), while, the IB exiting from the Diego Cao channel (DCC), loses the majority of its speed and bed load, allowing deposition in the sheeted drift that compose the deep Algarve basin (AB; Fig. 4.5).

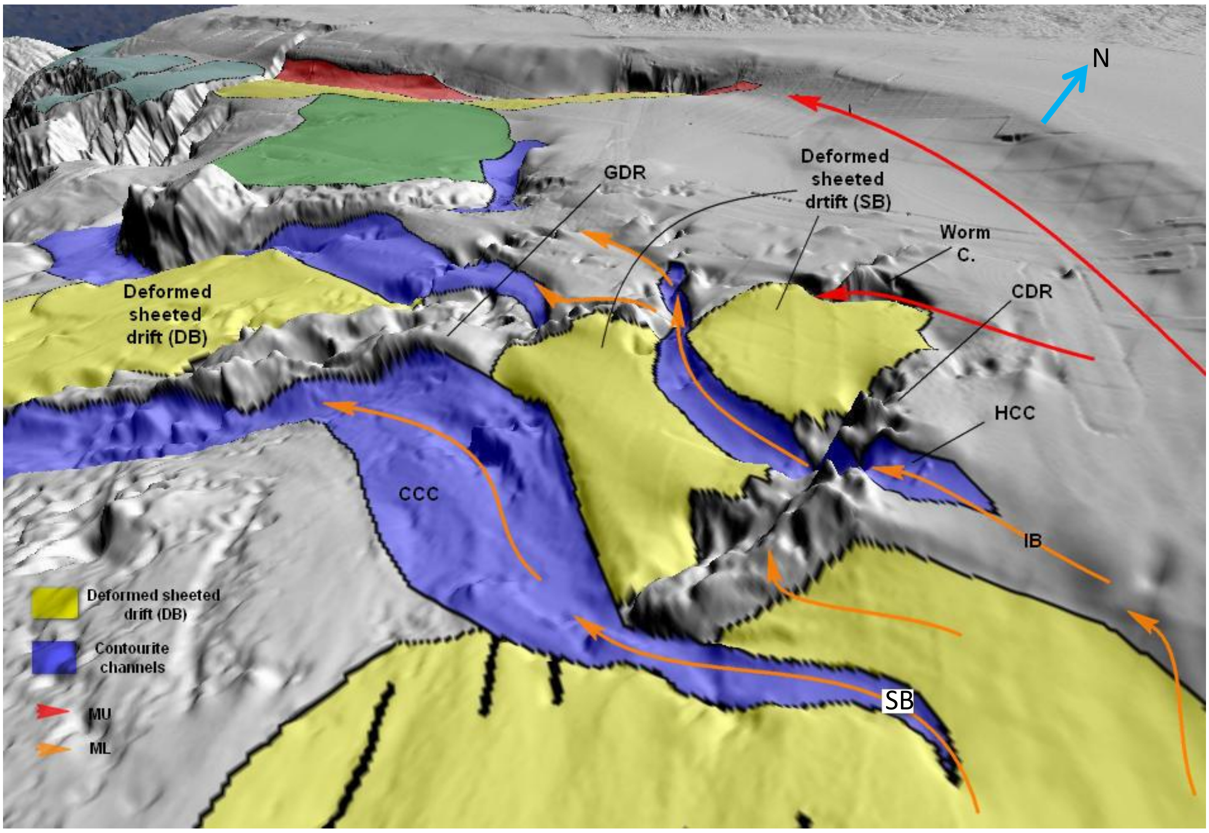

Figure 4.4 Diapiric ridges area, CCC = Cadiz contourite channel, HCC = Huleva contourite channel, CDR = Cadiz diapiric ridge, GDR = Guadalquivir diapiric ridge, Red arrow = Mediterranean Outflow upper core (MU), Orange arrow = Mediterranean Outflow lower core (ML), SB = MOW Southern branch, IB = MOW intermediate branch SB = Sanlucar basin.

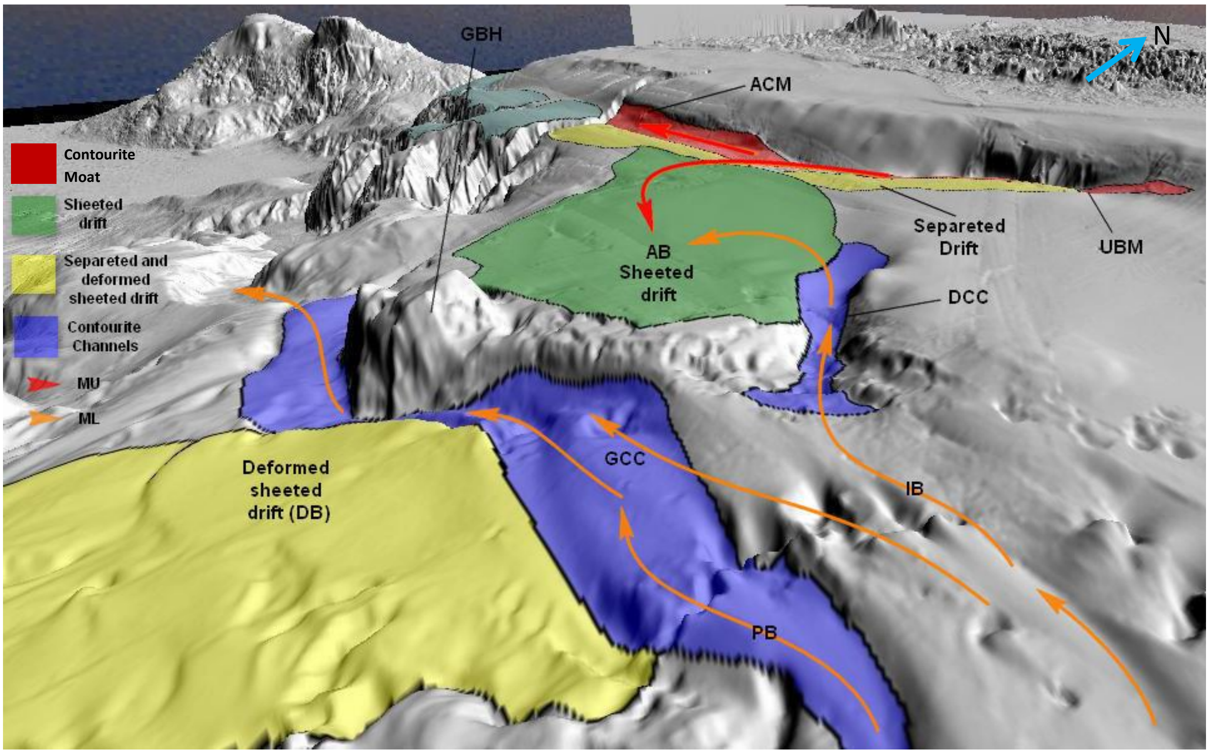

Figure 4.5 Contuorite main depositional area with Guadalquivir Bank interaction, GCC = Guadalquivir contourite channel, DCC = Diego Cao contourite channel, ACM = Alvarez Cobral moat, UBM = Upper slope basal moat, Red arrow = Mediterranean Outflow upper core (MU), Orange arrow = Mediterranean Outflow lower core (ML), PB = MOW Principal branch, IB = MOW intermediate branch AB = Deep Algarve basin.

The deep Algarve basin is also fed by a detached branch of the MU and is the main depocenter of the study area, as is showed in the seismic profiles reported by Hernandez Molina et al. (2016).

On the other side, the Mediterranean upper core (MU), passing North of the diapiric ridge continues to flow along the upper-middle slope intersection, forming a plastered drift all along its path. At about 7.6° W the MU enters in the Upper slope basal moat (UBM), eroding inside the moat and depositing on the adjacent separated drift (Fig. 4.6). The separated drift attached to the Alvarez Cobral moat (ACM) shows the sediment accumulation area mainly on its eastern flank while on the western side the capturing action of the Portimao canyon eat away the deposits (Fig. 4.6), as the bottom shear stress simulation reproduces (Fig. 3.10 and 3.12). The part of the MU that pass westwards of the Portimao canyon loses part of its water mass and speed, but it remains able to deposit over the Portimao, Lagos and Sagres drifts.

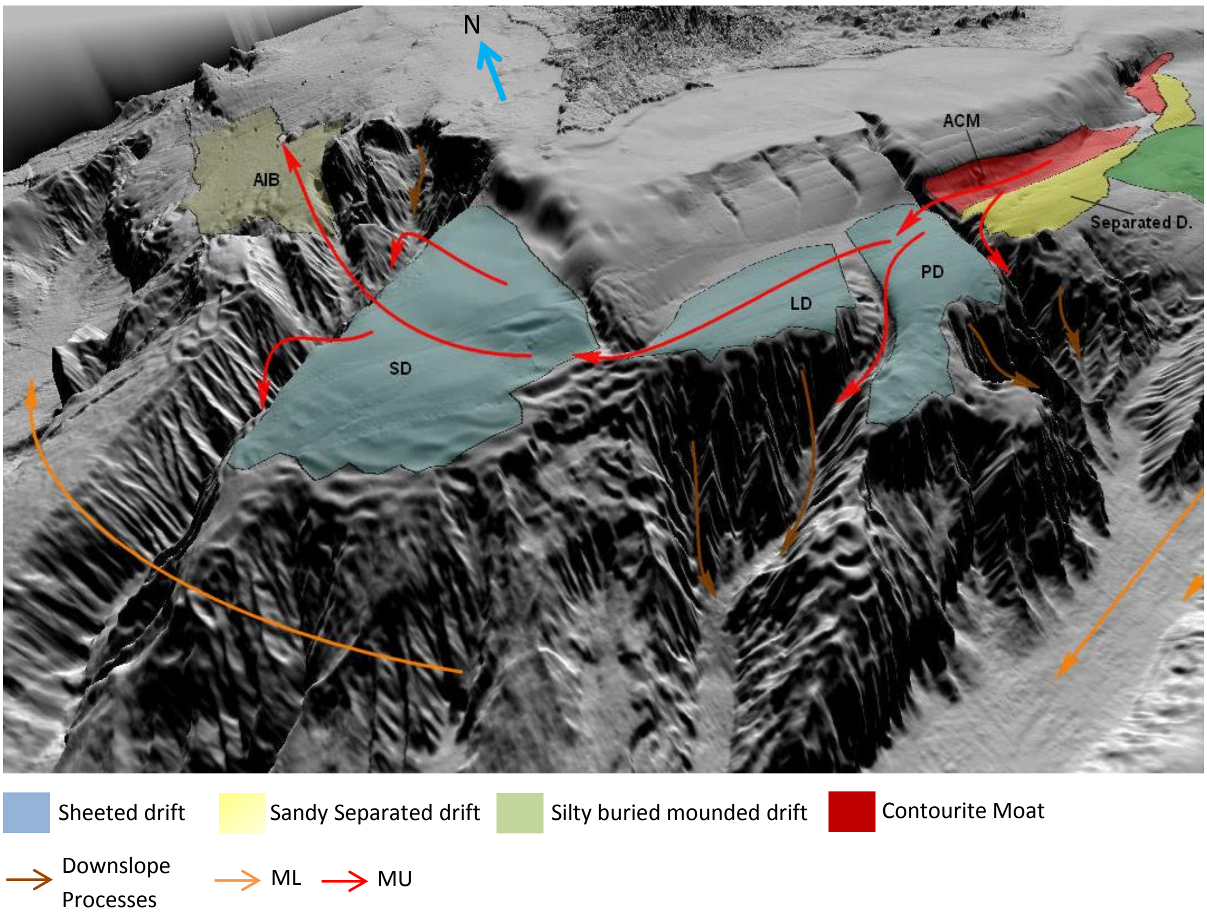

Figure 4.6 Submarine canyon area, Red arrow = Mediterranean Outflow upper core (MU), Orange arrow = Mediterranean Outflow lower core (ML), ACM = Alvarez Cobral moat, PD = Portimao drift, LD = Lagos drift, SD = Sagres drift, AIB = Alentejo basin.

At about 8.2°W both current cores, the lower one exiting from Guadalquivir contourite channel and the upper one passing the Portimao canyon, reach a neutral buoyancy and start to flow detached from the seafloor. In this location, the MOW loses the majority of its erosional power, as it shows by the absence of erosional features produced by the current in the Canyons sector. In fact, Ambar et al. (1999) found that at about 8°W the MOW reaches quasi-equilibrium as a density current and flows as a wall-bounded current, over the NADW and below the NACW. Finally, turning around Cabo San Vicente, the part of the current that has kept the thermohaline and speed characteristics needed to jump the San Vicente canyon reaches the western Algarve margin, feeding the silty buried drift founded in the Alentejo basin (AIB, Fig. 4.6).

Our results represent a first approach in order to estimate the bed shear stress produced by the MOW interaction with the seafloor of the Gulf of Cadiz. However, the absence of observed bottom shear stress data in the study area don't allow us to compare our simulation with the real situation. A similar approach, based on numerical modelling, has been applied to other areas. Chen et al., (2019), for the South China Sea, found a simulated bottom stress of 0.06 pa related to a current speed of about 15 cm/s, while the results of Guarnieri et al. (2014), for the Adriatic Sea, show a maximum simulated bottom shear stress reaching 3.8 pa, linked with a bottom orbital velocity of about 35 cm/s (current-wave interaction). In our simulation, by assuming a bottom speed amplitude of about 15 cm/s and 40 cm/s as a reference (Fig. 3.1a and 3.10), we estimate a bottom shear stress of about 0.35 pa and about 1.7 pa, respectively. The maximum shear stress value estimated in our study area exceeds 18 pa, and is associated to 120 cm/s of speed amplitude, found over the FBH (Fig. 3.10). On this base we consider our results quite realistic, although overall they appear to be slightly overestimated.

One of the important results of this work is the proposed yearly time scale distribution of depositional and erosional areas in the Gulf of Cadiz, showed by the maps in Figure 3.12 as the percentage of time in the year 2017 in which the bottom shear stress (τ_b) exceeds the erosional threshold (τ_c). Comparing the maps in figure 3.12 with the previously defined distribution of the contourite channels and drift of the CDS (Hernández-Molina et al., 2006, 2016), the value of critical bed shear stress that better fits is 0.8 N/m^2 (pa). This erosional threshold seems to be relatively high if compared with other studies. Guarnieri et al. (2014), for the Adriatic Sea used a critical bed shear stress of 0.02 pa, while Berenbrock and Tranmer (2008), for the Coeur d'Alene River (Idaho, USA), considered different critical bed shear stress depending on a given grain size (0.08 pa for silt with 0.031 mm of diameter and 0.19 pa for sand with 0.25 mm of diameter). However, considering that our study area is in a deep ocean environment, where the weight of the thick water column can increment the grade of consolidation of seabed deposits, and also may not facilitate sediment transport and erosion with respect to a shallow environment, thereby increasing the erosional threshold.

4.3 Med-currents ocean model capability and error

The regional Med-currents ocean model produced by INGV (Istituto Nazionale di Geofisica e Vulcanologia) considers the main freshwater input in the Mediterranean basin, such as precipitations and river runoff, and it's able to reproduce the dense water formation in the North Adriatic, Gulf of Lyon and in the Eastern Mediterranean, taking into account also the water output from evaporation (Copernicus Marine Service Ocean State, sec. 3.4, 2018). On this base, the Med-currents model is capable to reproduce the MOW spreading pattern in a consistent way. The results of our simulations essentially agree, in current speed intensity and direction, with *in situ* data compilation (Madelain, 1970; Kenyon and Belderson, 1973; Mèlières, 1974; Zenk, 1975; Baringer and Price, 1997; Nelson et al., 1999; Cherubin et al., 2000, all reported by Hernández-Molina et al., 2006). The reconstruction of the MOW spreading pattern by Hernandez Molina et al. (2006), principally deduced from a morpho-sedimentological analysis and observed oceanographic data (Fig. 1.9), is also in agreement with our results (Fig. 4.7).

Obviously, any model has got some limits and errors (for ocean models see also Desroziers et al., 2005). The Mediterranean bottom current simulated metrics are limited by the model's horizontal resolution (4x4 Km), therefore, the model is not able to reproduces filaments and branches of the MOW that are at a smaller scale. Furthermore, the interpolation of the bottom grid fields allows to better reproduce the patterns of the flow on the bathymetry, but it spreads the high value of the fields, located inside the erosive features, also over the drifts. This might be the case over the smooth platform (Fig. 3.1b,c, 3.10 and 3.12) where, instead of reproducing the higher bottom current activity in correspondence of the erosive lineaments, the model reproduces a high velocity over the whole platform, comprising also the dune crests (Fig. 3.1). Again, in the area located between the diapiric ridges (Fig. 3.10), the values of high bottom stress and current speed fields localized in the Huelva and Cadiz contourite channel are quite diffuse all over the Sanlucar drift.

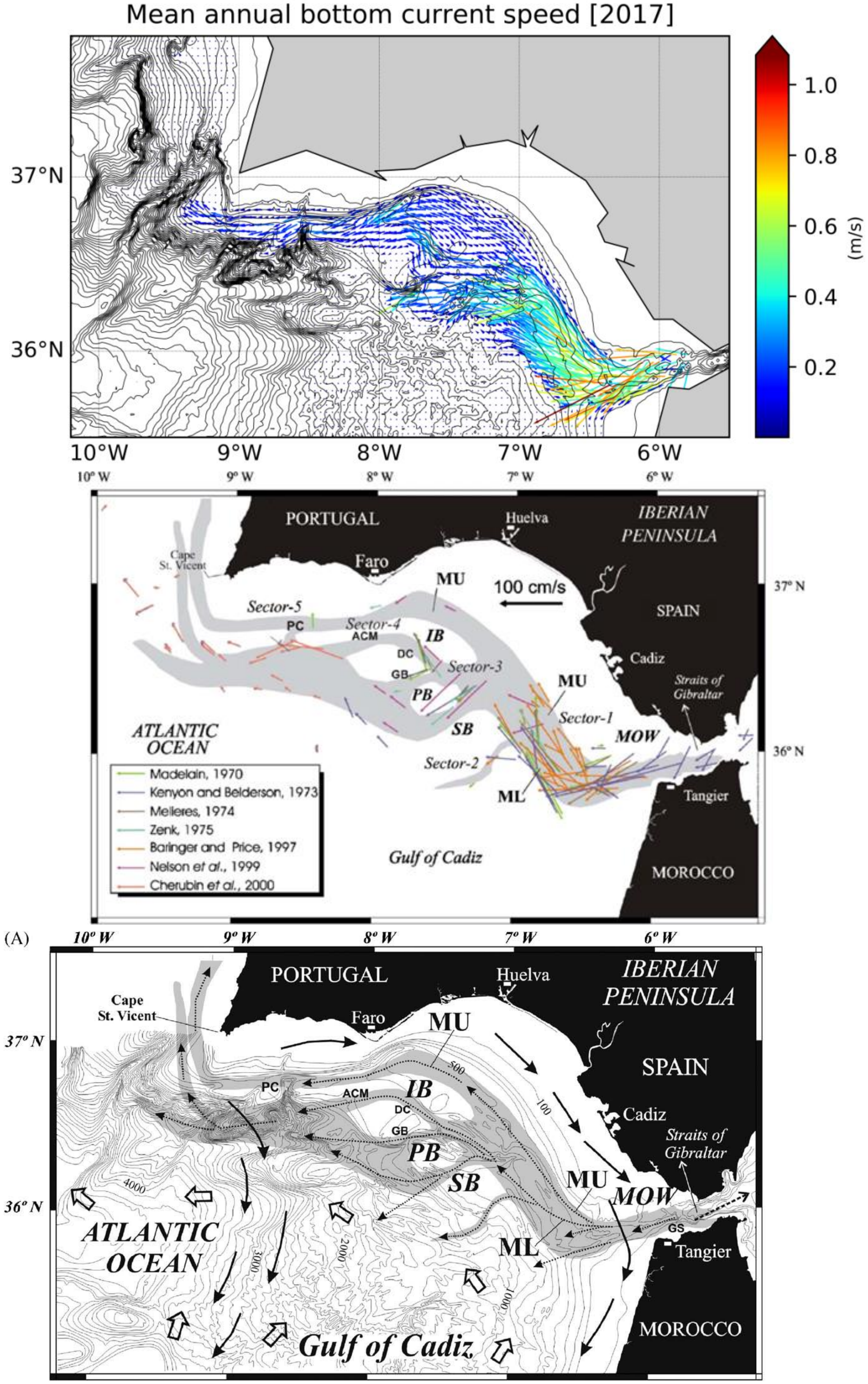

Figure 4.7 Simulated Bottom current speed in comparison with real data and reconstruction reported by Hernandez Molina., (2006).

Another limitation is due to the bathymetric offset between the “real” SWIM bathymetry and the bathymetry used by the model. This offset delocalizes the main core of the flow with an error grade appreciable in the model bathymetry error map (Fig. 2.5), as it is the case for the ACM and the attached separated drift, in which the high current activity fields appear shifted from the moat to the drift (profile in Fig. 3.4c). Furthermore, this bathymetric offset also influences the determination of the speed height from the bathymetry (z) used in the equations (2).

Regarding the shear stress estimation, the approximations done to calculate the Drag coefficient (C_d) through the equations (2) in chapter 2, in order to fill the equation (1), are the principal causes of uncertainty. The determination of the roughness (Z_0) calculated as “relative bathymetry position”, as described in section 2.3, permits to assume a roughness value for each bathymetric cell of the model, instead of taking a single value for the whole seafloor, but obviously it cannot completely describe the high variability of the seafloor morphology. Furthermore, to compute the bottom shear stress we use the bottom speed module field, calculated by applying the quadratic law with the meridional and zonal velocity components taken from the Med-currents ocean model.

Nowadays the observations of current speed are to sporadic, thus the model speed fields error could be estimated by more real data in the future. The eastward and westward net water transport through the Strait of Gibraltar is the first index used as a numerical current validation and is done comparing the model with the observed data taken from the literature. The Med-currents numerical geostrophic currents have been compared to the ones derived from satellite SLA gridded data in terms of daily basin speed averages, showing a good ability of the model to represent the temporal variation of the satellite derived currents and kinetic energy (Clementi et al., 2018).

Conclusions

In this study the dynamics by which the Mediterranean outflow interacts with the seafloor in the Gulf of Cadiz, forming the Contourite depositional system, have been analyzed at the daily time scale in one year. Through the use of high-resolution multibeam bathymetry and numerical ocean modelling, we show how the complex interaction between geology and oceanography shape the morphology of the Gulf of Cadiz seafloor. Bathymetry largely steers and modifies the flow; on the other side, high-speed currents events are driven by several forcing (i.e. Mediterranean dense water formations, atmospheric forcing and tides), highlighting the role of intermittent bottom current activity in sediment erosion, transport and subsequent drift accumulation. The main conclusions from this investigation are:

1. The Med-currents ocean model shows a good capability to reproduce the MOW spreading pattern and the simulated bottom current speed amplitude and directions are in agreement with *in situ* data reported by Hernandez Molina et al. (2006) and with the morpho-sedimentary setting.

2. We propose a first attempt to calculate the bottom shear stress produced by the MOW interaction with the seafloor of the Gulf of Cadiz. The comparison with the assumed bed critical shear stress enabled us to individuate the principal erosional areas (characterized by erosive lineaments, contourite channels and moats) and the main depositional centers (basins and drifts), and to simulate the related interannual spatial and temporal variability.

The results from this study represent a first step for modeling the effects of the Mediterranean Outflow on the seabed at the basin scale. For a better determination of the spatially highly variable parameters related to the seafloor characteristics, as the roughness (Z_0) and the bed critical shear stress (τ_c), new advanced investigation methods and more *in situ* measurements are requested. Also, we look forward for a quantitatively balance of the associated sediment transport dynamics that bring sediment to the drift.

Ringraziamenti

Un sentito grazie va alla professoressa Claudia Romagnoli che mi ha seguito e aiutato durante la stesura di questa tesi. Grazie alla professoressa Nadia Pinardi per avermi ospitato al dipartimento di Geofisica e per i suoi consigli sul bottom shear stress. Un grande ringraziamento anche a Alfredo Izquierdo e Miguel Bruno Mejías, per avermi introdotto all'affascinate mondo dell'oceanografia. Grazie a Emanuela Clementi del CMCC per i consigli tecnici sul modello. Un grazie speciale a Augusto, Kanval, Elise, Isabella, Francesco e Leonardo per i bei momenti vissuti insieme, siete mitici. Un super grazie alla Romagnoli crew, Luca e Camilla, senza di voi sarebbe stato tutto più difficile. Un grazie infinito a tutti i miei compagni di avventure di questi anni, di Cesena, di Bologna e anche a los hermanos de Cadiz, siete dei bombers. Un calorosissimo grazie va alla mia ragazza e segretaria Beatrice. Ma il più importante ringraziamento va ai i miei genitori Leonardo e Francesca, per l'amore e le grandi possibilità che mi hanno dato per esprimermi e crescere.

References

Ambar, I., Armi, L., Bower, A., & Ferreira, T. (1999). Some aspects of time variability of the Mediterranean Water off south Portugal. *Deep-Sea Research Part I: Oceanographic Research Papers*, *46*(7), 1109–1136. https://doi.org/10.1016/S0967-0637(99)00006-0

Ambar, I., Serra, N., Brogueira, M. J., Cabeçadas, G., Abrantes, F., Freitas, P., Gonzalez, N. (2002). Physical, chemical and sedimentological aspects of the Mediterranean outflow off Iberia. *Deep-Sea Research Part II: Topical Studies in Oceanography*, *49*(19), 4163–4177. https://doi.org/10.1016/S0967-0645(02)00148-0

Baringer, M. O. N., & Price, J. F. (1999). A review of the physical oceanography of the Mediterranean outflow. *Marine Geology*, *155*(1–2), 63–82. https://doi.org/10.1016/S0025-3227(98)00141-8

Berenbrock C. and Tranmer W. T., (2008). Simulation of Flow, Sediment Transport, and Sediment Mobility of the Lower Coeur d'Alene River , Idaho. Environmental, B., Commission, I., & Agency, U. S. E. P.

Chen, D., Wang, Y., Melville, B., Asce, M., Huang, H., & Zhang, W. (2018). Unified Formula for Critical Shear Stress for Erosion of Sand, Mud and Sand-Mud mixture, *144*(8), 1–14. https://doi.org/10.1061/(ASCE)HY.1943-7900.0001489.

Chen, H., Zhang, W., Xie, X., & Ren, J. (2019). Sediment dynamics driven by contour currents and mesoscale eddies along continental slope : A case study of the northern South China Sea. *Marine Geology*, *409*(October 2018), 48–66. https://doi.org/10.1016/j.margeo.2018.12.012

Clementi, E., Oddo, P., Drudi, M., Pinardi, N., Korres, G., Grandi A., (2017b). Coupling hydrodynamic and wave models: first step and sensitivity experiments in the Mediterranean Sea. Ocean Dynamics. doi: https://doi.org/10.1007/s10236-017-1087-7.

Clementi, F., Pierdicca, A., Milani, G., Gazzani, V., Poiani, M., Lenci, S., 2018. Numerical model upgrading of ancient bell towers monitored with a wired sensors network, in: Milani, G., Taliercio, A., Garrity, S., 10th International Masonry Conference (IMC_10). Milano, pp. 1–11.

Desroziers, G., Berre, L., Chapnik, B. and Poli, P., (2005). Diagnosis of observation, background and analysis-error statistics in observation space. Q.J.R. Meteorol. Soc. 131: 3385–3396. doi: 10.1256/qj.05.108.

Dewey, J. F. and Horsfield, B., (1970). Plate tectonics, orogeny, and continental growth: Nature, v. 224, p. 1031-1035.

Diez, S., National, S., & Luis, M. (2005). Bathymetric map of the Gulf of Cadiz, NE Atlantic Ocean: The SWIM multibeam compilation, (January), 3–5. https://doi.org/10.1029/2005GL023098.

Dobricic Srdjan and Nadia Pinardi (2008). An oceanographic three-dimensional variational data assimilation scheme. Ocean Modelling, 22 (3-4) 89-105.

Fekete, B. M., Vorosmarty, C. J., Grabs, W., (1999). Global, Composite Runoff Fields Based on Observed River Discharge and Simulated Water Balances, Tech. Rep. 22, Global Runoff Data Cent., Koblenz, Germany.

García, M., Hernández-Molina, F. J., Llave, E., Stow, D. A. V., León, R., Fernández-Puga, M. C., Somoza, L. (2009). Contourite erosive features caused by the Mediterranean Outflow Water in the Gulf of Cadiz: Quaternary tectonic and oceanographic implications. *Marine Geology*, *257*(1–4), 24–40. https://doi.org/10.1016/j.margeo.2008.10.009

Grant, W. D. and Madsen, O. S. (1979): Combined wave and current interaction with a rough bottom, J. Geophys. Res., 84, 1797–1808.

Grant, W. D. and Madsen, O. C. (1986): The continental shelf bottom boundary layer, Annu. Rev. Fluid Mech., 18, 265–305.

Gradstein, F. M., & Ogg, J. G. (2004). Geologic time scale 2004 - Why, how, and where next! *Lethaia*, *37*(2), 175–181. https://doi.org/10.1080/00241160410006483

Guarnieri, A., Souza, A. J., Pinardi, N., & Traykovski, P. (2014). *Numerical modelling of sediment transport in the Adriatic Sea*. https://doi.org/10.5194/osd-11-1391-2014

Gutscher, M.-A., Malod, J., Rehault, J. P., Contrucci, I., Klingelhoefer, F., Mendes-Victor, L., & Spakman, W. (2003). Evidence for active subduction beneath Gibraltar: Comment and Reply. *Geology*, *31*(1), e23–e23. https://doi.org/10.1130/0091-7613-31.1.e23

Hernández-Molina, F. J., Llave, E., Preu, B., Ercilla, G., Fontan, A., Bruno, M. Arnaiz, A. (2014). Contourite processes associated with the Mediterranean Outfl ow Water after its exit from the Strait of Gibraltar: Global and conceptual implications. *Geology*, *42*(3), 227–230. https://doi.org/10.1130/G35083.1

Hernández-Molina, F. J., Llave, E., Stow, D. A. V., García, M., Somoza, L., Vázquez, J. T., Gardner, J. (2006). The contourite depositional system of the Gulf of Cádiz: A sedimentary model related to the bottom current activity of the Mediterranean outflow water and its interaction with the continental margin. *Deep-Sea Research Part II: Topical Studies in Oceanography*, *53*(11–13), 1420–1463. https://doi.org/10.1016/j.dsr2.2006.04.016

Hernández-Molina, F. J., Serra, N., Stow, D. A. V., Llave, E., Ercilla, G., & van Rooij, D. (2011). Along-slope oceanographic processes and sedimentary products around the Iberian margin. *Geo-Marine Letters*, *31*(5–6), 315–341. https://doi.org/10.1007/s00367-011-0242-2

Hernández-Molina, F. J., Sierro, F. J., Llave, E., Roque, C., Stow, D. A. V., Williams, T., Brackenridge, R. E. (2015). Evolution of the gulf of Cadiz margin and southwest Portugal contourite depositional system: Tectonic, sedimentary and paleoceanographic implications from IODP expedition 339. *Marine Geology*, *377*, 7–39. https://doi.org/10.1016/j.margeo.2015.09.013

Hernández-Molina, J., Llave, E., Somoza, L., Fernández-Puga, M. C., Maestro, A., León, R., Gardner, J. (2003). Looking for clues to paleoceanographic imprints: A diagnosis of the Gulf of Cadiz contourite depositional systems. *Geology*, *31*(1), 19–22. https://doi.org/10.1130/0091-7613(2003)031<0019:LFCTPI>2.0.CO;2

Iorga, M. C., & Lozier, M. S. (1999). Signatures of the Mediterranean outflow from a North Atlantic climatology: 2. Diagnostic velocity fields. *Journal of Geophysical Research: Oceans*, *104*(C11), 26011–26029. https://doi.org/10.1029/1999JC900204

Izquierdo, A., Kagan, B. A., Sein, D. V, & Mikolajewicz, U. (2016). MODELLING IN THE STRAIT OF GIBRALTAR: FROM OPERATIONAL OCEANOGRAPHY TO SCALE INTERACTIONS. Удк 551.465.55 ©, 15–25.

Jenness. (2002). Topographic Position Index (TPI) v. 1.2. *Www.Jennessent.Com*.

Llave, E., Hernández-Molina, F. J., Somoza, L., Díaz-del-Río, V., Stow, D. A. V., Maestro, A., & Alveirinho Dias, J. M. (2002). Seismic stacking pattern of the Faro-Albufeira contourite system (Gulf of Cadiz): A Quaternary record of paleoceanographic and tectonic influences. *Marine Geophysical Researches*, *22*(5–6), 487–508. https://doi.org/10.1023/A:1016355801344

Louarn, E., & Morin, P. (2011). Antarctic Intermediate Water influence on Mediterranean Sea Water outflow. *Deep-Sea Research Part I: Oceanographic Research Papers*, *58*(9), 932–942. https://doi.org/10.1016/j.dsr.2011.05.009

Madec, Gurvan and the NEMO team, (2016). NEMO ocean engine: version 3.6 stable. Note du Pole de modelisation, Institut Pierre-Simon Laplace N 27. ISSN No 1288-1619. https://www.nemo-ocean.eu/wp-content/uploads/NEMO_book.pdf

McKenzie, D. P., (1970), Plate tectonics of the Mediterranean region: Nature, v. 226, p. 239-243.

Mulder, T., Voisset, M., Lecroart, P., Le Drezen, E., Gonthier, E., Hanquiez, V., Morel, J. (2003). The Gulf of Cadiz: An unstable giant contouritic levee. *Geo-Marine Letters*, *23*(1), 7–18. https://doi.org/10.1007/s00367-003-0119-0

Pinardi, N., Allen, I., De Mey, P., Korres, G., Lascaratos, A., Le Traon, P.Y., Maillard, C., Manzella G., Tziavos, C., (2003). The Mediterranean ocean Forecasting System: first phase of implementation (1998-2001). Ann. Geophys., 21, 1, 3-20.

Pinardi, N., and G. Coppini, (2010). Operational oceanography in the Mediterranean Sea: the second stage of development Ocean Sci., 6, 263-267.

Raicich, F. (1996). On fresh water balance of the Adriatic Sea, J. Mar. Syst., 9, 305–319.

Rebesco, M., Hernández-Molina, F. J., Van Rooij, D., & Wåhlin, A. (2014). Contourites and associated sediments controlled by deep-water circulation processes: State-of-the-art and future considerations. *Marine Geology*, *352*, 111–154. https://doi.org/10.1016/j.margeo.2014.03.011

Rogerson, M., Rohling, E.J., Bigg, G.R., and Ramirez, J., (2012), Paleoceanography of the Atlantic-Mediterranean exchange: Overviewand first quantitativeassessment of climatic forcing: Rev. Geophys., v. 50, RG2003, doi:http://dx.doi.org/10.1029/2011RG000376.

Roveri, M., Flecker, R., Krijgsman, W., Lofi, J., Lugli, S., Manzi, V., Sierro, F.J., Bertini, A., Carnerlenghi, A., De Lange, G., Govers, R., Hilgen, F.J., Huebscher, C., Meijer, P.T., Stoica, M., (2014). The Messinian salinity crisis: past and future of a great challenge for marine sciences. Mar. Geol. 352, 25–58.

Schwab, D. J., D. Beletsky, and J. Lou (2000), The 1998 coastal turbidity plume in Lake Michigan, Estuarine, Coastal and Shelf Science,50,49–58

Serra, N., Ambar, I., Boutov, D., & Oceanografia, D. (2010). Surface expression of MediterraneanWater dipoles and their contribution to the shelf/slope – open ocean exchange, Ocean Sci., 6, 191–209.

Srivastava, S.P., et al., 1990. Motion of Iberia since the Late Jurassic; results from detailed aeromagnetic measurements in the Newfoundland Basin. Tectonophysics 184 (3–4), 229–260.

Storto, A., Masina, S., Navarra, A., (2015). Evaluation of the CMCC eddy-permitting global ocean physical reanalysis system (C-GLORS, 1982-2012) and its assimilation components. Quarterly Journal of the Royal Meteorological Society, 142, 738–758, doi: 10.1002/qj.2673.

Teixeira, M., Terrinha, P., Roque, C., Rosa, M., Ercilla, G., & Casas, D. (2019). Interaction of alongslope and downslope processes in the Alentejo Margin (SW Iberia) – Implications on slope stability. *Marine Geology*, *410*(July 2018), 88–108.

Terrinha, P., Matias, L., Vicente, J., Duarte, J., Luís, J., Pinheiro, L., … Víctor, L. M. (2009). Morphotectonics and strain partitioning at the Iberia-Africa plate boundary from multibeam and seismic reflection data. *Marine Geology*, *267*(3–4), 156–174. https://doi.org/10.1016/j.margeo.2009.09.012

Thran, A. C., Dutkiewicz, A., Spence, P., & Müller, R. D. (2018). Controls on the global distribution of contourite drifts: Insights from an eddy-resolving ocean model. *Earth and Planetary Science Letters*, *489*, 228–240. https://doi.org/10.1016/j.epsl.2018.02.044

Tonani, M., Teruzzi, A., Korres, G., Pinardi, N., Crise, A., Adani, M., Oddo, P., Dobricic, S., Fratianni, C., Drudi, M., Salon, S., Grandi, A., Girardi, G., Lyubartsev, V., Marino, S., (2014). The Mediterranean Monitoring and Forecasting Centre, a component of the MyOcean system. Proceedings of the 6th Int. Conference on EuroGOOS 4-6 October 2011, Sopot, Poland. Edited by H. Dahlin, N.C. Fleming and S. E. Petersson. First published 2014. Eurogoos Publication no. 30. ISBN 978-91-974828-9-9.

Trowbridge J. H. and Lentz S. J. (2018). The Bottom Boundary Layer. Annual Review of Marine Science, 397-420.

Zenk, W., & Armi, L. (1990). The complex spreading pattern of Mediterranean Water off the Portuguese continental slope. *Deep Sea Research Part A, Oceanographic Research Papers*, *37*(12), 1805–1823. https://doi.org/10.1016/0198-0149(90)90079-B

Zitellini, N., Gràcia, E., Matias, L., Terrinha, P., Abreu, M. A., De Alteriis, G., Diez, S. (2009). The quest for the Africa-Eurasia plate boundary west of the Strait of Gibraltar. *Earth and Planetary Science Letters*, *280*(1–4), 13–50. https://doi.org/10.1016/j.epsl.2008.12.005